VISUAL SIMULATION OF

DIFFERENT OPTICAL DESIGNS

PROGRAMA DE DOCTORADO EN OPTOMETRÍA Y CIENCIAS DE LA VISIÓN

Doctorando:
Eleni Papadatou

Directores de Tesis:
Alejandro Cerviño Exposito
David Madrid Costa

Burjasot, Noviembre de 2016

VISUAL SIMULATION OF

DIFFERENT OPTICAL DESIGNS

PROGRAMA DE DOCTORADO EN OPTOMETRÍA Y CIENCIAS DE LA VISIÓN

Doctorando:
Eleni Papadatou

Director de Tesis:
Alejandro Cerviño-Exposito
David Madrid Costa

Burjasot, Noviembre de 2016

VISUAL SIMULATION OF

DIFFERENT OPTICAL DESIGNS

Memoria presentada por

Eleni Papadatou

Para optar al grado de

DOCTOR en OPTOMETRÍA Y CIENCIAS DE LA VISIÓN

IV

DECLARATION

No portion of the work referred to in the thesis has been submitted in support of an application for another degree or qualification of this or any other university or other institution of Learning.

El Dr Alejandro Cerviño Exposito, Profesor Titular de Universidad en la Universidad de Valencia, y el Dr David Madrid Costa, Profesor Ayudante Doctor en la Universidad Complutense de Madrid,

CERTIFICAN que la presente memoria Visual Simulation of Different Optical Designs, resume el trabajo de investigación realizado, bajo su dirección, por Dª Eleni Papadatou y constituye su Tesis para optar al Grado de Doctor en Optometría y Ciencias de la Visión.

Y para que así conste, y en cumplimiento de la legislación vigente, firma el presente certificado en Valencia, a Noviembre de dos mil dieciséis.

Fdo. Alejandro Cerviño Exposito   Fdo. David Madrid Costa

x

Acknowledgments

Θα ήθελα να ευχαριστήσω την οικογένεια μου, ιδιαίτερα τη μητερα μου, που πάντα στήριζε τις προσπάθειες μου και μου έδωσε όλα τα ηθικά εφόδια για να πορεύομαι στη ζωή.

Τους καθηγητές μου που μου εμφύσησαν το «μικρόβιο» της έρευνας και με ώθησαν να προχωρήσω τις σπουδές μου και να κυνηγήσω τα όνειρα μου.

Τους ανθρώπους που συνεργάστηκα αυτά τα τρία χρόνια και καταφέραμε μικρές συνεισφορές στο επιστημονικό πεδίο.

Τους φίλους μου, πάλιους και νέους, που εκτός από όμορφες στιγμές, πρόσφεραν και ηθική υποστήριξη.

Τέλος, τον συντροφό μου που στάθηκέ σύμβουλος και οδηγός σε αυτό το εγχείρημα και πάντα πιστεύε στις δυνατότητές μου.

«Αἰὲν ἀριστεύειν καὶ ὑπείροχον ἔμμεναι ἄλλων»
Ιππόλοχος προς Γλαύκο, Ομήρου Ιλιάδα

«Ὅταν μιλάει η αταξία η τάξη να σωπαίνει· έχει μεγάλη πείρα ο χαμός»
Κική Δημουλά

Resumen

La presbicia es la pérdida de la capacidad de acomodar del ojo, debida a la senescencia del mismo. Las causas principales de ésta pérdida son la aparición de agregados proteínicos en el cristalino, lo que conlleva una pérdida progresiva de flexibilidad y de elasticidad de esta lente, que ulteriormente desemboca en la imposibilidad de acomodar o, en otras palabras, de ver nítidos objetos situados relativamente cercanos al ojo. La presbicia, o como es más comúnmente conocida, la vista cansada, suele aparecer algo más tarde de los 40 años de edad. Al tratarse de un defecto asociado al envejecimiento, el 100% de la población mayor de 40 años sufrirá de presbicia. Este hecho, junto con el aumento en la proporción de ancianos experimentado en los últimos años en la población general, hace que el estudio y desarrollo de nuevas y cada vez más sofisticadas tecnologías para la compensación de la presbicia sea de vital importancia.

Actualmente existe una amplia oferta de soluciones compensadoras de la presbicia, las cuales se dividen en varios grupos. El método más usado actualmente es la compensación mediante gafas, que pueden ser sólo para visión cercana, bifocales o multifocales. Además, existen lentes de contacto multifocales, lentes intraoculares y cirugía refractiva corneal. Lo que une a todas estas soluciones es el mismo objetivo: intentar proporcionar al sujeto una visión óptima a lo largo del mayor rango de distancias de trabajo posible, compensando así la pérdida de la acomodación. La gran mayoría de lentes de contacto multifocales, lentes intraoculares e incluso algunas cirugías refractivas se basan en el principio conocido como visión simultánea. Ésta se basa en la formación de varias imágenes en la retina al mismo tiempo. Una de estas imágenes está enfocada, mientras que el resto están desenfocadas y el ojo las aprecia como borrosas. Por tanto, el éxito de este tipo de soluciones depende de la capacidad de cada individuo de ignorar las imágenes borrosas y seleccionar la imagen nítida a cada distancia de trabajo. Bajo esta categoría se engloban lentes de contacto y lentes intraoculares multifocales refractivas que poseen distintas zonas dedicadas a diferentes distancias de trabajo, y lentes difractivas. La gran mayoría de lentes, tanto de contacto como intraoculares se basan en el principio de visión simultánea. Otro principio para compensar la presbicia es conocido como monovisión. La monovisión consiste en la compensación de uno de los dos ojos para ver de forma nítida a distancias lejanas, mientras que el otro ojo se compensa para ver de forma nítida en visión cercana. De

esta forma, el sujeto puede ver de forma adecuada tanto objetos lejanos, como cercanos. Esta estrategia de compensación de la presbicia suele ir acompañada de menos éxito que la visión simultánea. Existen también lentes intraoculares acomodativas, cuyo objetivo es restaurar la acomodación del ojo aprovechando el hecho de que el músculo ciliar aún mantiene su habilidad. Sin embargo, hasta ahora este tipo de lentes no parece cumplir su objetivo de forma adecuada.

A pesar de la gran cantidad de lentes para presbicia que existe en el mercado, aún no se ha dado con una solución adecuada para la gran mayoría de la población présbita, que desea tener la posibilidad de ver de forma adecuada a un gran rango de distancias diferentes, sin necesidad de recurrir a la compensación clásica con gafa. Es por esto que es de gran importancia el entender y evaluar de forma adecuada las diferentes soluciones para la presbicia existentes en el mercado, así como proponer nuevas metodologías y análisis que permitan el desarrollo de nuevos elementos compensadores de presbicia, ya sea por medio de la mejora de los diseños existentes hoy día, o mediante la introducción de nuevas técnicas.

Los objetivos de esta Tesis Doctoral pueden resumirse en dos: la evaluación objetiva y precisa de soluciones compensadoras de la presbicia, mediante nuevas métricas y análisis; así como la introducción y desarrollo de nuevas metodologías que ayuden a mejorar los diseños existentes hoy día.

Existe una amplia variedad de métricas diferentes para la evaluación objetiva de la calidad óptica, estando algunas de ellas basadas en el frente de ondas propagado por dicho sistema, en la "Point Spread Function" (PSF), en la función de transferencia de modulación (MTF), o incluso en la imagen que forman dichos sistemas.

En el caso de lentes intraoculares multifocales, el estudio objetivo de su calidad óptica se realiza siguiendo una serie de normas establecidas por unos estándares ISO, que deben ser cumplidos. Dado que, como norma general, los estudios sobre calidad óptica in vitro de lentes intraoculares multifocales, carecían de comparaciones objetivas entre lentes mediante el uso de alguna métrica, era importante el desarrollo de una forma rápida y precisa de poder realizar comparaciones entre dichas lentes para conocer cuáles son sus ventajas e inconvenientes y para discernir qué lente puede ser más útil para determinados individuos.

Es por ello que se creó una métrica basada en la función de modulación de transferencia axial (aMTF). Esta aMTF se obtiene fácilmente con los equipos que miden lentes

intraoculares multifocales teniendo en cuenta los estándares ISO. En este caso se usó el PMTF (Lambda-X), que es un dispositivo que básicamente forma la imagen de un borde vertical u horizontal (dependiendo si interesa la MTF sagital o tangencial) de una lente intraocular variando de forma secuencial la vergencia. En cada paso de vergencia, el software del dispositivo se encarga de calcular la MTF, obteniendo así valores de contraste para una serie de frecuencias espaciales (MTF) y para un conjunto de vergencia diferentes (through-focus). Este dispositivo utiliza una fuente de luz con el pico espectral en 546 nm y permite la opción de modificar la apertura utilizada para las medidas, con posibilidad de seleccionar 2, 3, 3.75 y 4.5 mm. La razón por la cual la métrica está basada en la aMTF es sencilla; la aMTF es precisamente el conjunto de MTFs obtenidos a diferentes vergencias o distancias de trabajo. Esto hace que la métrica pueda ser aplicada directamente sobre los datos obtenidos con este tipo de dispositivos, siguiendo todos los estándares propuestos por la ISO. Esta métrica fue bautizada como VUaMTF (Volume Under the axial MTF), debido a que se basa en el cálculo del volumen existente bajo la superficie definida por la aMTF. La VUaMTF posee una característica que hacen de ella una métrica interesante y versátil; el volumen puede ser calculado en diferentes intervalos de frecuencias espaciales y de vergencias. Esto significa que esta métrica puede ser utilizada para calcular la calidad óptica objetiva de una lente intraocular completa, o para calcular dicha calidad sólo en el foco destinado a visión lejana, o cercana o intermedia. Además, puede seleccionarse el rango de frecuencias espaciales y estudiar qué lente es mejor para formar imágenes con contenido frecuencial bajo y cuál para formar imágenes con contenido frecuencial alto. Esto abre las puertas a un rango amplio de comparaciones y a una caracterización de las lentes intraoculares multifocales no visto hasta ahora, que permitirá conocer de forma más profunda las características de cada lente. Para una mayor simplicidad en la lectura de los resultados, se optó por normalizar la VUaMTF usando el foco dedicado a visión lejana de una lente intraocular monofocal.

Diferentes lentes intraoculares multifocales fueron seleccionadas con el objetivo de probar la nueva métrica desarrollada, así como de caracterizarlas objetivamente y de forma lo más completa posible. Se seleccionaron un total de cuatro lentes, de entre las más conocidas en el mercado, que abarcaran un amplio abanico de diseños diferentes (bifocal, trifocal, rango extendido…). Dichas lentes fueron caracterizadas de dos formas: se evalúo su calidad óptica mediante el uso del instrumento PMTF (Lambda-X) y de la métrica desarrollada en esta Tesis Doctoral (VUaMTF), así como también se

evaluó la dispersión no deseada de luz, o scattering, que estas lentes pueden provocar, y que se conoce como straylight. El straylight puede causar brillos y disminución del contraste que supone incomodidad para el paciente, de ahí la importancia de realizar este tipo de evaluaciones con lentes intraoculares. El straylight de las diferentes lentes intraoculares fue objetivamente determinado mediante el uso de un dispositivo conocido como C-Quant (Oculus), gracias a una modificación realizada sobre éste que permite medir el straylight de lentes intraoculares. También se caracterizó una lente intraocular monofocal que sirvió de comparación.

Como era de esperar, la lente monofocal ofreció una calidad óptica mayor para lejos que el resto de multifocales estudiadas. Esto es lógico, ya que las lentes multifocales necesitan dividir la luz que les llega a más de un foco, con lo cual existe una compensación en la que, para ofrecer visión nítida a más de una distancia, la calidad óptica para visión de lejos debe disminuir. En otras palabras, parte de la calidad óptica para la visión lejana debe ir destinada a visión cercana o intermedia. Gracias a la métrica VUaMTF, los diferentes diseños pueden ser distinguidos inmediatamente, según el número de máximos que presenta la MTF axial. También se pudo observar como la lente de rango extendido presentó valores de VUaMTF prácticamente constantes para visión lejana e intermedia, disminuyendo para visión cercana. La lente monofocal, como su propio nombre indica, sólo presentó un pico, localizado en visión lejana, mientras que el resto de multifocales superaron los valores de VUaMTF proporcionados por la monofocal para distancias intermedias y cercanas.

Con respecto a los valores de straylight de las lentes intraoculares, todos ellos fueron muy similares entre sí y muy pequeños. De hecho, los valores obtenidos para todas las lentes fueron mucho menores que el valor de straylight típico para ojos jóvenes, y también menores que el valor de straylight típico de un cristalino joven. Esto quiere decir que las lentes intraoculares estudiadas no deberían causar brillos indeseados o straylight en los pacientes implantados con ellas, siempre y cuando la implantación sea óptima.

El análisis objetivo de calidad óptica mediante la VUaMTF, permite caracterizar cada diseño de lente intraocular y puede ayudar a la selección de la lente más apropiada para cada paciente, según sus necesidades visuales.

Como se mencionó con anterioridad, otra solución típica para la presbicia es el uso de lentes de contacto multifocales. La representación de la potencia refractiva de la lente

con respecto a la distancia radial se conoce como perfil de potencia. Estos perfiles de potencia gozan de una gran popularidad, sobre todo para evaluar lentes multifocales. Sin embargo, presentan algún inconveniente, como el hecho de que sólo pueden ser interpretados de forma adecuada para lentes que poseen simetría radial. Además, como ocurría con la evaluación objetiva de lentes intraoculares por medio de la MTF, no existen prácticamente análisis que permitan caracterizar estos perfiles de potencia de forma objetiva. Es por ello que se en este documento se proponen una serie de análisis de perfiles de potencia que permiten caracterizarlas de forma más óptima, así como permiten evaluar de forma objetiva el efecto que el diámetro pupilar tiene en la distribución de potencias refractivas de este tipo de lentes. Esto es de gran importancia, dado que la gran mayoría de lentes de contacto multifocales son refractivas y están divididas en distintas zonas, y cada una de ellas provee una potencia refractiva diferente. Además, los diseños más típicos en el mercado son concéntricos, con lo cual el tamaño de la pupila del ojo es crucial, ya que si ésta es muy pequeña, la lente no proveerá al ojo con determinadas potencias. Es por esto que la distribución de potencias de la lente proporciona al ojo depende enormemente del tamaño pupilar de éste, y de ahí la importancia de conocer cómo cada diseño de lentes de contacto multifocales se ve afectado por diferentes tamaños pupilares. Para este análisis se utilizaron tres diseños diferentes de lentes de contacto multifocales: un diseño bifocal centro-cerca con tres adiciones diferentes, un diseño asférico que aumenta su potencia de forma progresiva desde la periferia al centro, y un diseño multifocal basado en cinco anillos concéntricos, también con tres adiciones diferentes.

Para estudiar cómo varía la distribución de las distintas potencias refractivas que proporciona cada lente al variar el tamaño pupilar, se calculó el porcentaje del perfil de potencia que poseía una potencia refractiva determinada. En otras palabras, y dado que las lentes utilizadas en este estudio poseían todas simetría radial, se calculó el porcentaje de área de la lente dedicada a proporcionar una potencia dióptrica determinada con respecto al área total medida. La potencia dióptrica, en este caso, fue considerada en intervalos de 0.25 D. De esta forma, lo que se obtienen son una especie de histogramas en los que se representa un porcentaje de área de la lente para cada intervalo de potencias. Esto se realiza para los tres diseños de lentes diferentes, y para varios diámetros pupilares diferentes (3, 4.5 y 6 mm).

Por otra parte, se establecieron unos límites de visión a diferentes distancias. El límite seleccionado para visión cercana fue 40 cm (2.5 D, consideradas desde la potencia

nominal de la lente), así toda la zona de las lentes que posean 2.5 o más D de potencia, respecto de la potencia nominal de la lente, que era de -3 D en todos los casos, fue atribuido a visión cercana. La visión intermedia de definió entre 100 y 40 cm (1 y 2.5 D, desde la potencia nominal), mientras que la visión lejana se consideró desde el infinito hasta 1 metro (1 D). Con estos límites, se caracterizaron las lentes multifocales de adición alta. Se representó la variación de porcentaje de lente dedicado a cada una de las tres zonas de visión diferente con respecto al diámetro pupilar.

Por último, un análisis de porcentaje de zona de lente dedicada a cada potencia dióptrica fue llevado a cabo mediante una suma acumulada de porcentajes. Esto es similar a las distribuciones cumulativas de probabilidad, y permitió una caracterización objetiva, rápida y sencilla de la distribución de potencias refractivas en las distintas lentes, con diferentes diámetros pupilares.

Normalmente, la distribución de potencias de las distintas lentes multifocales se esparció al aumentar el diámetro pupilar y cuando la adición de las lentes era mayor. Esto es, más valores de potencia aparecían al aumentar el diámetro pupilar y la adición. Esto es lógico y razonable, ya que al aumentar el diámetro pupilar, se abarcaba más perfil de potencia, y al aumentar la adición manteniendo la potencia nominal de -3 D, más valores de potencia aparecieron a consecuencia de tener más adición. Diferencias entre los diseños fueron apreciadas en los distintos histogramas de potencia refractiva.

Con respecto al segundo tipo de análisis, diferencias entre los diferentes diseños de alta adición fueron evidentes. La lente que poseía varias zonas en forma de anillos no alcanzó en ningún momento el límite establecido para visión cercana. A diámetros pupilares inferiores a 2 mm, la lente se comportaba bien para visión intermedia, mientras que para pupilas de, aproximadamente 3.8 mm, la lente dedicaba el mismo porcentaje de área a visión lejana que a visión intermedia. Para las otras dos lentes sí que existían porcentajes para las tres zonas de visión, empezando con visión lejana para pupilas muy pequeñas, y, conforme la pupila incrementaba su tamaño, el resto de zonas de visión comenzaban a aparecer. Con una pupila de 6 mm, la lente asférica presentaba alrededor de un 80 % de su área dedicada a visión lejana, mientras que la lente bifocal presentaba alrededor de un 40-40-20 % dedicado a visión lejana, cercana e intermedia, respectivamente.

El análisis de porcentaje de área de lente acumulado dio resultados similares a los histogramas mencionados anteriormente, pero son más precisos y más elegantes.

Pueden ser utilizados para calcular rápidamente porcentajes de área de la lente dedicados a diferentes potencias refractivas.

Estos análisis pueden ayudar a mejorar la prescripción de lentes de contacto multifocales, ya que conociendo la dinámica pupilar del sujeto, se puede elegir la mejor lente que le proporcione un rango de visión adecuado a sus necesidades y según su diámetro pupilar.

Otro de los objetivos marcados en esta Tesis Doctoral fue la introducción y desarrollo de nuevas metodologías que permitan mejorar las soluciones compensadoras de la presbicia. Para ello, lo primero que se ideó fue una metodología que produjera visión simultánea, pero en este caso, en vez de utilizar diferentes zonas de la óptica para formar diferentes imágenes simultáneamente, se utilizó la misma óptica, en este caso un espejo deformable, para generar distintas imágenes en el tiempo. Esto se llevó a cabo cambiando la forma del espejo deformable muy rápidamente (50 Hz), lo que se conoce como multiplexación temporal, de tal modo que el ojo integra las imágenes y aprecia lo mismo que apreciaría con visión simultánea proporcionada por lentes multifocales. Esto es, una imagen nítida y otra imagen "fantasma" desenfocada. Para ello, es crucial que la frecuencia con la que el espejo deformable cambie de forma sea mayor que la frecuencia crítica de fusión del ojo.

Para llevar a cabo esta metodología se utilizó un sistema de óptica adaptativa, compuesto, básicamente, por un espejo deformable, un sensor de frente de onda, un sistema Badal motorizado, un microdisplay de 800x600 píxeles, un láser He-Ne que permitió medir y corregir aberraciones del sistema, así como generar aberraciones en los distintos diseños realizados, y una cámara digital que funcionó como ojo artificial, con una pupila de 5 mm de diámetro.

La visión simultánea se generó cambiando la forma del espejo a 50 Hz. Por ejemplo, para generar un diseño bifocal sin ningún tipo de aberración, el espejo pasaba de generar un desenfoque de 0 D a generar uno de 2.5 D de forma muy rápida. Se generaron un total de nueve diseños: bifocal en el que el espejo pasaba el mismo tiempo en cada desenfoque, bifocal en el que el espejo pasaba un 60 % en el foco de lejos y un 40 % en el de cerca, bifocal tórica con un cilindro de -1 D a 0°, bifocales con aberración esférica de 0.1 micras (para pupila de 5 mm), variado el signo de la aberración en cada uno de los focos (positivos ambos, negativos ambos, positivo y negativo, y negativo y positivo), y dos diseños a los que se añadieron aberraciones corneales de un modelo de

córnea típico para 60 años de edad. La diferencia entre los dos últimos radicó en que en uno se compensó parte de la aberración esférica corneal.

Para la evaluación objetiva de cada uno de estos diseños, se realizó un "through-focus" con el sistema Badal, o lo que es lo mismo, se fue variando el desenfoque en pasos de 0.125 D, desde +0.5 a -3 D de vergencia. En cada paso, se realizaron fotografías con la cámara digital de distintos estímulos: red rectangular vertical, red rectangular horizontal, ambas con una frecuencia espacial de 15 ciclos por grado, y un optotipo ETDRS. Las redes rectangulares se usaron para calcular el contraste que ofrecía cada diseño a la frecuencia especificada, tal y como indica la ISO, mientras que el optotipo se usó para realizar una correlación cruzada con el optotipo perfectamente enfocado y sin aberraciones.

Los resultados obtenidos fueron similares a los que se obtienen en lentes intraoculares reales y la adición de aberración esférica con distintos signos hace que las curvas varíen de forma distinta, en algunos casos desplazando ligeramente los picos, y, a veces, mejorando la visión a distancias intermedias, esto es, mejorando la profundidad de foco. La adición de aberraciones corneales afectó muy negativamente al contraste a 15 ciclos por grado, mejorando la calidad en los picos ligeramente cuando se compensó parcialmente la aberración esférica corneal.

Se puede decir, por tanto, que se trató de un método válido para evaluar diferentes diseños para compensar la presbicia de forma totalmente no invasiva, que puede ayudar a seleccionar la lente adecuada para pacientes que deseen la implantación de una lente intraocular o el uso de lentes de contacto multifocales. Además, esta metodología puede ser usada para mejorar los diseños actuales.

La segunda metodología desarrollada, tiene como objeto estudiar cómo influyen diferentes diseños de compensaciones para presbicia en la agudeza visual de los sujetos, tanto en alto como en bajo contraste. En este caso, se realizaron simulaciones de diferentes diseños multifocales utilizando Matlab (Mathworks) y basados en óptica de Fourier.

Las curvas de desenfoque muestran la variación de la agudeza visual de los sujetos a varias vergencias, lo que las hace tremendamente importantes a la hora de evaluar si las compensaciones multifocales son adecuadas. Por este motivo, este tipo de curvas son ampliamente utilizadas en oftalmología y optometría.

Cinco diseños diferentes fueron creados para evaluar esta metodología: monofocal, bifocal angular, bifocal radial, trifocal radial y un diseño de rango extendido. Estos diseños resumen de forma adecuada las distintas posibilidades disponibles en el mercado. Los diseños se crearon mediante la generación de frentes de onda con diferente desenfoque (o potencia refractiva), con tantos frentes de onda distintos como zonas poseía cada diseño particular. Una aberración esférica de -0.27 micras para 6 mm de pupila fue añadida a todos los diseños, dado que se trata de un valor típico que se encuentra en las lentes disponibles comercialmente. Además, se añadieron aberraciones corneales provenientes de un modelo de córnea de 60 años típico, para estudiar el efecto de dichas aberraciones en las curvas de desenfoque. Al frente de onda perteneciente a cada diseño se le añadió diferentes cantidades de desenfoque, con el fin de realizar una curva de desenfoque. La vergencia se varió desde 1 hasta -3.5 D, en pasos de 0.25 D, y en cada uno de estos pasos, se calculó la PSF y se realizó una convolución con dos optotipos ETDRS: uno de alto contraste (prácticamente 100 %) y otro de bajo contraste (alrededor del 10 %). Se le presentaron dichos optotipos a tres sujetos, y se obtuvo para cada uno de ellos y para cada diseño dos curvas de desenfoque: una sin aberraciones corneales y otra con aberraciones. Los sujetos miraban monocularmente a través de una pupila artificial de 3 mm de diámetro, para disminuir drásticamente el efecto de sus propias aberraciones, a una pantalla en la que se presentaban los distintos optotipos. El efecto Stiles-Crawford se tuvo en cuenta en las simulaciones, al calcular una apodización Gaussiana típica y aplicarla sobre la función pupila.

Las curvas de desenfoque obtenidas son similares a las obtenidas en otros estudios con pacientes que fueron implantados con lentes intraoculares, lo cual refuerza el uso de esta metodología. Como es obvio, se obtuvieron valores de agudeza visual mayores para alto contraste que para bajo. Un hallazgo importante es el hecho de que, a mayor complejidad del diseño multifocal, más afectada se ve la agudeza visual a bajo contraste, siendo a veces bastante pequeña. Las aberraciones corneales no parecieron afectar demasiado a la agudeza visual, aunque se observó un desplazamiento en algunos picos, debido a la aberración esférica corneal. De todos modos, esto puede ser fácilmente corregido variando la potencia refractiva del diseño, lo que equivale a un desplazamiento lateral de la curva de desenfoque. Otro aspecto importante es el hecho de que la adición de aberraciones corneales a ciertos diseños parece incrementar el intervalo total de las curvas de desenfoque en el que la agudeza visual es igual o mejor a 0.2 logMAR, o lo que es lo mismo, parece incrementar la profundidad de foco de

dichos diseños en el caso de alto contraste. Para bajo contraste, lo disminuye siempre, debido a que las aberraciones suelen afectar más a la sensibilidad al contraste que a la agudeza visual.

Parece, por tanto, que esta metodología es adecuada para testear diferentes diseños a pacientes para obtener la compensación más adecuada posible a sus necesidades.

Como conclusiones generales de esta Tesis Doctoral cabe citar que los diferentes análisis propuestos, tanto para lentes intraoculares (VUaMTF) como para lentes de contacto multifocales, permiten una caracterización objetiva, rápida y precisa de este tipo de soluciones para la presbicia. También permiten una comparación concisa entre diferentes diseños de lentes. La calidad óptica proporcionada por cada lente depende, obviamente, del diseño específico de la lente. La evaluación de la calidad óptica no suele ser suficiente, es por ello que la medida del straylight de este tipo de soluciones para la presbicia es necesario, a pesar de que las lentes evaluadas presentan valores muy bajos. Por otra parte, es de gran importancia el desarrollo y validación de nuevas metodologías que permitan testear diferentes diseños multifocales en pacientes de forma no invasiva y previo a la posible cirugía para la implantación de una lente intraocular. De este modo, se puede seleccionar el diseño más adecuado para cada paciente, según sus características y sus necesidades visuales. Tanto la multiplexación temporal anteriormente descrita como la generación de diferentes diseños y la posterior obtención de curvas de desenfoque son metodologías que permiten tanto la selección de la compensación más adecuada para cada paciente, como la posibilidad de mejora de los diseños que existen actualmente, mediante la adición de distintas aberraciones o el uso de diferentes geometrías que optimicen el rendimiento visual de los pacientes.

Abstract

Presbyopia is the age-related, irreversible loss of the accomodative ability of the human eye, which affects near visual performance. The present PhD Thesis aimed to evaluate optical and visual aspects of multifocal designs for presbyopia treatment that can be found in contact and intraocular lenses. First, a metric was implemented that facilitates the in vitro evaluation of intraocular lenses. The idea of the metric is based on the axial modulation transfer function of the intraocular lenses which can be obtained with a proper laboratory equipment. The metric assesses the volume under the surface defined by the axial modulation transfer function within adjustable defocus and spatial frequency intervals. It allows for fast and objective comparisons between different types and designs of intraocular lenses, therefore, it can be a useful tool in laboratory evaluation of presbyopic optical elements.

The metric was applied for evaluating the in vitro optical quality of four different types of intraocular lenses that consisted of the most common designs: a monofocal, a bifocal, a trifocal and an extended range intraocular lens, revealing the optical quality that these elements can offer according to their design. The evaluation was performed for two different pupil diameters (3-mm and 4.5-mm) and the results suggested that the optical quality of the monofocal design for far vision was superior than that exhibited by the multifocal designs. On the other hand, the multifocal intraocular lenses provided better optical quality at more than one vergence. Since some pseudophakic patients implanted with multifocal intraocular lenses show elevated straylight levels, the abovementioned lenses were tested with an apparatus for assesing in vitro their straylight levels; the results showed no differences between the monofocal and the multifocal designs. Moreover, the straylight levels of all the lenses were lower than the straylight exhibited by the young healthy crystalline lens.

For multifocal contact lenses the pupil dynamics have a crucial role in the visual performance. For this purpose, the power profiles of center-near and center-distance designs were obtained and a thorough analysis of the effect of pupil size upon the power distribution of these lenses was performed. The results of this study, if combined with pupil data from presbyopes, can provide useful information for improving the fitting of presbyopes, thus increasing visual performance with multifocal contact lenses.

Since simultaneous vision is the most common approach for multifocal solutions, a methodology for non-invasive control of visual performance with simultaneous vision

solutions was presented. This methodology is based on adaptive optics technology and the ability of a deformable mirror to change its shape in a quick fashion between two vergences (temporal multiplexing). It can simulate different bifocal designs, including toric and combinations of spherical aberration and investigate subjective visual performance for different multifocal contact or intraocular lens designs.

Lastly, a pilot study was conducted where high (100%) and low contrast (10%) visual acuity with simulated optical designs was evaluated by obtaining defocus curves. The simulations were generated using Fourier optics and included a monofocal, an angular bifocal, a radial bifocal, a radial trifocal and an extented range design. To those simulations, higher order aberrrations from an aging cornea were added. The preliminary results showed that corneal higher order aberrations could increase the depth of focus in expense of visual acuity and also that low contrast visual acuity was worse with multifocal designs in particular.

Table of Contents

Chapter 1
Introduction

1.Introduction

This introduction aims to cover the ophthalmic solutions and strategies that are available for presbyopia correction, mainly in contact and intraocular lenses, and the advantages of using adaptive optics technology in presbyopia treatment.

1.1 Crystalline lens

The crystalline lens is located behind the iris and belongs to the anterior segment of the human eye. This transparent, biconvex structure is responsible (along with the cornea) for refracting light to form clear images of objects on the retina. The refractive ability of the crystalline lens comes from the fact that its refractive index, which is not homogeneous (gradually decreasing from the center to the periphery), is different from that of the surrounding structures (aqueous humor, vitreous body). As for its structure (Figure 1.1), the crystalline lens is composed of four layers that from its surface to its center are: the capsule (a collagen membrane that surrounds the lens), the subcapsular epithelium (only on the anterior portion), the cortex and the nucleus. The lens is held in place by suspensory thin ligaments, known as zonular fibers, emerged from the epithelium cells (Lens, Nemeth, and Ledford 2008).

1.2 Accommodation of the human eye and presbyopia

The human eye has the ability to change its refractive power for bringing into focus objects at different distances. This ability, known as accommodation of the human eye, is crucial for maintaining constant, smooth and clear vision (Cox 2001; Charman 2014a). Scheiner (1619) is reported to be the first who demonstrated accommodation using a double pinhole, and later Potterfield (1738) used the term "accommodation" to describe the ability of the human eye to focus at different distances (Agarwal, Agarwal, and Apple 2002).

Although there are several theories (L. Werner et al. 2000; Schachar 2004; Strenk, Strenk, and Koretz 2005) that attempt to explain the mechanism of accommodation, the present understanding is based on Helmholtz's theory (1856). Helmholtz noticed changes on the size of the Purkinje's image on the anterior surface of the crystalline lens and supported that it was responsible for accommodation (Strenk, Strenk, and Koretz 2005). The Helmholtz's theory (or capsular theory) of accommodation (Hartridge 1925; Strenk, Strenk, and Koretz 2005; Agarwal, Agarwal, and Apple 2002;

Petrash 2013) (Figure 1.2) states that while viewing a far object (unaccommodated state) the ciliary muscle is relaxed and the zonular fibers are tensed resulting in a flattening of the lens that decreases the dioptric power of the eye. According to Helmholtz, the source of this tension is caused by the pressure that the vitreous and the aqueous humor wield outwards onto the sclera. When viewing a near object (accommodated state), the ciliary muscle contracts causing a relaxation of the zonular fibers which allows for the lens to obtain a more convex shape and to increase the eye's dioptric power.

Although the young human eye can easily change its focal length to focus objects placed at different distances, the amplitude of accommodation (Figure 1.3) has been found to decline almost linearly with age (Charman 2014a; Charman 2008; Pascal JI and Ludvigh E 1938; Pallikaris, Plainis, and Charman 2012). In the first two decades of life accommodative amplitude has been found to be between a range of 7-10 D. The most significant decrement in accommodative amplitude occurs between the ages of 20 and 50, and, by the age of 52 is usually zero (Charman 2014a; Charman 2008; L. Werner et al. 2000). This gradually, irreversible loss of accommodative amplitude will lead at approximately mid-forties to near vision difficulties (e.g. in reading or working at the computer), a state known as presbyopia. Presbyopia is an age-related process and it will affect all humans' vision. According to the World Health Organization, in 2005, more than a billion people in the world were presbyopic and around 517 million of them did not receive adequate correction for presbyopia (Holden et al. 2008).

1.3 Other age-related changes of the human eye

Except of presbyopia and accommodative loss, the structures of the human eye undergo further changes with aging. These changes can increase for example the amounts of ocular aberrations (Amano et al. 2004; Artal et al. 2002) and of light scattering (van den Berg 1995; Van Den Berg et al. 2007), or reduce the transmittance of the ocular structures (Koretz et al. 1989). Consequently, they affect the refraction and the retinal image quality. Starting with the eye's axial length, it has been found to undergo a decrease through life. This has been interpreted as an emmetropization mechanism to prevent the eye from becoming myopic due to refractive changes with age (Grosvenor 1987).

The tear film production is reduced with aging. However, an increase in tear evaporation rate ("watery eye") can occur due to malposition of the eyelids (Salvi, Akhtar, and Currie 2006).

The cornea undergoes changes to its toricity, which can alter the astigmatism from "with the rule" to "against the rule" (Lyle 1971). Its transparency remains unaffected if there are no scars or degenerations that could affect its refractive properties (e.g. increasing scattering light).

As for the pupil, it has been found that both size and pupil's reflexes decrease linearly with age under every illumination level (Winn et al. 1994; Bitsios, Prettyman, and Szabadi 1996).

The crystalline lens undergoes changes in its shape, curvatures and refractive index (Salvi, Akhtar, and Currie 2006). The most typical change is the hardening of the lens due to biochemical and photochemical effects. This condition, known as *nuclear sclerosis* will eventually result to cataract (Salvi, Akhtar, and Currie 2006). Another change, which is related to cataract's appearance, is the absorption of more blue light due to biochemical changes.

As for the vitreous body's aged-related changes, it has been found that it looses part of its volume and collapses (syneresis) (Sebag 1987). Lastly, the retina undergoes various psychophysical, structural and cellular changes with aging (Bonnel, Mohand-Said, and Sahel 2003).

1.4 Ophthalmic solutions for presbyopia treatment

The difficulties in near vision that older people experience have been described since the antiquity. Roger Bacon (1250 AD) was the first European to describe presbyopia and to propose a solution (Charman 2014a). At the same era, the first reading spectacles for presbyopes appeared (Charman 2014a). Since then, the field of presbyopia has evolved to offer satisfying vision solutions for counteracting presbyopia symptoms. The increasing longevity will result for most of the people to spend almost half of their lives being presbyopes, hence the importance of the presbyopia correction. Nowadays, there is a wide range of available solutions for counteracting presbyopia symptoms including several designs of ophthalmic lenses, contacts lenses (CLs), intraocular lenses (IOLs), along with surgical techniques (Charman 2014a; Charman 2014b; Glasser 2008; Pallikaris, Plainis, and Charman 2012). These solutions can be

applied to the cornea, the anterior or the posterior chamber, the crystalline lens or the sclera (Figure 1.4). Despite the plethora of methods, there is not an ideal, repeatable solution that guarantees the optimal visual outcome yet. For the selection of a proper solution, multiple factors (e.g. lifestyle, visual demands) should be taken into account (Pallikaris, Plainis, and Charman 2012).

1.4.1 Ophthalmic lenses

The most common solution for presbyopia treatment is the prescription of ophthalmic lenses (Figure 1.5). Single-vision ophthalmic lenses incorporate an addition power for accomplishing near vision tasks. Although they offer satisfactory near vision, they do not cover the visual demands for near and intermediate vision. In the case the presbyope suffers of other refractive errors (i.e. myopia, hyperopia) he/she should use another pair of glasses or CLs for covering the visual demands at other distances (Pallikaris, Plainis, and Charman 2012). A solution for solving the issue of needing several spectacles, is the use of bifocal lenses (already proposed in 1784 by Benjamin Franklin), where the lower part of the lens has the correction for near vision and the upper part has the correction for distance vision (Charman 2014a). A later evolution of the bifocal lenses was the trifocal lens, where a part for enhancing the intermediate vision was also incorporated on the lens surface. The problem with these segmented designs is discomfort (known as "image jump"), the subjects experience in vision due to the abrupt power changes between the regions of the lenses (Pallikaris, Plainis, and Charman 2012; Charman 2014a). The creation of progressive lenses aimed to eliminate this undesirable phenomenon. Progressive ophthalmic lenses (Pallikaris, Plainis, and Charman 2012; Charman 2014a; Callina and Reynolds 2006) aim to provide smooth and clear vision at every viewing distance. In these lenses the lens power changes gradually in small steps from far to near vision within a relatively narrow corridor. The problems with these lenses are that some people cannot get used to them and the distortion of peripheral vision due to the narrow power channel. Other solutions of ophthalmic lenses for presbyopia treatment include mechanically-varied power liquid filled lenses or electric-varied power lenses based on liquid-crystal technology (Charman 2014a).
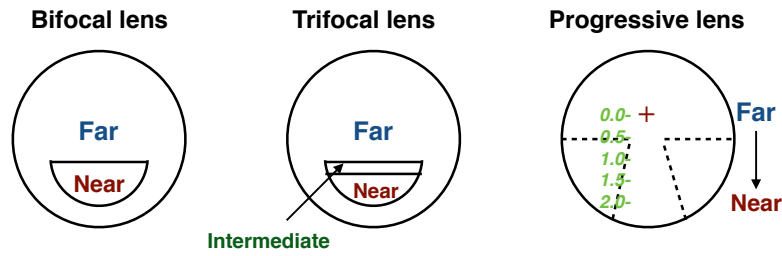
Figure 1.5: Examples of bifocal, trifocal and progressive lens designs.

1.4.2 Contact lenses

CLs have gained popularity for correcting the refractive errors of the eye. The pre-presbyopic population that is fitted with CLs has a large potential to take advantage of presbyopic solutions based on CLs corrections. The success of these solutions are based on a variety of factors, ranging from fitting techniques followed by the practitioners to age-dependent changes of the eye. Nowadays, the main strategies (Charman 2014a; Pallikaris, Plainis, and Charman 2012) followed for presbyopia compensation with CLs are:

(a) CLs for correcting the far vision and single-vision spectacles for correcting the near vision. This option is the simplest and least expensive for CL users and offers excellent far and near vision. However, for some presbyopes who are already CL users, maybe is not a satisfying solution since it increases spectacle dependence.

(b) Another option is monovision, where one eye (usually the dominant one) is fitted with a CL for correcting distance vision (some residual myopia is usually left) and the other one with a CL for correcting near vision. Monovision, first introduced by Westsmith in 1950s, is based on the brain's ability to match with the best-focused image while suppressing the blurred one (Charman 2014a; Pallikaris, Plainis, and Charman 2012). One drawback of this method is that the suppression ability varies among individuals and moreover, for some individuals this ability is absent (Alais and Blake 2005). A crucial factor for monovision success is the required amount of addition power to achieve near correction and its influence on binocular depth-of-focus (DoF). Monovision works satisfactory if the the two DoF (one for each eye) are overlapping for providing functional vision in a range of distances (Figure 1.6) (Charman 2014a; Pallikaris, Plainis, and Charman 2012). If the addition power for near correction is relatively high, then important differences can be noticed between the dioptric power

of far and near corrections leading to a dramatic stereoacuity decrease (Bennett 2008; Charman 2014a; Morgan et al. 2011). Although monovision with CLs has good success rates (between 70% and 76%) (Morgan et al. 2011), especially in early presbyopes where the addition powers are lower, it still holds a small portion in presbyopia correction with CLs. Globally, only 8% of all CLs fittings account for monovision with the highest rates reported in USA and United Kingdom (20% - 25%) (Morgan et al. 2011).

In addition to the classical monovision technique, other techniques (Charman 2014a; Bennett 2008) exist aiming to increase the DoF and optimize the visual outcome: the *extended monovision* (the non-dominant eye is fitted with a bifocal or a multifocal CL), the *modified monovision* (both eyes are fitted with bifocal or multifocal CLs), the *partial monovision* (the near addition power is reduced for enhancing the intermediate distance) and the *cross-monovision* (the non-dominant eye receives the far correction). (c) CLs with bifocal or multifocal designs (Figure 1.7) are another option for presbyopia correction. These designs aim to increase the DoF for providing satisfactory vision at different distances and reduce spectacle dependence (Charman 2014a; Pallikaris, Plainis, and Charman 2012). Bifocal CLs can have alternating, concentric or diffractive designs whereas multifocal CLs can have aspheric, concentric or diffractive-refractive designs (Charman 2014a; Toshida et al. 2008; Pallikaris, Plainis, and Charman 2012; Callina and Reynolds 2006).

1.4.2.1 Alternating Design

The alternating design in CLs is similar to that of bifocal spectacles, consisting of two distinct power segments where the distance correction is placed on the upper portion of the lens and the near correction is placed at the lower portion (Charman 2014a; Bennett 2008; Pallikaris, Plainis, and Charman 2012; Callina and Reynolds 2006). When the eye looks straight-forward receives the far correction and when it looks downwards, it receives the near correction. Similarly, as in trifocal spectacles, there are also some lenses that provide an area for intermediate vision. This design is almost exclusively applied to rigid gas permeable (GP) CLs, since for achieving near vision correction an adequate upwards movement of the lens (1.5-2.5 mm) is required (Pallikaris, Plainis, and Charman 2012). A successful fitting requires good stabilization of the lens,

regarding the cornea and the pupil, while the gaze is shifting up and down. For achieving stabilization (Figure 1.8), a ballast prism of 1.0-1.4 prism D is incorporated at the lower part of the lens (Pallikaris, Plainis, and Charman 2012). Another stabilization method used in GP lenses is truncation, where from the lower edge of the CL, a chord of 1.0-1.5 mm is removed (Toshida et al. 2008; FAAO and FIACLE 2010).
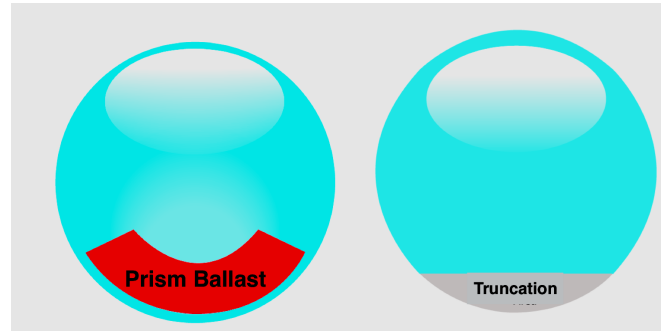

Figure 1.8: Stabilization techniques for GP bifocal CLs.

1.4.2.2 Concentric Design

Bifocal CLs with concentric designs incorporate in their optical zone two concentric rings with different refractive power for far and near (Pallikaris, Plainis, and Charman 2012; Callina and Reynolds 2006). Concentric design is also used in multifocal CLs design. In the case of multifocal CLs, the lens incorporates more than two concentric rings in order to provide multiple-distance correction. One major difference between alternating and concentric design is that the last is independent of viewing direction (Charman 2014a; Bennett 2008). The central region of the lens can be dedicated either to distance correction (center-distance), or near correction (center-near). The concentric rings for distance and near vision both partially cover the pupil. The visual function of these lenses is based on simultaneous vision, a strategy widely used in presbyopic solutions (Charman 2014a; Pallikaris, Plainis, and Charman 2012). In simultaneous vision, images corresponding to different vergences are projected on the retina at the same time. The brain has to choose among the superimposed images one in-focus image and suppress the rest out-of-focus images (Charman 2014a; Charman 2014a; Bennett 2008). If the suppression ability of the subject is not adequate, then a reduction in image-contrast, especially in high spatial frequencies, is expected due to the out-of-focus images. The proportion of light that forms the in-focus images and of the light that forms the out-of-focus images, depends on pupil size which varies depending on the luminance (Pallikaris, Plainis, and Charman 2012). Consequently, pupil size will affect the correction provided for far and near and each ring will provide an optimum

correction at a certain pupil size (Pallikaris, Plainis, and Charman 2012; Callina and Reynolds 2006). Another factor which has been found to affect the visual performance with concentric designs is the ocular higher order aberrations (HOAs) and in particular the spherical aberration (SA) (Charman 2014a; Bennett 2008).

1.4.2.3 Diffractive Design

Diffractive design provides bifocality and is found in GP and hydrogel CLs (Charman 2014a). This design is independent of pupil size and offers satisfactory far and near vision but due to high manufacturing cost is not commonly used in CLs (Pallikaris, Plainis, and Charman 2012). Its visual function is based on simultaneous vision principle and for optimal visual performance good centration and little movement on blinking are required. Diffractive design is commonly used in IOLs manufacturing and its principles will be described in detail in other section.

1.4.2.4 Aspheric design

Aspheric designs aim to provide multifocality and their visual function is based on simultaneous vision principle (Charman 2014a; Callina and Reynolds 2006; Pallikaris, Plainis, and Charman 2012). These lenses are characterized by a gradual change in the dioptric power from the center to the periphery of their optical zone. To achieve this gradual change, at least one aspheric surface (usually the back surface of the lens) is needed. The aspheric surface can result either to greater dioptric power at the center of the lens (center-near) either to greater dioptric power at its periphery (center-distance). For achieving center-near designs, the incorporation of a controlled amount of negative SA is required, whereas for center-distance designs a controlled amount of positive SA is required. Moreover, the incorporation of SA enhances DoF, which compensates for the accommodative loss (Pallikaris, Plainis, and Charman 2012).

The provided addition power can be controlled by the eccentricity value of the aspheric surface: the highest the eccentricity, the highest the addition power is. However, eccentricity and SA can deteriorate the retinal image quality, hence influencing the visual performance (Pallikaris, Plainis, and Charman 2012). For producing aspheric CLs designs with high additions values, bi-aspheric surfaces are used where the change in power is not gradual (Pallikaris, Plainis, and Charman 2012).

Aspheric designs exist both in GP and soft CLs (Pallikaris, Plainis, and Charman 2012). For achieving the optimal visual outcome, it is required good centration of the lens and relatively little movement on blinking. Other crucial factor is the pupil size that if it is too large maybe the zones of far and near vision fail to cover it adequately. This is particularly important for GP CLs since they have smaller diameter than the soft CLs and smaller optical zones (Pallikaris, Plainis, and Charman 2012). Also, with aspheric center-near designs it is likely that the effective correction for near vision will decrease due to interactions between the negative SA of the lens and the ocular SA (Pallikaris, Plainis, and Charman 2012).

1.4.3 Intraocular lenses

IOLs implantation is a surgical technique for restoring large refractive errors of the eye and restoring vision after cataract extraction. The main types of IOLs are the aphakic and the phakic models (Bellucci 2013; Charman 2014b). The aphakic IOLs are inserted into the capsular bag for replacing the cataractous crystalline lens, whereas the phakic IOLs are placed into the eye between the corneal and the crystalline lens. The first IOL implantation was performed by Sir Harold Ridley in London at 1949 (Sarwar and Modi 2014) and the implanted IOL was manufactured in polymethyl methacrylate (PMMA). Since then, several materials (e.g. PMMA, silicone, hydrophobic or hydrophilic foldable acrylic, collamer) have been used in IOLs manufacturing and several types and models exist for covering different visual demands (Bellucci 2013).

1.4.3.1 Aphakic IOLs

Aphakic IOLs can be distinguished into monofocal, bifocal, multifocal, accommodating or light adjustable IOLs. Their designs vary and can be spherical, aspherical, toric for astigmatism correction, refractive or diffractive, hybrid (combination of refractive and diffractive design) or even a combination among them.

Monofocal IOLs

Monofocal IOLs are a popular solution used over the last decades for restoring vision after cataract removal (Charman 2014b). These lenses provide excellent far vision and normally require the use of supplementary spectacles for achieving near vision. The

first monofocal IOLs had a spherical design (incorporating positive SA), whereas later models had aspheric design (incorporating negative or zero SA) (Rocha et al. 2007). This change occurred because it was found that the positive SA of spherical designs was interacting with the positive SA of the cornea, thus affecting the visual performance. However, it has been reported that although positive SA can affect the image quality, it can potentially increase the DoF (Marcos, Barbero, and Jiménez-Alfaro 2005).

Although monofocal IOLs by design provide correction only for one distance, some patients can achieve satisfactory vision for near without the need of spectacles (Tucker and Rabie 1980). This phenomenon is known as pseudoaccommodation and is related to the small pupil size that the elderly population has, small residual amounts of against-the-rule astigmatism (Datiles and Gancayco 1990), HOAs (Barbero, Marcos, and Jiménez-Alfaro 2003), adaptation to blur imagery (Pallikaris, Plainis, and Charman 2012) or even interactions between the ciliary muscle and the IOLs axial movement (Charman 2014b). Monofocal IOLs combined with monovision strategy can enhance further the DoF and optimize pseudoaccommodation in order to reduce spectacle dependence (Charman 2014b).

Multifocal IOLs

Until 1997 in Unites States the only available IOLs were of monofocal design. The first multifocal IOL that was approved by the FDA was the Array SA40N (AMO, USA) which had a refractive design (Lane et al. 2006). In general, multifocal IOLs can have refractive or diffractive design or hybrids design, with asperical surfaces and incorporate also astigmatic correction.

Refractive IOLs

Refractive IOLs consist of annular refractive zones for providing far, near and intermediate visual function based on simultaneous vision principle. The most representative IOL of this category is the rotationally symmetrical three-piece ReZoom IOL (AMO, USA) (Figure 1.9), which was approved by the FDA in 2005 and has a similar design to Array SA40N. The ReZoom IOL (Lane et al. 2006) consists of five annular refractive zones for providing satisfactory vision over a range of distances under different illumination levels, hence its performance is pupil-dependent. Zones 1,

3, and 5 are dedicated to distance corrections while zones 2 and 4 are dedicated to near corrections. Between the zones there are aspheric transitions for enhancing the intermediate vision.

Another refractive IOL, in this case characterized by non-rotational symmetry, is the Lentis Mplus IOL (Oculentis, Germany) (Figure 1.9). This IOL (also available in toric design) has an aspheric zone for distance vision combined with a 3.0 D posterior sector-shaped segment for near vision. In theory, light that hits the transition area of the segment is not reflected on the optical axis preventing in this way superposition of interference or diffraction (Gatinel and Houbrechts 2013).
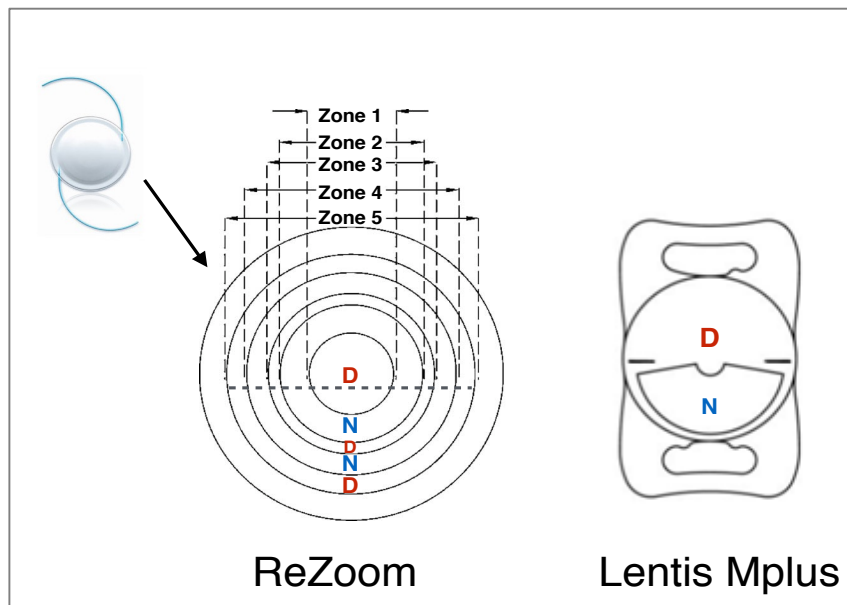
Figure 1.9: ReZoom (left) and Lentis Mplus (right) refractive IOLs. "D" reads for distance correction and "N" for near correction.

Diffractive IOLs

The concept of Fresnel zone (1820) helped to understand the fundamental properties of the light. It also set the basis for the optical principles of diffractive lenses, leading later to the creation of zone plates (Kusel and Rassow 1991; Davison and Simpson 2006). A diffractive lens is a special Fresnel lens where: a) the difference in optical path among the fragments is integer times the wavelength, b) the height of the steps is in order of the wavelength and c) the image is created due to positive interference among the waves from each point of each fragment (Kusel and Rassow 1991).

Bifocal diffractive IOLs are constructed by a diffractive surface on a refractive platform (Davison and Simpson 2006). They use the zero and first orders of diffraction to direct the light rays symmetrically (or asymmetrically) towards far and near points, respectively. In this way, two principal foci are created concentrating a great percentage of the incoming light (around 82% in total) whereas the rest of the light (around 12%) is lost in higher diffraction orders or diffused (Davison and Simpson 2006; Pallikaris, Plainis, and Charman 2012). To achieve bifocality, the surface of the lens is modified by a series of blaze-shaped annular diffractive zones (Figure 1.10) which have a phase delay at the optical path of typically half wavelength: this step is essential for creating bifocality (Davison and Simpson 2006; Pallikaris, Plainis, and Charman 2012; Charman 2014b). For example, if the phase delay is one wavelength the lens will be monofocal. The height and the width of the zones determine the energy distribution between the foci and the addition power respectively (Pallikaris, Plainis, and Charman 2012).

Diffractive IOLs are considered to be pupil independent. Changes in pupil size theoretically do not affect the image quality since every point of the diffractive surface contributes for the creation of far and near images (Nema, n.d.; Davison and Simpson 2006; Pallikaris, Plainis, and Charman 2012).

For enhancing the far vision under larger pupil sizes, some diffractive IOLs incorporate apodization (Pallikaris, Plainis, and Charman 2012; Davison and Simpson 2006; Charman 2014b) technology which aims to reduce the diffractive effect at the edge of the lens. With apodization, the height of the diffractive steps is gradually decreased from the center to the periphery of the lens so that the peripheral zones contribute more light to far vision.

The first diffractive lens was introduced in 1988 by 3M, constructed in PMMA material, and was a full-optic diffractive IOL (Davison and Simpson 2006). Although nowadays there are several diffractive IOLs, the most typical example is AcrySof ReSTOR IOL (Figure 1.9) (Charman 2014a; Lane et al. 2006; Davison and Simpson 2006). This is an apodized, diffractive-refractive, single piece IOL constructed in acrylic foldable hydrophilic material. The lens has a central area of 3.6 mm, which consists of 12 annular diffractive zones with gradually changing height placed on the anterior surface of the lens, for providing the near correction. The height of the zones decreases from 1.3 μm at the center to 0.2 μm at the periphery. The far correction is

provided by a refractive base that starts after the 3.6 mm of the central zone. Its design leads to 41% light distribution to far focus and 41% light distribution to the near focus. A problem with bifocal diffractive IOLs is the poor intermediate vision they provide. By superimposing two diffractive profiles, trifocal IOLs for enhancing intermediate vision are also available (Gatinel et al. 2011). An example of trifocal design is the apodized FineVision IOL (PhysIOL, Belgium) with two diffractive structures, which are adjusted to provide two power additions aiming for near (+3.0 D) and intermediate (+1.75 D) correction (Charman 2014b; Madrid-Costa et al. 2013).

AcrySof ReSTOR   FineVision
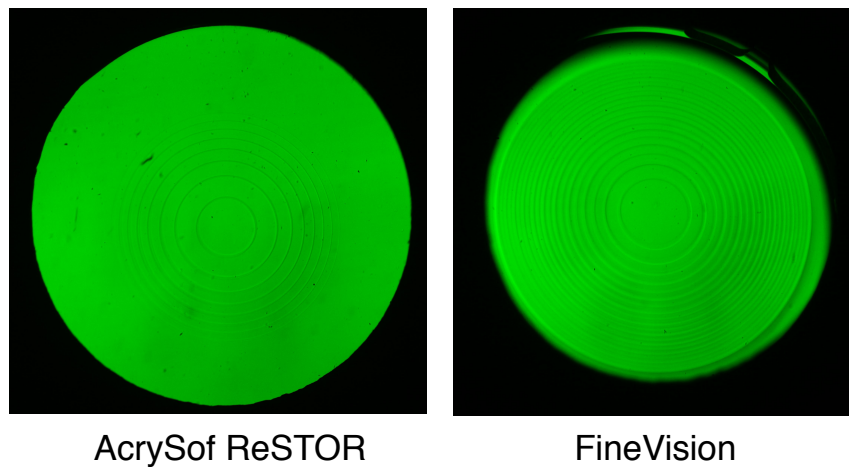
Figure 1.11: Apodized diffractive IOLs. The images were taken by a slit-lamp and the help of a digital camera. Bifocal AcrySof ReSTOR and trifocal FineVision IOLs.

Issues with diffractive and refractive IOLs

Diffractive and refractive IOLs enhance more the DoF in the pseudophakic eye comparing to monofocal IOLs and also provide better near visual acuity (VA) (Charman 2014b). Nevertheless, since they present more complex designs, they are associated with undesirable visual artifacts. The most common problem, in both refractive and diffractive designs, is the decrease in photopic contrast sensitivity (CS) when compared to monofocal IOLs (Charman 2014a; Żelichowska et al. 2008; Montés-Micó et al. 2004). This loss is mainly noticeable at high and medium spatial frequencies and is a result of multiple foci existence, which creates superimposed images (Charman 2014b; Montés-Micó et al. 2004; Barisić et al. 2008) and the loss of light energy in diffractive designs. Under dim illumination where the out-of-focus images are more

noticeable, patients implanted with diffractive or refractive IOLs complain for haloes or other glare effects that, in some cases, can be the reason for IOL's explantation (Charman 2014b; Barisić et al. 2008; Woodward, Randleman, and Stulting 2009). Patients implanted with refractive IOLs have reported more severe haloes and glare phenomena under dim light conditions compared to patients implanted with diffractive IOLs (Barisić et al. 2008; Lane et al. 2006). Nevertheless, there is some evidence that at least near CS with a refractive multifocal IOL can be improved over time (Montés-Micó and Alió 2003). Other unwanted effect related with multifocal IOLs is straylight. The literature reports decreased straylight levels in pseudophakic eyes implanted with multifocal IOLs that are comparable to monofocal IOLs' straylight levels (Cerviño et al. 2008; Hofmann et al. 2009; de Vries et al. 2008). However, in some pseudophakic eyes increased straylight levels have been reported (Łabuz, Reus, and van den Berg 2015). That could be an issue related to the designs of these lenses (i.e. existence of intermediate zones, increased SA due to aspheric transitions between the zones), but since little information exists about their designs, further investigation is needed (Charman 2014b). For reducing halos and glare effects at night, bilateral implantation of the same IOL type has been proposed (Olson et al. 2005).

Regarding VA with multifocal IOLs, satisfying results in both far uncorrected and corrected VA have been reported with refractive and diffractive IOLs designs under photopic conditions (Żelichowska et al. 2008; Barisić et al. 2008; Kohnen et al. 2009; Kohnen et al. 2006; Alfonso et al. 2007; Yamauchi et al. 2013; Lane et al. 2006). Intermediate VA has been found to be better with refractive IOLs compared to bifocal diffractive IOLs (Lane et al. 2006; Barisić et al. 2008; Żelichowska et al. 2008). As for uncorrected near VA, both refractive and diffractive IOLs provide satisfactory correction under photopic conditions (Lane et al. 2006; Żelichowska et al. 2008; Alió, Plaza-Puche, et al. 2011) but diffractive IOLs achieve slightly better performance, increasing that way spectacle independence (Barisić et al. 2008).

The pupil size is particularly important on the visual performance with refractive intraocular lenses, where the geometry of the lens has a key role. For example, even though the asymmetrical Lentis Mplus IOL shows higher pupil independence (Figure 1.12), there have been observed elevated coma aberration values after implantation with this IOL (Alió, Piñero, et al. 2011).

Other factors that can influence the visual performance with intraocular lenses are decentration and tilt (Yang, Chung, and Baek 2000; Montés-Micó et al. 2012;

Woodward, Randleman, and Stulting 2009), especially in the case of aspheric IOLs (D. A. Atchison 1991) or in the existence of ocular pathology like closed-angle glaucoma (Hayashi et al. 1999), rotation in toric (Garzón et al. 2015; Veselá et al. 2016) or in non-rotationally symmetrical designs, history of previous refractive surgery (Aramberri 2003) as well as patient's expectations (Barisić et al. 2008).

Figure 1.12: Ratio of the IOLs' area dedicated to far and near focus, as a function of pupil diameter. The two multifocal IOLs shown are the refractive rotationally symmetric Array and the asymmetric Lentis Mplus. (Charman 2014b)

Accommodating IOLs

Accommodating IOLs (AOLs) are another option for restoring vision after cataract extraction. These lenses aim to mimic the eye's natural crystalline lens and restore accommodative ability by taking advantage of the ciliary muscle's strength and the elasticity of the capsular bag (Charman 2014b; D. F. Chang 2008; Tomás-Juan and Murueta-Goyena Larrañaga 2015; Glasser 2008). Although further investigation is ongoing for AIOLs, they can be distinguished into two categories: single-optic AOLs and dual-optic AOLs.

Single-optic AOLs (e.g. Crystalens, Bausch and Lomb in Figure 1.13) theoretically work by forward movement of the lens optic (D. F. Chang 2008) caused by constriction of the ciliary muscle or by pressure from the vitreous body (D. F. Chang 2008; Tomás-Juan and Murueta-Goyena Larrañaga 2015; Glasser 2008). The provided accommodative power depends on both the amounts of the forward axial movement of the lens and its dioptric power (Charman 2014b; D. F. Chang 2008). Studies where the accommodative effectiveness of single-optics AOLs was compared with the pseudoaccommodation caused by monofocal IOLs reported no differences (Dogru et al. 2005; Wolffsohn et al. 2006; Beiko 2013; Alió, Piñero, et al. 2011). The accommodative gain with single-optic IOLs was found to be around 0.5 D. Moreover, Wolffsohn et al. found that this accommodative effect is decreasing with time resulting in deterioration of near VA. Compared to refractive multifocal IOLs, they have been reported to offer poorer near VA (Claoué 2004).

Dual-optic AOLs is the next generation of single-optic AOLs and their function is based on Helmhotz's theory (Tomás-Juan and Murueta-Goyena Larrañaga 2015; D. F. Chang 2008; Glasser 2008). The most typical example of this category is the Synchrony IOL (AMO) (Figure 1.13). This lens is composed by an anterior high convergent optic and posterior divergent optic. In the unaccommodated state the distance between the optics is minimized due to capsular tension whereas in near vision the capsular tension is decreased (due to ciliary muscle's constriction) and the anterior optic is moving forward (D. F. Chang 2008; Tomás-Juan and Murueta-Goyena Larrañaga 2015). Compared to monofocal IOLs and single-optic AOLs, dual-optic AOLs offer better through-focus performance (Alió et al. 2012; Ossma et al. 2007). However, their accommodative effectiveness is uncertain (Charman 2014b). Another problem that has been observed for the dual-optic AOLs is the separation of the optics for near vision performance (Alió et al. 2012; Ossma et al. 2007).

Crystalens   **Synchrony**
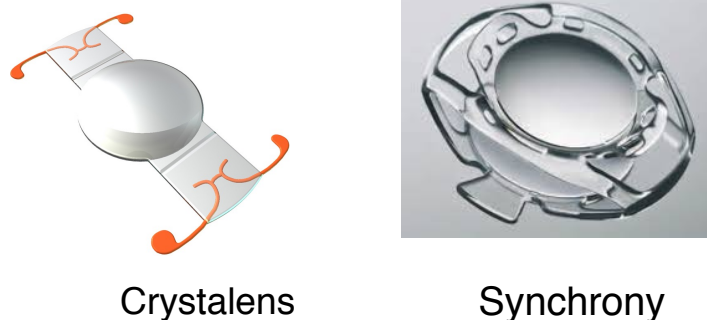
Figure 1.13: AOLs illustrations. Single-optic Crystalens and dual-optic Synchrony.

Extended DoF IOLs

Extended or elongated DoF IOLs (EDoF) aim to provide better near visual performance than monofocal IOLs and AOLs and to reduce also the haloes and glare phenomena that have been observed with refractive and diffractive IOLs ("Looking Deep at Extended Depth-of-Focus IOLs" 2016). The most typical example of EDoF is the Tecnis Symphony (AMO), which aims to enhance the DoF by using: a) diffractive optics for elongating the focus and for compensating chromatic aberration, and b) the incorporation of negative SA for compensating the positive SA of the cornea and increasing the DoF ("TECNIS® - Safer, Sharper Vision after Cataract Surgery" 2016).

Tecnis Symphony is available in Europe since 2014 and it has been stated that it can provide 2.5 D of usable DoF ("SYMFONY IOL | Eurotimes.org" 2016).

After Tecnis Symphony implantation in patients, clinical studies (Auffarth 2015; Cochener 2015; Marques 2015; Mesa 2015; Kaymak et al. 2016) so far have stated satisfactory outcomes including: high patient's satisfaction, high spectacle independence, excellent far and intermediate uncorrected visual acuity, functional near vision, good reading ability for normal print size and reduced optical artifacts. Other EDoF IOLs are the the small-aperture IC-8 IOL (AcuFocus, USA) that uses pinhole optics for enhancing DoF and the refractive Mini Well IOL (SIFI Medtech, Catania, Italy).

Light adjustable IOLs

Monofocal and multifocal IOLs along with AOLs and EDoFs may lead postoperatively to significant residual errors (Charman 2014b; Gale et al. 2009). A light adjustable IOL (Calhoun Vision, USA) can be an alternative method of aphakic IOL implantation for avoiding additional refractive surgery (Charman 2014b; Brierley 2013; Villegas, Alcon, et al. 2014; Sáles and Manche 2015; Ford, Werner, and Mamalis 2014). The macromers of this cross-linked, silicone matrix lens can change their shape when they are exposed to spatially profile ultraviolet light (355 nm), changing the lens refractive power (Figure 1.14). A three-week period is normally required to stabilize the refraction effect and permanently fix ("locked-in") the refractive power of the lens (Brierley 2013; Charman 2014b; Ford, Werner, and Mamalis 2014; von Mohrenfels et al. 2010).

In presbyopia treatment, the light adjustable IOL can be involved in monovision correction (implanted to the non-dominant eye) or in customized aspheric treatments (e.g. for adjusting the proper amount of SA that a patient needs to improve the DoF) (Villegas, Alcón, et al. 2014). However, for improving the performance of these lenses further investigation is required.

1.4.3.2 Phakic IOLs

Phakic IOLs can be implanted either to the anterior either to the posterior chamber of the eye and are a good solution for high or moderate myopia treatment and astigmatism (Espandar, Meyer, and Moshirfar 2008; D. H. Chang and Davis 2006; Rosen and Gore 1998). However, these lenses are related to endothelial cell loss due to the decrease of

the anterior chamber length with aging and cataract formation (Charman 2014b; Espandar, Meyer, and Moshirfar 2008; D. H. Chang and Davis 2006). One advantage they have over the aphakic IOLs is that they can be removed from the eye with less implications (Lovisolo and Reinstein 2005).

1.4.3.3 Other techniques for presbyopia treatment

In addition to CLs and IOLs, a variety of other techniques exist for correcting presbyopia, but with less success up to date:

- Scleral procedures such as anterior ciliary sclerotomy (Ito et al. 2005; Malyugin, Antonian, and Lohman 2008) or laser scleral microincisions with Er:YAG laser (Torricelli et al. 2012) for increasing accommodative amplitude.

- Efforts for regeneration of the crystalline lens by stem cells (Barbosa-Sabanero et al. 2012), crystalline lens refiling (Nishi et al. 2009), lens photodisruption with femtosecond lasers (Reggiani Mello and Krueger 2011).

 - Corneal refractive surgery techniques for creating a pseudoaccommodative cornea

(i.e. presbyLASIK) (Telandro 2004; Pallikaris and Panagopoulou 2015; Alió et al. 2009).

1.5 Adaptive optics technology in vision science

The introduction of adaptive optics (AO) technology into the visual optics field launched the beginning of a new era in vision science. Initially, AO optics systems were used in astronomy (Babcock 1953) and later Liang et al., applied this technology for improving visual performance in terms of CS and VA (J. Liang, Williams, and Miller 1997). AO technology gave the opportunity to measure and manipulate the real-time wavefront errors of the human eye and to explore the visual benefit of correcting HOAs (Roorda 2011; Artal et al. 2010; Yoon and Williams 2002; David A. Atchison et al. 2009; J. Liang, Williams, and Miller 1997). Moreover, AO technology has been applied to study the accommodative response (Fernández and Artal 2005; Gambra et al. 2009; Chin, Hampson, and Mallen 2009; Roorda 2011) and to develop new solutions for presbyopia correction (Roorda 2011; Manzanera et al. 2007; Piers et al. 2004; Dai 2008) by, for instance, manipulating the SA in a way that can extend the DoF to the

minimal cost in retinal image quality (Piers et al. 2004). In addition to testing visual function, AO technology is also applied in retinal imaging for assessing the density of the photoreceptor cells, the spacing between the photoreceptors, the mosaic regularity, the pigment epithelium, the fiber layer of the optic nerve, the lamina cribrosa and the retinal vessels (Roorda 2011; Miller and Meshel 1993; Kozak 2014; Putnam et al. 2005; Rossi and Roorda 2010).

1.5.1 AO system description

An ideal wavefront is planar or spherical, but inhomogeneous media, where the light passes through, can cause distortions to the shape of the wavefront (Tyson 2015). These distortions, known as aberrations, can lead to severe degradation in image quality. The human eye suffers from heterogeneities due to imperfections of its own media (e.g. corneal irregularities, tear film irregularities) (A. and Doble 2012). The role of an AO system in vision is to enhance the visual performance by manipulating the shape of the wavefront (i.e. the aberrations) of the human eye.

The key components of an AO system are a wavefront sensor and an adaptive element that can change its shape when a control signal is applied. Such an adaptive element is a membrane deformable mirror (DM), which aims to apply the inverse of the wavefront's deformation for optimizing the image quality (Friese et al. 2007; Roddier 1988). For achieving this, the DM has on its surface several electrodes (actuators) where different voltage values can be applied for changing the membrane's shape (Friese et al. 2007; Perreault et al. 2002; Roddier 1988; Fernández and Artal 2003). Commercially available DM are usually made of silicon materials (Friese et al. 2007; Perreault et al. 2002). The number of actuators that a DM has on its surface defines the precision and the efficacy of the mirror (Dalimier and Dainty 2005). Other types of DM used in AO systems include bimorph DMs, micro-eletromechanical (MEM) devices, liquid crystal spatial light modulators (LQ-SLM) or magnetic DMs (Dalimier and Dainty 2005; Manzanera et al. 2007; Tyson 2015).

The wavefront sensor aims to detect and characterize the shape of the incoming wavefront. A typical wavefront sensor such as a Sack-Hartmann (Junzhong Liang et al. 1994; Prieto et al. 2000; Junzhong Liang and Williams 1997) consists of a microlens array of the same focal length. Each lenset focuses the light on a photon sensor (e.g. a CCD array). In the case of an ideal wavefront each lenset will focus the light at the center of a pixel grid on the photon sensor. Each grid is associated with a different

lenset of the array (Figure 1.15). In the case of a distorted wavefront the focus of each lenset will deviate from the center of the grid. The analysis of these deviations characterizes the shape of the wavefront (Jiang and Li 1990).

Briefly, in an AO system for testing the visual function works in a close-loop (E. J. Fernández, Iglesias, and Artal 2001). A light source (normally a laser beam) is used for assessing the wavefront of the human eye. The light passes through the system's optics to end up at the wavefront sensor. The wavefront sensor will determine the shape of the wavefront and then commands will be calculated for the deformable mirror to alter its shape and reconstruct the distorted wavefront (Figure 1.16).

1.5.2 AO technology for presbyopia treatment

AO technology can be a useful tool for presbyopia treatment for providing customized solutions and new designs for presbyopia. This can potentially increase patient's satisfaction by overcoming some of the problems with CLs and IOLs (Hong and Choi 2010; Artal et al. 2010).

As previously mentioned, the aim of multifocal CLs and IOLs is to enhance the DoF of the presbyopic eye. Several studies have reported that HOAs are not static but change in magnitude with accommodation (D. A. Atchison et al. 1995; Ninomiya et al. 2002; Cheng et al. 2004; Lopez-Gil and Fernandez-Sanchez 2010). Correcting HOAs with AO technology can optimize the visual performance but decreases DoF (Nio et al. 2002). However, with AO technology the effect of HOAs in DoF can be restricted to a point that is not a problem for visual performance. AO technology is not only used for correcting aberrations but also for inducing aberrations. This means that aberrations like the SA can be induced in controlled amounts for exploring the optical benefits and for increasing the DoF to the minimum cost in image quality. Werner et al., combined vision testing with induction of SA by an AO system and they conclude that small amounts of positive SA (0.06 μm) can enhance DoF (J. S. Werner et al. 2009). Moreover, it has been found that the introduction of positive and negative SA can shift and expand the DoF in contrast to trefoil and coma which do not have such effects (Rocha et al. 2009). Yi et al., also found that combinations of 4th and 6th order SA with different signs can enhance DoF (Yi, Robert Iskander, and Collins 2011).

AO technology has been used also for testing the visual performance of IOLs prior implantation by correcting a subject's aberrations and inducing the aberrations of the lens (Pérez-Vives, Montés-Micó, et al. 2013; Pérez-Vives, Ferrer-Blasco, et al. 2013). Another application of AO technology is to guide the patient in the selection of the presbyopic solution that is more suitable for optimizing the visual outcome. A binocular adaptive optics visual simulator (Fernández, Prieto, and Artal 2009) can be used for manipulating the eyes' aberrations simultaneously providing independent corrections for each eye. With this technology HOAs can be manipulated and optical designs (i.e. diffractive or refractive) can be simulated offering an important correcting advantage for the patient (Manzanera et al. 2007).

Chapter 2

A method to assess the in vitro optical quality of presbyopic solutions based on the axial modulation transfer function

2. A method to assess the in vitro optical quality of presbyopic solutions based on the axial modulation transfer function

2.1 Introduction

For assessing the imaging performance of an optical system it is necessary to set image quality criteria. These criteria are commonly defined by metrics derived by the Wavefront Error (WFE), the Point Spread Function (PSF) and the Optical Transfer Function (OTF) (Marsack, Thibos, and Applegate 2004; Thibos et al. 2004; Chen et al. 2005). Nevertheless, one single metric is not adequate to characterize entirely the quality of an optical system(Brigantic et al. 1997). In previous studies focusing on human eye (Marsack, Thibos, and Applegate 2004; Thibos et al. 2004; Chen et al. 2005), a plethora of 31 metrics have been classified into two types: pupil plane metrics (based on WFE) and image plane metrics (based on PSF and OTF). The correlation between these metrics in terms of optical quality and visual performance has been examined. Albeit some metrics proved to be better predictors than others, still there is not an ideal combination among them (Marsack, Thibos, and Applegate 2004; Thibos et al. 2004).

In order to characterize the optical quality of an IOL, Modulation Transfer Function (MTF), the modulus of the Fourier Transform of the PSF, is the established scientific method widely used("ISO 11979-2:2014 - Ophthalmic Implants -- Intraocular Lenses -- Part 2: Optical Properties and Test Methods" 2016; "ISO 11979-9:2006 - Ophthalmic Implants -- Intraocular Lenses -- Part 9: Multifocal Intraocular Lenses" 2016). By definition, MTF expresses the variation of image contrast with spatial frequency for an object with 100% contrast (Thibos et al. 2004; "ISO 11979-9:2006 - Ophthalmic Implants -- Intraocular Lenses -- Part 9: Multifocal Intraocular Lenses" 2016), or, in other words, how minutely a lens forms the image of an object. The MTF of an aberration-free optical system limited only by diffraction is called the diffraction limited MTF. The radial average MTF (rMTF) is the one-dimensional curve obtained by averaging the two-dimensional MTF across all directions. The majority of measuring devices dedicated to MTF estimation calculate the rMTF obtained in sagittal and tangential directions (Wells and Dobbins 2012).

Based on MTF, several metrics(Chen et al. 2005; "ISO 11979-9:2006 - Ophthalmic Implants -- Intraocular Lenses -- Part 9: Multifocal Intraocular Lenses" 2016; Boreman 2001; Holladay et al. 2002; Adelina Felipe et al. 2010) have been developed. These metrics include the average modulation (the mean value of modulation at a range of frequencies), the area under the MTF, the Strehl Ratio by means of MTF (the ratio of the area under the actual MTF curve with the area under diffraction limited MTF curve) and the cut-off spatial frequency (the spatial frequency at which the modulation reaches or approaches to zero), among others.

An important factor that characterizes the optical performance of an IOL and of any optical system is the tolerance to defocus. This is particularly important for the MIOLs that have different foci. The measurement of MTF at a particular spatial frequency as a function of defocus is known as the Through Focus MTF (TF-MTF) (Boreman 2001). A variety of studies (Holladay et al. 2002; Adelina Felipe et al. 2010; Artigas et al. 2009; Gatinel and Houbrechts 2013a; David Madrid-Costa et al. 2013; Remón et al. 2012; Montés-Micó et al. 2013; D. Madrid-Costa et al. 2014; Carson et al. 2014; Ruiz-Alcocer et al. 2014) has presented the TF-MTF in order to determine the optical quality of IOLs.

Another method to describe the performance of an optical system is the axial MTF (aMTF). The aMTF of an optical system is formed by successive MTF curves at different focal points across a range of spatial frequencies (Remón et al. 2012). Therefore, the successive MTF curves create a surface that contains the information from the MTF and the TF-MTF. Thus, the aMTF describes the image-forming capability of an optical system as a function of defocus and spatial frequency.

In this paper we propose a metric, the Volume Under the aMTF (VUaMTF), for assessing the in vitro optical quality of rotationally symmetric optical elements. VUaMTF focuses on calculating the volume under the surface defined by aMTF at a certain maximum spatial frequency and within defined defocus intervals. Therefore, it aims to provide information about the optical tolerance to defocus and the optical quality at different spatial frequencies.

2.2 Methodology
2.2.1 Volume under the axial MTF scheme

Figure 2.1, a, represents the aMTF of a bifocal IOL in a selected range of spatial frequencies (0 c/degree to 36 c/degree). The color bar that accompanies the figure indicates the MTF values. Far (0 D) and near foci (3.75 D) are clearly distinct in the graph: the far focus yields higher MTF values whereas the near focus yields lower MTF values. As the spatial frequency increases, the MTF values drop for both foci.

Figures 2.1, b, and 2.1, C, show in which way Figure 2.1, a, can be interpreted in order to obtain optical quality information. Figure 2.1, b, shows that a horizontal profile (line 1) corresponds to the MTF of the far focus in the spectrum of spatial frequencies. On the other hand, Figure 2.1, c, shows that a vertical profile (line 2) can give information about the MTF in every IOL's plane at a particular spatial frequency. In this case, the 15 c/degree spatial frequency was selected, which nearly corresponds to an optotype for 20/40 equivalent visual acuity in white light (Carson et al. 2014). The aforementioned profile corresponds to the TF-MTF, which is related to the defocus tolerance.
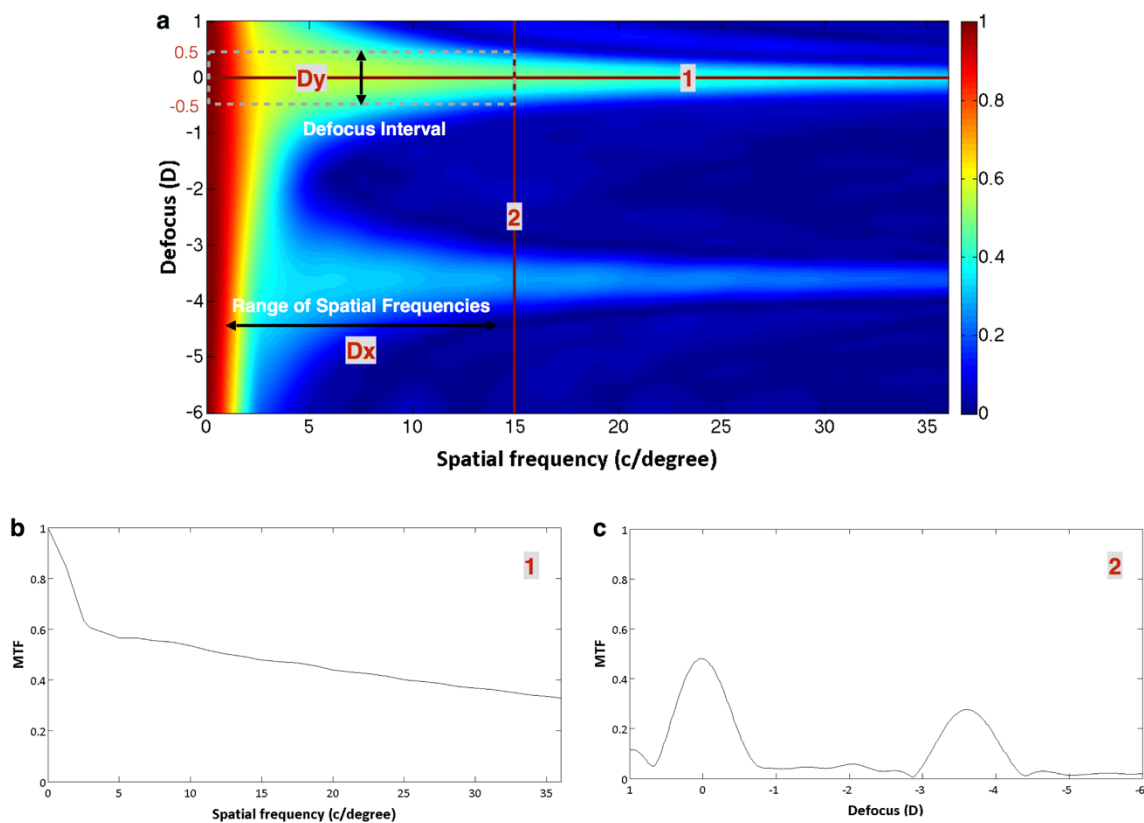
Figure 2.1: a: Shows the axial MTF of the bifocal lens as a function of spatial frequency and defocus. The color bar indicates the values of the MTF. Dx and Dy represent examples of intervals of spatial frequency and defocus, respectively, that will be used to compute the VUaMTF. **b**: is the MTF of the far focus as a function of spatial frequency, and it corresponds to a horizontal profile (line 1) in a. **c:** is the TF-MTF at 15 c/degree and it corresponds to a vertical profile (line 2) in a.

The calculation of the volume can be performed by setting intervals that isolate areas of interest. For example, the foci of a MIOL aim to provide good vision at different vergences and thus it is important to evaluate their optical quality. By setting intervals at the dioptric range of the lens, it is feasible to isolate and calculate the volume under the main foci. Figure 1(a) shows how the far focus of the bifocal lens can be isolated when a defocus interval (1 D) is set at a selected range of spatial frequencies (0 c/degree to 15 c/degree). Then, VUaMTF can be applied to calculate the volume within the defocus interval (Dy) for that range of spatial frequencies (Dx).

The selection of the intervals relies on the characteristics of the optical system (MIOLs in this case) that someone wants to examine. The different intervals can be set in both axes of the aMTF. Different ranges at the spatial frequency axis can be related directly to different visual acuities (e.g. 30 c/degree corresponds to an approximate VA of 20/20). Moreover, several intervals can be selected in the defocus axis and compare the optical performance at different vergences.

2.2.2 MIOLs Designs

In order to test the capability of VUaMTF, aMTF data from two MIOLs were used. According to the manufacturer, both MIOLs were aspherical with a diffractive design. One lens was bifocal and the other trifocal. Both lenses have optical diameter of 6.0 mm, overall diameter of 11.0 mm, incorporate ultraviolet blockers and are available in the market from 0 D to +32 D (in steps of 0.5 D).

The bifocal lens was the AT LISA 809M IOL (Carl Zeiss Meditec AG, Jena, Germany), with a +3.75 D near addition and nominal power of +20 D. The lens' optics distributes the light energy asymmetrically, directing 65% to the far focus and 35% to the near focus. The trifocal lens was the AT LISA tri 839MP IOL (Carl Zeiss Meditec AG, Jena, Germany), with a +3.33 D near addition and +1.66 D intermediate addition within the central 4.34 mm optical zone of the lens. The nominal power was +19 D. For pupils up to 4.34 mm the light energy distribution is 50% for the far focus, 20% for intermediate focus, and 30% for the near focus. Beyond the 4.34 mm central zone, the lens is solely devoted to far and near vision.

29

2.2.3 Optical Quality Assessment

The optical quality of the MIOLs was assessed with the PMTF instrument (Lambda-X, Nivelles, Belgium) using an aberration-free artificial cornea. The device complies with the ISO standards 11979-2("ISO 11979-2:2014 - Ophthalmic Implants - - Intraocular Lenses -- Part 2: Optical Properties and Test Methods" 2016) and 11979-9("ISO 11979-9:2006 - Ophthalmic Implants -- Intraocular Lenses -- Part 9: Multifocal Intraocular Lenses" 2016) for MTF measurements based on eye models. The device has a light source that emits at 546 nm. For different apertures it performs MTF measurements until the maximum spatial frequency, depending on aperture size. To measure the MTF of an IOL, the device uses a transilluminated pattern-edge, which is always located at an infinite distance. The instrument scans the image plane by moving the microscope at different focal points within the IOL's optical zone to collect best-focus planes. When joining all the scans together, the result is the aMTF. Both MIOLs' optical quality was assessed at a well-centered position. The lenses were immersed in saline solution (refractive index: 1.335) and then were placed in a wet cell.

2.3 Results

Figure 2.2 shows the aMTF of the bifocal 2.2, a, and the trifocal lens 2.2, b, for a range of spatial frequencies up to 36 c/degree. In these graphs, the optical behavior of the two different MIOLs designs can be observed at different focal planes and spatial frequencies. The color bar that accompanies the figure indicates the MTF values. Both lenses provide a focus for far (0 D) and near vision. As it can be observed from the graphs, the far focus of the bifocal IOL yields better optical quality than the far focus of the trifocal. In addition, the trifocal lens provides a distinct focus for the intermediate vision (around -2 D).
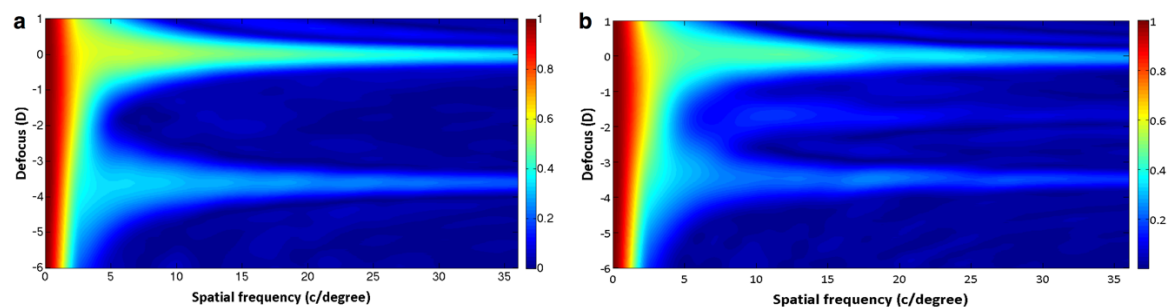

Figure 2.2: aMTF representation of the bifocal (a) and the trifocal (b) lens up to 36 c/degree spatial frequency, for a 3mm aperture size. The color bar indicates the MTF values. In the graphs are clearly

distinct the far and the near focus of the bifocal and the far, the near and the intermediate focus of the trifocal lens.

The behavior of the main foci of MIOLs under different defocus conditions and spatial frequencies is a very important factor to evaluate. For that reason, several defocus intervals (0.50 D, 0.75 D and 1 D) were set at the main foci of the lenses. These intervals allowed for quality evaluation in terms of defocus tolerance. Moreover, within the same defocus intervals we evaluated the optical quality that the foci yielded for different maximum spatial frequencies (7.5 c/degree, 15 c/degree, 30 c/degree).
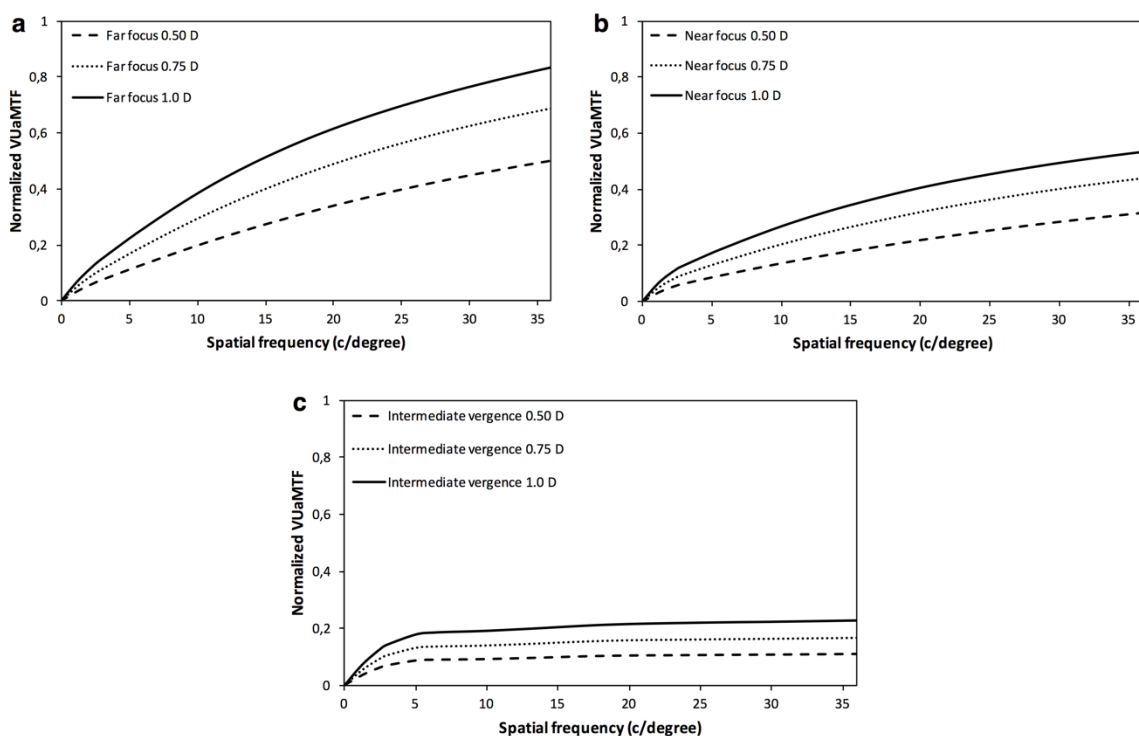
Figure 2.3. VUaMTF for different defocus intervals (0.5 D, 0.75 D, 1 D), for the far (a) and the near foci (b) of the bifocal lens at different spatial frequencies (up to 36 c/degree). (c) shows the VUaMTF for the intermediate vergence to allow a comparison with the intermediate focus of the trifocal lens. The values are normalized by the VUaMTF of a monofocal IOL in a 1 D defocus interval for 30 c/degree spatial frequency.

Figures 2.3 and 2.4 show the variation in volume's values within different defocus intervals in a range of spatial frequencies until 36 c/degree, when VUaMTF was applied to evaluate the main foci of the IOLs under study. The calculations were done for the different selected defocus maximum spatial frequency intervals mentioned above. The values have been normalized by the VUaMTF of a monofocal IOL in an interval of 1

31

D for a maximum spatial frequency of 30 c/degree that corresponds to a 20/20 Snellen visual acuity. Figure 2.3 represents the VUaMTF values for the far 2.3, a, and the near focus of the bifocal IOL 2.3, b. In addition, figure 2.3, c, represents the VUaMTF values for the intermediate vergence of the lens to allow a comparison with the intermediate focus of the trifocal lens. Figure 2.4 shows the VUaMTF values for the far 2.4, a, the near 2.4, b, and the intermediate 2.4, c, focus of the trifocal IOL. Due to its design that allows a distribution of light in three foci, the trifocal IOL provides notable results in terms of optical quality for intermediate vergences.
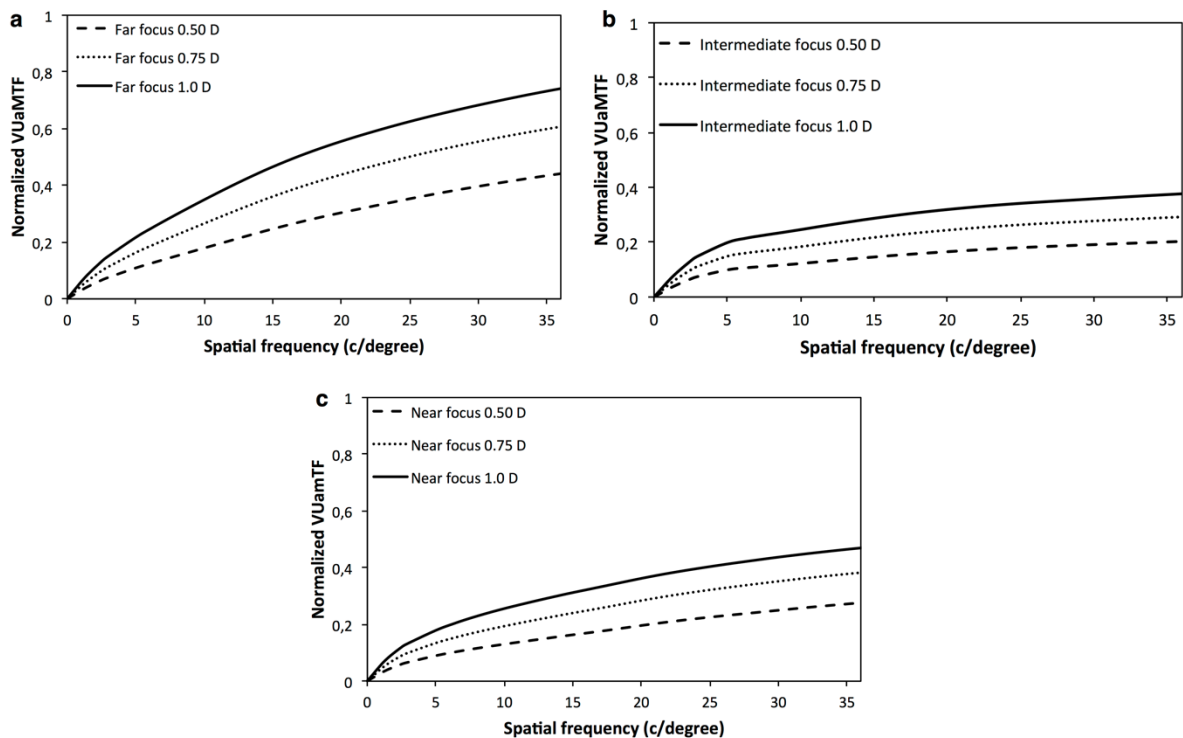
Figure 2.4. VUaMTF for different defocus intervals (0.5 D, 0.75 D, 1 D), for the far (a), the near (b) and the intermediate (c) foci of the trifocal lens at different frequencies (up to 30 c/degree). The values are normalized by the VUaMTF of a monofocal IOL in a 1 D defocus interval for 36 c/degree spatial frequency.

In addition to Figures 2.3 and 2.4, Table 2.1 shows the numeric values of VUaMTF (normalized by the VUaMTF values of the monofocal IOL) for the different maximum spatial frequency and defocus intervals of the far, the near focus of the bifocal lens and for the intermediate vergence. Subsequently, Table 2.2 shows the VUaMTF values for the far, the near and the intermediate focus of the trifocal IOL.

2.4 Discussion

An ideal optical system exists only under ideal conditions that are not possible to reach in the real world. When the performance of an optical system is evaluated, a number of factors that influence its function must be taken into account (e.g. diffraction, relative illumination, etc.). The existence of metrics based on WFE, PSF and OTF (Marsack, Thibos, and Applegate 2004; Thibos et al. 2004; Chen et al. 2005) is essential to estimate an optical system's performance and to ensure that the system will be able to meet its objectives.

Normalized VUaMTF values of the Bifocal IOL									
Frequency (c/degree)	Far focus			Intermediate Focus			Near Focus		
	Defocus Interval (D)			Defocus Interval (D)			Defocus Interval (D)		
	0.5	0.75	1	0.5	0.75	1	0.5	0.75	1
7.5	0.14	0.21	0.27	0..09	0.14	0.19	0.10	0.15	0.20
15	0.24	0.36	0.46	0.10	0.15	0.20	0.16	0.24	0.31
30	0.4	0.56	0.68	0.11	0.16	0.22	0.25	0.36	0.44

Table 2.1. VUaMTF values for the far, the near focus of the bifocal lens and for the intermediate vergence, at different maximum spatial frequencies and defocus intervals. The values are normalized by the values of a monofocal IOL in a 1 D defocus interval for 30 c/degree spatial frequency.

Normalized VUaMTF values of the Trifocal IOL									
Frequency (c/degree)	Far focus			Intermediate Focus			Near Focus		
	Defocus Interval (D)			Defocus Interval (D)			Defocus Interval (D)		
	0.5	0.75	1	0.5	0.75	1	0.5	0.75	1
7.5	0.13	0.19	0.25	0.10	0.15	0.20	0.10	0.15	0.20
15	0.22	0.32	0.42	0.13	0.19	0.26	0.15	0.21	0.28
30	0.35	0.49	0.61	0.17	0.25	0.32	0.22	0.31	0.39

Table 2.2. VUaMTF values for the far, the intermediate and the near focus of the trifocal lens, at different maximum spatial frequencies and defocus intervals. The values are normalized by the values of a monofocal IOL in a 1 D defocus interval for 30 c/degree spatial frequency.

Metrics based on the MTF are commonly used for evaluating in vitro the optical quality of IOLs. In previous studies (David Madrid-Costa et al. 2013; Montés-Micó et al. 2013; D. Madrid-Costa et al. 2014; Carson et al. 2014; Ruiz-Alcocer et al. 2014), the average MTF is a widely used metric. The average MTF is the value of modulation averaged in the range of spatial frequencies from 0 c/mm to 100 c/mm. This metric has been proved (Gatinel and Houbrechts 2013b; Montés-Micó et al. 2013) to be proportional to the area under the MTF (Artigas et al. 2009; Remón et al. 2012), which has been used in other studies (Pons et al. 1998) for optical quality assessment. In some studies, the TF-MTF (Gatinel and Houbrechts 2013a; Ruiz-Alcocer et al. 2014) has been used to assess the defocus tolerance of IOLs. In the aforementioned studies, the MTF and the TF-MTF

of IOLs have been presented as separate entities to describe the optical quality of the lenses.

In this paper, a metric for assessing in vitro the optical quality of optical elements has been proposed. The VUaMTF is based on VUaMTF by setting different defocus and spatial frequency intervals. VUaMTF depends on three parameters (dimensions): the defocus interval, the range of spatial frequencies and the optical performance (MTF values).

A similar method, the Defocus Transfer Function (DTF) that is a 2 dimensional function which can be useful to characterize optical systems with circularly symmetric pupils, was previously proposed (FitzGerrell, Dowski, and Cathey 1997). The function analyzes the effect of defocus on the OTF taking advantage of the symmetry of the circularly symmetric pupil. DTF was proposed as a theoritical scheme for assesing the optical quality of IOLs. Most comercially available devices for assesing the optical quality of IOLs comply with the ISO standards (ISO 11979-2 and ISO 11979-9) and calculate the MTF curves through an intensity profile that does not give information about the PSF or the optical transfer function.

Calculations with VUaMTF can be performed at any desirable vergence. In the case of MIOLs, the key is their main foci, which aim to provide optimum optical quality at different distances. To evaluate the optical quality of the MIOLs in this study, it was essential to set up intervals on their dioptric range to define the main foci. The number of intervals that were used for each lens relied on their design. The number of intervals that were used for each IOL relied on their design. For the bifocal IOL, 2 intervals were used; for the trifocal, 3 were used.

The VUaMTF can be used to compare the optical quality of different IOLs in vitro, showing their optical performance and highlighting the advantages and disadvantages between different IOL types. For example, a comparison between 2 IOLs can be performed keeping the defocus interval fixed and varying the spatial frequency interval or vice versa. Thus, the IOL with the greatest VUaMTF value will be the IOL with the best optical performance. In this study, the far focus of the bifocal IOL always yielded higher values than the far focus of the trifocal IOL. This difference is a result of the different IOL designs. As described in the methodology, the optics of the bifocal IOL allow for higher distribution of light in the far focus compared with the trifocal IOL.

De Gracia et al. (de Gracia, Dorronsoro, and Marcos 2013) studied the effect of different multifocal phase designs on the optical quality and the depth of focus of presbyopic corrections. This theoretical approach outlined that the optimal number of foci (or phase zones) for these designs lied between three and four. According to their results, trifocals solutions yielded better optical quality and larger depth of focus than the bifocal ones. This increase in depth of focus can be observed in Figure 2.3, c, and Figure 2.4, c, where it is obvious that the trifocal lens provides better vision for intermediate distances. The VUaMTF could be also used to evaluate these theoretical designs before they are considered for manufacturing.

The range of the intervals with VUaMTF is adjustable. This is an advantage that can be used to test the defocus tolerance of the lens (by increasing or decreasing the defocus interval) and also to estimate the optical quality that it provides at different spatial frequencies. Figures 2.3 and 2.4 and Tables 2.1 and 2.2, demonstrate that VUaMTF gave the possibility of optical quality assessment of both MIOLs in several spatial frequencies and defocus intervals. This can be related to different visual tasks (depending on the spatial frequency) and to the defocus tolerance (different distances at which the tasks are performed).

A possible limitation of using the VUaMTF is that it summarizes the information about the three parameters to one numeric value. For example, an IOL with high MTF values but with a pronounced MTF decay can have the same VUaMTF value as an IOL that yields lower MTF value but shows a mild decay. This limitation comes from the volume calculation (eg, the area under the MTF for a limited maximum frequency).

Another limitation of the VUaMTF is that it can be applied only for rotationally symmetric lenses, tested in a well-centered position to avoid phenomena such as decentration and tilt. The position of an IOL changes after it is implanted. This is a result of contracting forces generated mainly by the capsular's bag shrinkage, which leads to postoperative axial movement of the IOL (Petternel et al. 2004). Therefore, phenomena such as decentration, tilt and rotation (the latter is the most important factor in optical quality degradation in cases of toric IOLs (A. Felipe et al. 2012)) can occur. These phenomena can have an important impact on the visual outcome (e.g. decreased depth of focus or out of focus images) if the amounts are larger than the acceptable limits (Baumeister, Bühren, and Kohnen 2009). Under such conditions, the rotational symmetry of an IOL, like the ones evaluated in this study, is lost. In such cases, more complex methods should be used to adequately assess the effects.

Clinicians should always treat the results of in vitro MTF evaluations of IOLs carefully. A previous study (Alió et al. 2011), found that an increment of a certain amount in MTF does not correspond to an increment of the same amount in the contrast sensitivity function (CSF) of the human eye. By using an adaptive optic system, the authors corrected the higher order aberrations (HOAs) and the astigmatism of four subjects. Afterwards, they compared the optical improvement by means of MTF with the visual improvement by means of CSF before and after correcting HOAs and astigmatism. Although the improved MTF was close to the diffraction limited case, the improvement in CSF was moderate. The authors justified this fact by the limitation that the neural CSF imposes.

In summary, the VUaMTF is a metric that aims to objectively compare optical solutions in an easy and fast way by the use of a commercial bench and some basic calculations. In this paper we chose to focus on MIOLs due to the fact that nowadays they make a headway progress (Alió et al. 2011; Pepose, Wang, and Altmann 2012) in the field of refractive surgery. VUaMTF can provide valuable information about the optical tolerance to defocus and the optical quality of a MIOL allowing also for comparisons between different lenses. Nevertheless, VUaMTF is not restricted only to MIOLs: it can be applied to evaluate the optical quality of every IOL and furthermore, can be generalized to determine the optical quality of any rotationally symmetric optical system by means of aMTF.

Chapter 3
Assessing the optical quality of commercially available intraocular lenses by means of modulation transfer function and straylight

3. Assessing the optical quality of commercially available intraocular lenses by means of modulation transfer function and straylight

3.1 Introduction

Implantation of IOLs is a common procedure for restoring vision after cataract extraction. Monofocal IOLs can provide excellent vision at one distance, normally the far, but additional spectacles or CLs are required for achieving satisfactory vision at other distances such as the near (Charman 2014). It has been reported that some patients implanted with monofocal IOLs can achieve adequate near vision without the need of extra correction (Tucker and Rabie 1980; Datiles and Gancayco 1990; Barbero, Marcos, and Jiménez-Alfaro 2003). This condition is known as pseudoaccommodation (Charman 2014; Pallikaris, Plainis, and Charman 2012) but is not the case for every patient.

Diffractive multifocal IOLs have gained popularity during the past decades over monofocal IOLs in cataract surgery. These IOLs use the principles of the diffraction to distribute the light energy between two principal foci dedicated for far and near vision (Davison and Simpson 2006; Pallikaris, Plainis, and Charman 2012), aiming to provide spectacle independence (Davison and Simpson 2006; Pallikaris, Plainis, and Charman 2012; Charman 2014). Trifocal designs are also available for enhancing intermediate vision (Gatinel et al. 2011). Although diffractive IOLs are considered to be pupil-independent (Davison and Simpson 2006; Pallikaris, Plainis, and Charman 2012), the pupil size determines the amount of energy that reaches each foci, hence, it influences the retinal image contrast. In vitro studies for the evaluation the optical quality of diffractive IOLs by means of MTF, have been performed (Papadatou et al. 2016; Gatinel and Houbrechts 2013; Montés-Micó et al. 2013; Ruiz-Alcocer et al. 2014; David Madrid-Costa et al. 2013; Domínguez-Vicent et al. 2015). All the studies reported decreased MTF values as the pupil size and the spatial frequency increased.

Diffractive IOLs have been associated with photopic phenomena such as glare and haloes experienced by patients under dim illumination (Barisić et al. 2008; Lane et al. 2006). These phenomena can have a severe impact on the visual performance and can be the cause for IOLs' extraction (Charman 2014; Barisić et al. 2008; Woodward, Randleman, and Stulting 2009).

One source of these photopic phenomena is straylight. Straylight is the result of scattered light due to imperfections in the eye's optical media that creates a veil of straylight over the retina (Van Den Berg et al. 2007) which can result to disability glare (Vos 1984). In visual performance, straylight is perceived as light radiation around bright sources. Although straylight remains stable until the fifth decade of life, it is doubled at 65 years and tripled at 77 years for eyes with good VA (Van Den Berg et al. 2007). This increase leads to visual artifacts such as disability glare in night driving and hindrance from low sun during the daytime (T. J. T. P. van den Berg et al. 2009; Van Den Berg et al. 2007). In the presence of cataract these disturbances are much more pronounced (T. J. van den Berg 1995; Van Den Berg et al. 2007; Elliott and Bullimore 1993).

Straylight level of pseudophakic eyes has been found to be comparable or even better than straylight level of the young normal eye (Lapid-Gortzak et al. 2014). Previous studies have evaluated the effect of IOL's design in postoperative straylight level in eyes implanted with monofocal and diffractive multifocal IOLs (Hofmann et al. 2009; Cerviño et al. 2008; Wilkins et al. 2013; Peng et al. 2012; de Vries et al. 2008). Some studies reported no significant differences in straylight level between eyes implanted with monofocal and multifocal diffractive IOLs (Hofmann et al. 2009; Cerviño et al. 2008; Wilkins et al. 2013) whereas other studies reported higher straylight level in eyes implanted with multifocal diffractive IOLs (de Vries et al. 2008; Peng et al. 2012).

This study aimed to assess the in vitro optical quality of commercially available diffractive multifocal IOLs by means of MTF and straylight when compared to a monofocal IOL. The MTF was measured using the PMTF instrument (Lambda-X, Nivelles, Belgium). Several studies have used this instrument to report optical quality of IOLs in the past (Papadatou et al. 2016; Gatinel and Houbrechts 2013; Ruiz-Alcocer et al. 2014; Montés-Micó et al. 2013; D. Madrid-Costa et al. 2015). For measuring the straylight, the C-Quant device (Oculus Optikgeräte GmbH, Germany) (Franssen, Coppens, and van den Berg 2006; Coppens, Franssen, and van den Berg 2006) including a modification for performing objective in vitro straylight measurements in IOLs (Łabuz et al. 2015), was used.

3.2 Methods

3.2.1 IOLs designs

Four posterior-chamber IOLs with different designs were used in this study; a hydrophobic acrylic single-piece aspheric monofocal IOL, a hydrophilic acrylic (with hydrophobic surface) single-piece aspheric diffractive bifocal IOL, a hydrophilic acrylic single-piece aspheric diffractive trifocal IOL and a hydrophobic acrylic single-piece aspheric diffractive EDoF IOL. All the samples were fresh, free of glistenings or other defects.

3.2.2 Optical quality assessment by means of MTF

The optical quality of the IOLs by means of MTF was assessed using the PMTF device with an aberration-free artificial cornea (see in Chapter 2). Each lens was evaluated at 3 mm and at 4.5 mm aperture sizes. The IOLs were immersed in a cell filled with saline solution (refractive index: 1.335) and then were placed at the translation table of the instrument. For each lens, three consecutive measurements were performed at each aperture size for collecting data of their axial MTF.

The VUaMTF metric (Papadatou et al. 2016) was used as the tool for evaluating the optical performance of the IOLs (see also in Chapter 1). The optical quality of each IOL at each pupil size was assessed in 0.5 D intervals at seven focal points (0 D, -1.5 D, -2 D, -2.5 D, -3 D, -3.5 D, -4 D) for two different spatial frequencies; 15 cpd and 30 cpd which correspond nearly to 0.5 and 1.0 VA respectively (Papadatou et al. 2016).

3.2.3 Optical quality assessment by means of straylight

The C-Quant straylight meter is a commercial apparatus for measuring ocular straylight based on the psychophysical compensation comparison method. Details about the functioning of the device can be found elsewhere (Franssen, Coppens, and van den Berg 2006; Coppens, Franssen, and van den Berg 2006). Briefly (Figure 4.1), an annular straylight source (5° to 10° radius) flickers at various intensities in black and white. The device has an annular central test field (3.3° radius) divided in two halves. One half flickers in counter-phase modulating light and perceives also light from the straylight source, whereas the other half perceives light from the straylight source. In clinical practice, the task of the patient is to choose which half flickers stronger each time. At a certain moment both halves appear to be equal and the patient has to guess.

Recently, a modification for the C-Quant was proposed for performing in-vitro measurements in IOLs without the eye's scattering interference (Łabuz et al. 2015). The key points of this methodology (Figure 3.1) are a diaphragm which prevents the rays of the straylight source to reach the observer's eye and a lens (L_2) which projects a magnified image of the test field at the observer's eye.

For the measurements, each IOL was inserted in a cell filled with saline solution (refractive index: 1.335) and then was placed at the instrument (see in Figure 4.1). The measurements were performed for a fixed pupil of 5.5 mm. Two experienced observers performed the measurements in order to demonstrate that the measurements were independent of the straylight of the own eye.

First, the straylight of the wet cell without the IOL was measured and then the measurement was repeated with the IOL inside.
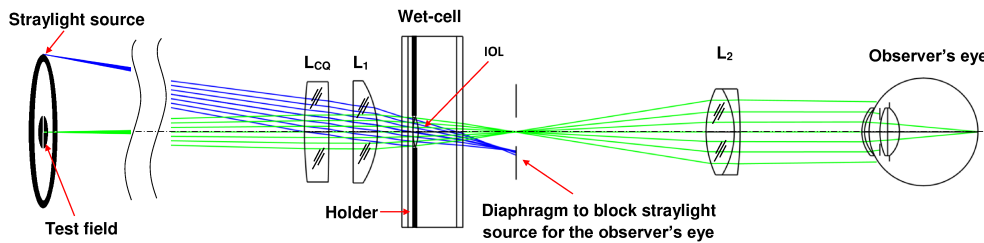

Figure 3.1: Modification of the C-Quant for measuring in-vitro straylight of IOLs (not scale). L_{CQ} is a fixed lens for seeing the straylight source and the test field. A plano-convex lens (L_1) is placed 5 mm behind L_{CQ}. The wet cell with the IOL is placed at 5 mm behind L_1. The diaphragm acts as a field-stop blocks the rays from the straylight source and L_2 projects a magnified image of the test field to the observer's eye. (From Łabuz et al. 2015)

The straylight value of each IOL was calculated by subtracting the two measurements according to the the equation:

$$\log(S_{IOL}) = \log (10^{\log (S_{set-up+IOL})} - 10^{\log (S_{set-up})}) \quad (4.1)$$

The values log(Sset-up + IOL) and log(Sset-up) were obtained with the C-Quant device and represent the log(s) values of the wet cell with and without IOL respectively. The straylight levels of the IOLs in this study are presented in linear scale by means of the straylight parameter (s) (T. J. van den Berg 1995), which is given in degrees per steradian (deg^2/sr).

3.3 Results

3.3.1 Axial MTF

For showing the overall optical behavior of the IOLs, the representation of the axial MTF was chosen. Figure 3.2 represents the axial MTFs of each IOL under study. The x-axis of each graph stands for the spatial frequency (up to 36 cpd) and the y-axis stands for the vergence (in D). The right column shows the results for the 3 mm pupil size whereas the left column shows the results for the 4.5 mm pupil size. The color bar indicates MTF's values.

Figure 3.2, a, shows the axial MTF of the bifocal IOL. The lens has two distinct foci located approximately at 0 D and at -3.75 D, for far and near vision respectively. At 4.5 mm, the axial MTF of both foci attenuates especially at higher spatial frequencies.

Figure 3.2, b, represents the results for the trifocal IOL. The lens shows two main foci for far and near vision located approximately at 0 D and at -3.5 D respectively. Around -1.75 D, a focus for intermediate vision is distinct but with lower MTF values. At 4.5 mm the optical quality of each focus, the near and the intermediate focus in particular, attenuate as the spatial frequency increases.

Figure 3.2, c, illustrates the axial MTF of the EDoF IOL. The monochromatic axial MTF of this lens reveals two main foci located close to each other (approximately at 0 D and -1.75 D). At 4.5 mm the optical quality of the foci attenuates, starting from the low spatial frequencies.

Finally, Figure 3.2, d, shows the axial MTF of the monofocal IOL. The lens shows one focus with high optical density which is located at 0 D. At 4.5 mm the optical quality of the focus decreases as the spatial frequency increases.

3.3.2 Volume under the axial MTF

Figure 3.3 shows the results of VUaMTF metric at different vergences (0 D, -1.5 D, -2 D, -2.5 D, -3 D, -3.5 D, and -4 D) calculated within an interval of 0.5 D.

Figure 3.3, a, presents the VUaMTF curves of all the IOLs at 3 mm at 30 cpd of spatial frequency. The values are normalized by the VUaMTF value of the monofocal IOL at 0 D for the 3 mm pupil. The monofocal IOL yields the best value at 0 D and then its curve drops rapidly. The bifocal and the trifocal IOL have similar curves. The bifocal shows slightly better values at 0 D and between -3 D and -4 D. The curve of the EDoF IOL reaches its highest level between -1.5 D to -2.5 D and then decreases.
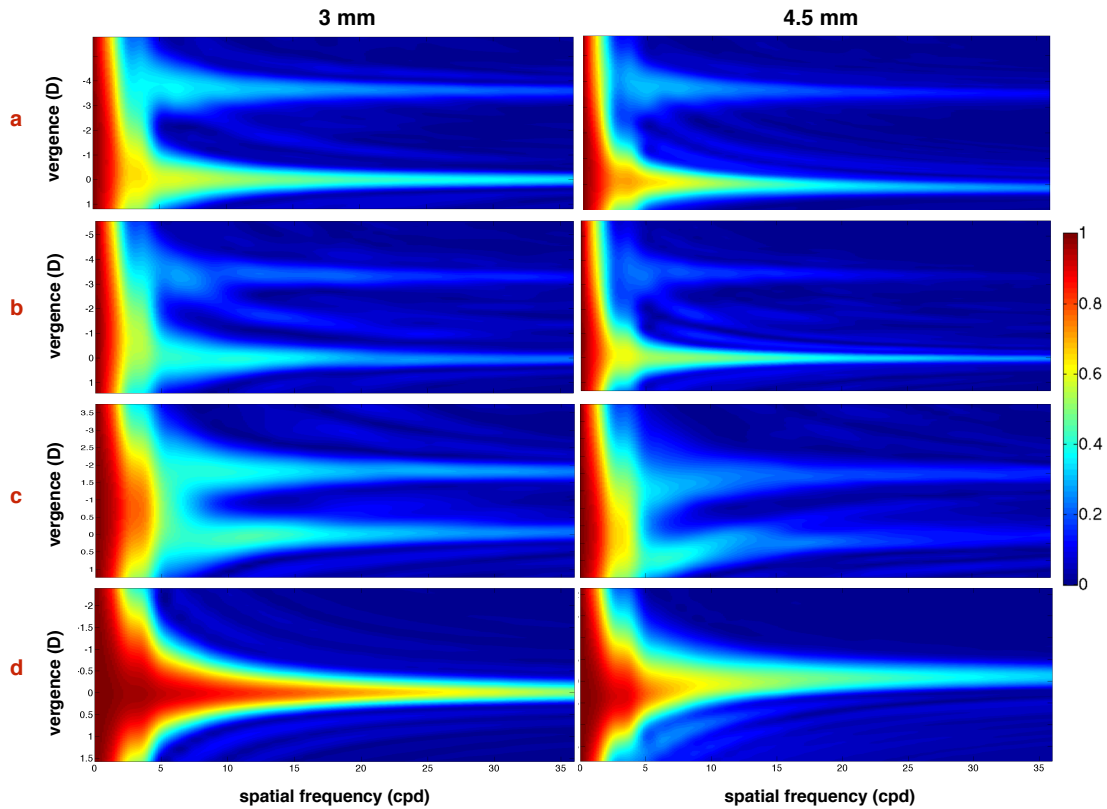
Figure 3.2: Representation of the axial MTFs of the IOLs at 3 mm and 4.5 mm pupil sizes. The color bar indicates the values of the MTF. The a, b, c, d notations indicate the bifocal, the trifocal, the EDoF and the monofocal IOL respectively.

Figure 3.3: VUaMTF curves of the IOLs at 3 mm and 4.5 mm pupil, at 30 cpd and 15 cpd. The values in a and c are normalized by the by the VUaMTF value of the monofocal IOL in 0 D at 30 cpd, for the 3 mm pupil whereas in b and d the values are normalized by the same value at 4.5 mm.

45

Figure 3.3, b, presents the VUaMTF curves at 4.5 mm for a spatial frequency of 15 cpd. The values are normalized by the VU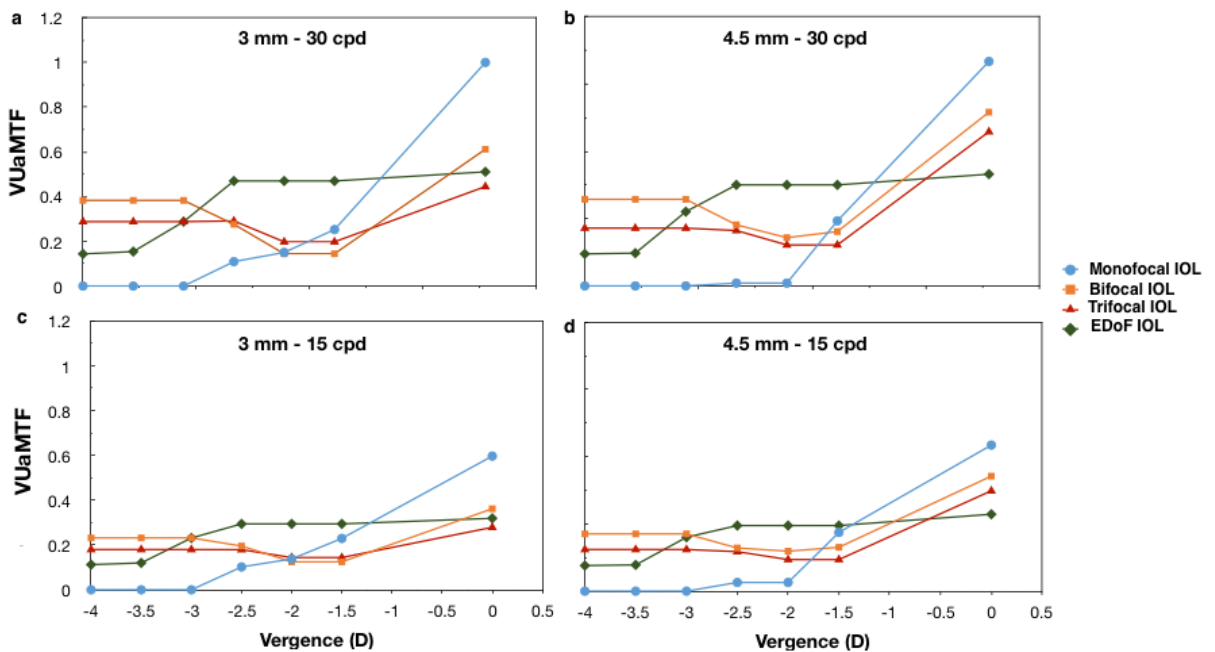aMTF value of the monofocal IOL at 0 D for the 4.5 mm pupil. The curve of the monofocal IOL falls to zero after -1.5 D of vergence. The bifocal and the trifocal IOL have their peak value at 0 D while the rest of their curves differs slightly from 3 mm. The curve of the EDoF IOL practically does not experience any change with pupil size.

Figures 3.3, c and d, show the VUaMTF curves of the IOLs for 15 cpd, at 3 mm and 4.5 mm respectively. The values in Figure 4.3, c, are normalized by the VUaMTF value of the monofocal IOL at 0 D for the 3 mm pupil at 30 cpd whereas in Figure 3.3, d, are normalized by the same value for the 4.5 mm. The trends of the curves are similar with figures a, and b, with the VUaMTF values decreasing.

3.3.2 Straylight results

Figure 3.4 shows the results of the straylight measurements expressed by the s parameter. For comparison purposes, the continuous line in the graph shows the mean straylight level of the young normal crystalline lens (van der Mooren et al. 2011) and the dashed line represents the mean straylight level of the young normal eye (Van Den Berg et al. 2007). The individual straylight values of the two observers along with the mean values of straylight are presented for each IOL type. The error bars at the observers' series show the individual standard deviation (SD) of the observer between the two measurements. The error bars at the IOLs' series show the SD between the two observers. All the values (mean ± SD) are summarized in table 3.1.

All the IOLs show very low straylight values when comparing to the straylight level of the young crystalline lens. Moreover, the straylight of the aspheric monofocal IOL was found to be in the same level with the ones of the diffractive IOLs.

	$s \pm SD$ (deg^2/sr)		
IOL Type	Observer 1	Observer 2	Average value
Monofocal	0.49 ± 0.44	0.59 ± 0.15	0.54 ± 0.30
Bifocal	0.68 ± 0.02	0.87 ± 0.32	0.77 ± 0.27
Trifocal	1.00 ± 0.17	1.12 ± 0.18	1.06 ± 0.26
EDoF	0.66 ± 0.11	0.35 ± 0.06	0.50 ± 0.13

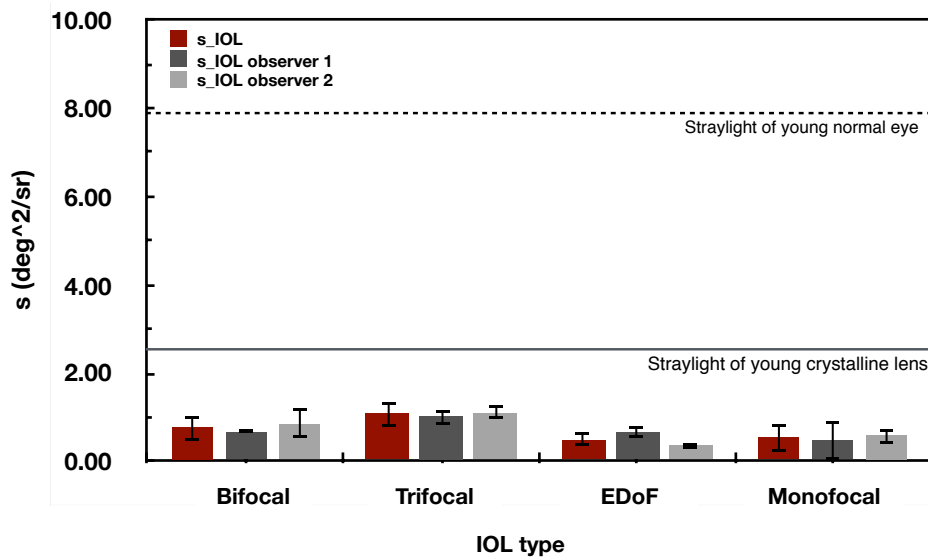**Table 3.1:** Straylight values of the IOLs under study.

Figure 3.4: Straylight values of the IOLs under study expressed by the s parameter. The dashed line indicates the straylight level of the young normal eye whereas the continuous line shows the straylight level of the young normal crystalline lens. The error bars at the observers' series show the individual SD of the observer. The error bars at the IOLs' series show the SD between the two observers.

3.4 Discussion

The aim of the present study was to evaluate in vitro the optical quality of four different IOLs types. For this purpose, we used different apparatuses for assessing the axial MTF and the straylight of the IOLs.

The axial MTF gave information about the optical quality of the IOLs regarding the vergence and the spatial frequency. In Figure 3.2, it can be observed that the optical quality of the monofocal IOL was superior at 0 D (far focus) for both pupil sizes compared to the optical quality of the diffractive IOLs at that same vergence. In addition to the far focus, the diffractive IOLs had other foci located at different vergences as a result of their diffractive designs (Davison and Simpson 2006). These findings are in accordance with previous studies were in vitro optical quality of IOLs was presented (Gatinel and Houbrechts 2013; David Madrid-Costa et al. 2013; Montés-Micó et al. 2013; Papadatou et al. 2016). Moreover, in Figure 3.2 it can be observed that the quality of the IOLs was affected by the pupil size and decayed as spatial frequency increased, more notably, in the case of the EDoF IOL.

The value of the addition power of a diffractive IOL sets the distance between its foci and determines the vergences where the IOL offers its optimum correction. In Figure 3.3, it can be observed that only the EDoF IOL seems able to provide correction in an

extended range where the optical quality remains almost unchangeable. This extended range for the EDoF starts from 0 D and continues up to -2.5 D. In that same interval the bifocal and the trifocal IOL had notably lower VUaMTF values compared to the EDoF IOL. Interestingly, although the axial MTF of the trifocal IOL (Figure 3.2, b) showed a peak around -1.75 D (intermediate focus), the VUaMTF values of the trifocal IOL were very close to the ones of the bifocal IOL at this vergence. On the other hand, the optical quality of the EDoF decreased after the -2.5 D of vergence in contrast with the optical quality of both the bifocal and the trifocal IOLs; both showed increased optical quality from -3 D and up to -4 D. Summarizing, this results support evidence that the EDoF provides better visual quality at an extended range of distances (up to 40 cm) whereas the bifocal and the trifocal IOLs seem to provide better visual quality at far and near (0.3 cm to 0.25 cm) distances. Nevertheless, it should be kept in mind that these measurements were done assuming perfect centration of the lens, under monochromatic light and without evaluating the effect of corneal aberrations. Once these lenses are implanted in the eye, the visual outcomes can be different than the ones predicted here. In vitro straylight measurements of IOLs are useful since they show the *per se* straylight levels of the IOLs without the influence of the eye's optical media (e.g. cornea, vitreous body, retina) (van der Mooren et al. 2011). Figure 3.4 shows the straylight values of the IOLs expressed by the s parameter. In the present study, the s values of the IOLs were found to be too low when compared to the s values of the young normal eye. These findings are in line with a previous study where the authors reported straylight values of different IOLs (Langeslag et al. 2014). In the same study the authors concluded that hydrophobic IOLs tend to have lower straylight values than hydrophilic IOLs for scatter angles more than 3° which was the case for the in vitro measurements of our study. In Figure 3.4, it can be observed that the bifocal and the trifocal IOLs, which are of hydrophilic material, showed relatively higher straylight values than the monofocal and the EDoF IOLs, which are of hydrophobic material. In our study we also found the straylight levels of the diffractive IOLs to be similar to the one of the monofocal IOL. Given both the range of angle that we measured the straylight and the material of the IOL, this finding is in accordance with the study of Langeslag et al, (Langeslag et al. 2014) but in contrast to a recent study (Pennos et al. 2016) where in vitro straylight values of monofocal and diffractive IOLs were measured with an instrument based on the principle of double-pass optical integration (Ginis et al. 2014). The methodology we used in our study for measuring in vitro straylight of IOLs has been validated before

(Łabuz et al. 2015) and our findings support evidence that diffractive effects *per se* of these IOLs are not expected to elevate the postoperative straylight level in the pseudophakic eye as some studies have indicated (de Vries et al. 2008; Peng et al. 2012).

In vitro study of explanted IOLs can shed some light on why some patients have elevated straylight levels. Glistenings in the IOL's bulk, caused for example by temperature fluctuations in the eye, can have an impact on the optical performance of the IOL (van der Mooren, Franssen, and Piers 2013). Van der Mooren et al, (van der Mooren et al. 2015) reported two cases where the multifocal Acrysof Restor SN60AD3 IOL (Alcon Laboratories, Inc.) was explanted and replaced with a monofocal IOL after the patients complained for blurry or hazy vision. Careful examination of the explanted IOLs revealed severe or moderate glistenings to the IOLs' bulk. The authors concluded that straylight caused by multifocal IOLs with glistenings may have an impact on visual performance. Another study (Labuz et al. 2016) tried to determine the size of the particles that are predominant in light scattering in explanted IOLs. These IOLs were found to have increased straylight values after they were explanted. The spectral analysis from these IOLs indicated the existence of particles larger than wavelength, which indicates MIE scattering (Das et al. 2013), but further analysis of the particles' origins is essential.

In conclusion, this study offers a dual evaluation of the optical quality of IOLs by determining the axial MTF and the straylight of commercially available diffractive IOLs versus a monofocal IOL. Although no connection can be established between straylight and MTF measurements, the present study is useful to extend our knowledge about the optical properties of the IOLs.

Chapter 4

Objective assessment of the effect of pupil size upon the power distribution of multifocal contact lenses

4. Objective assessement of the effect of pupil size upon the power distribution of multifocal contact lenses

4.1 Introduction

It is well-known that the accommodative ability of the human eye decreases almost linearly with age, starting as early as in puberty (Charman 2014a; Duane 1908; Kragha 1986). The consequences of this irreversible loss normally start to be noticeable in near vision between 40 and 45 years of age, where the amplitude of accommodation usually falls below 3 D (Charman 2014a) and the eye is said to be presbyopic.

The field of presbyopia is one of the most challenging in vision science since the increase in life expectancy will result in most of the people spending almost half of their lives being presbyopes. Several methods (Charman 2014a; Charman 2014b) have been proposed to compensate presbyopia symptoms, including spectacles for near vision, contact lenses (CLs) and surgical approaches. Although spectacle for enhancing near vision is the most common solution, social and practical reasons drive early presbyopes to seek alternative correcting methods (Charman 2014a; Charman 2014b). The contact lens industry has been evolving during the past decades aiming to offer presbyopic solutions that will decrease spectacle independence (Charman 2014a; Pallikaris, Plainis, and Charman 2012; Morgan et al. 2011). Nowadays, the majority of the commercially available multifocal CLs are based on the concept of simultaneous vision. These lenses incorporate multiple refractive powers and controlled amounts of negative or positive spherical aberration (Charman 2014a; Pallikaris, Plainis, and Charman 2012; Plainis et al. 2013).This design leads to simultaneous projection of both in-focus and out-of-focus images onto the retina. The success of simultaneous vision relies on the visual system's capability to suppress the blurred out-of-focus images. Although out-of-focus images can reduce the contrast of the in-focus image, spherical aberration offers a greater Depth of Focus (DoF) and therefore, the deterioration of the in-focus image is not apparent within a certain vergence range (Bennett 2008; Montés-Micó et al. 2011; Plainis, Atchison, and Charman 2013).

Despite the availability of various designs of simultaneous vision multifocal CLs, the proportion of presbyopic population that uses them is still relatively low (Morgan et al. 2011). Several studies (Plainis, Atchison, and Charman 2013; Bakaraju et al. 2012; García-Lázaro et al. 2015) have evaluated the visual and optical performance of multifocal CLs and the factors they may have an influence on it. These factors range

from the fitting technique applied by practitioners to optical factors and age-dependent ocular changes (e.g. as pupil size). Previous studies have revealed that the refractive power provided by simultaneous-vision multifocal CLs as a function of beam vergence is strongly dependent on pupil size (Plainis, Atchison, and Charman 2013; Cardona and López 2016; Madrid-Costa et al. 2015; Vasudevan, Flores, and Gaib 2014). Since pupil size decreases with age and varies significantly across individuals (Kragha 1986; Montés-Micó et al. 2014) this parameter, along with the specific lens design, should both be taken into account. Previous studies (Plainis, Atchison, and Charman 2013; Madrid-Costa et al. 2015; Montés-Micó et al. 2014; Wagner et al. 2015) have assessed the power profiles of commercially available simultaneous-vision multifocal CLs so as to gain a better understanding of the lens designs and optical performance.

In this context, we aimed to evaluate in vitro three models of simultaneous-vision multifocal CLs having different designs and addition powers in order to analyze the effect of pupil size upon their power profile, in an effort to explain the rationale behind their optical performance.

4.2 Methods
4.2.1 Multifocal Contact Lenses Designs

Three different types of CLs for presbyopia correction were included in this study (see Table 4.1): The first contact lens is the Acuvue Oasys for Presbyopia (Vistakon, Inc., Jacksonville, FL, USA), which is a multifocal contact lens consisting of concentric aspheric zones alternating between distance and near vision. The lens' central zone is dedicated to far vision (this center-distance design will be referred to as CD). The lens is available with powers ranging from +6 D to −9 D in steps of 0.25 D and it comes with three different addition powers (commonly known as "add"): namely, "Low", "Mid" and "High".

The second contact lens, the Fusion 1 day Presbyo (Safilens S.R.L., Staranzano, GO, Italy), has an optical design that aims to provide clear vision at any distance according to the manufacturer. The lens has a continuous power gradient and center-near (CN) design. The lens is available with powers ranging from +6 D to -6 D in steps of 0.25 D and from -6 to -10 D, and from +6 D to +8 D, in steps of 0.5 D.

Finally, the third contact is the Biofinity multifocal (Cooper Vision, Fairport, NY, USA), available in both CN and CD designs for monovision correction. The power

range of this lens goes from +6 D to -6 D in steps of 0.25 D and from -6 to -10 D in steps of 0.5 D. It comes with addition powers of +1 D, +1.5 D, +2 D and +2.5 D. For the purpose of this study only CD models were evaluated.

Parameter	Acuvue Oasys for presbyopia	Fusion 1 day Presbyo	Biofinity multifocal
Replacement	2 weeks	Daily	Monthly
Water Content (%)	38	60	48
Refractive index	1.42	1.42	1.4
BOZR (mm)	8.4	8.6	8.6
TD (mm)	14.3	14.1	14
DK/t (@ -3 D)	147	29	142
tc (mm) (@ -3 D)	0.07	0.07	0.09
Lens Design	Concentric rings	Afocal	Asymmetric D and N
Manufacturer	Johnson & Johnson	Safilens	Cooper Vision

Table 4.1: technical specifications of the contact lenses under study. **BOZR:** back optic zone radius; **TD:** total diameter; **DK/t:** oxygen transmissibility; **tc:** central thickness

4.2.2 Instrument

To obtain the power profiles of the multifocal CLs, the NIMO TR1504 (LAMBDA-X, Nivelles, Belgium) was used. This instrument is based on a quantitative deflectometry technique that combines the Schlieren principle with a phase-shifting method. The phase-shifting Schlieren technique makes it possible to calculate the lens' power distribution by measuring the light deviation. Previous studies (Bakaraju et al. 2012; Montés-Micó et al. 2014; Belda-Salmerón et al. 2013; Domínguez-Vicent et al. 2015), have described in detail the functioning of this device. According to a previous study (Joannes et al. 2010), the phase-shifting Schlieren technique prevails over any current ISO-referenced method for contact lenses evaluation in terms of accuracy and repeatability.

4.2.3 Experimental procedure

Three -3 D lenses were measured for each lens type and each addition power. Prior to the measurements, each lens was removed from its blister and submerged in saline solution (refractive index: 1.335) at room temperature for at least 12 hours for stabilizing the effect of the saline solution upon it. The lens was then inserted into a wet cell filled with that same saline solution. Finally, the cell was placed on the NIMO translation table and the required parameters for the measurements were set in the software: the refractive index of the saline solution, the refractive index of the lens, the lens diameter, the back optic zone radius of the lens, the lens optical zone diameter and the central thickness of the lens.

For each lens, five consecutive measurements were performed using the auto-centration mode (in order to align the lens' and the system's optical axis) at the multifocal mode of the instrument. The power distribution of each lens was recorded for a 6.00 mm aperture size.

4.2.4 Data Analysis

The results of this study are divided into the following parts: First, each lens' power profile is presented. Second, based on power profile, each lens' refractive power distribution is shown for different pupil diameters. For each pupil diameter, the refractive power from the lens' profile was divided into regions of 0.25 D. The proportion of the lens' profile providing refractive power in each region was then calculated, creating the power distributions. These power distributions gave information about the portion of the lens' power profile devoted to each refractive power at each pupil size.

Third, for the high addition lenses, we calculated the cumulative power distribution and the proportion of the lens' surface dedicated to different vergences (for far, intermediate and near vision) as a function of pupil size. For this purpose, three standard distances were considered. The vergence threshold between far and intermediate vision was set at 1 m (1 D with respect to the lens' nominal power), whereas the threshold separating intermediate and near vision was set at 40 cm (2.5 D with respect to the lens' nominal power).

4.3 Results

4.3.1 Power Profiles

Figure 4.1 shows the power profiles of the three contact lens types under study at a radial distance of 3 mm (6 mm pupil size) from the center of the lens. Each curve is the averaged result of 5 consecutive measurements.

Figure 4.1, a, shows the power profiles of the Acuvue Oasys for Presbyopia lens for the three addition powers. Alternating power zones characterize the profiles of these lenses, which turn towards more negative power values at the periphery. As the addition power increases, the step size between adjacent zones tends to be more abrupt. In this sense, the low-addition lens shows a power profile that is smoother and closer to the nominal value, compared to the mid- and high-addition lenses. The effective near refractive addition (Montés-Micó et al. 2014) was 0.46 D for the low-add lens, 0.71 D for the mid-add lens and 1.62 D for the high-add lens, whereas the maximum near refractive addition (Montés-Micó et al. 2014) was 1.57 D for the low-add lens, 2.76 D for the mid-add lens and 1.92 D for the high-add lens.

Subsequently, Figure 4.1, b illustrates the power profile of Fusion 1 day Presbyo lens. The power profile is characterized by a drop towards more negative values as the radial distance from the center of the lens increases. The lens has a central zone of much higher refractive power, surrounded by a smoother zone of lower power. The effective near refractive addition of the lens was 2.87 D whereas the maximum near refractive addition was 3.51 D.

Finally, Figure 4.1, c, illustrates the power profiles the Biofinity CN lenses for the three addition powers. These power profiles are characterized by a constant central plateau of much higher power, followed by a steep drop to lower power values at the periphery. The effective near refractive addition was 1.43 D for the +1.5 D addition lens, 1.97 D for the +2 D addition lens and 2.77 D for the +2.5 D addition lens, whereas the maximum near refractive addition was 1.69 D for the +1.5 D addition lens, 2.23 D for the +2 D addition lens and 2.92 D for the +2.5 D addition lens.
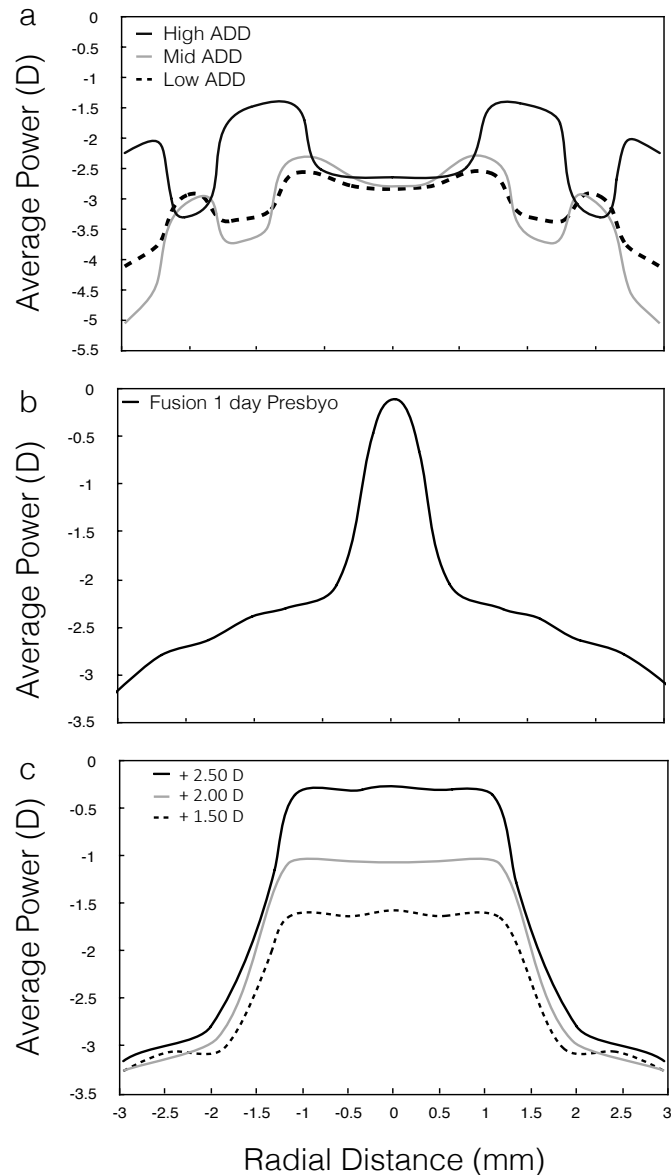
Figure 4.1: Power profiles of the multifocal contact lenses at 3.00 mm of radial distance. (a) Acuvue Oasys for Presbyopia, (b) Fusion 1 day Presbyo, (c) Biofinity CN Multifocal.

4.3.2 Refractive power distributions

Figures 4.2 to 4.4 show the power distributions of the lenses at different pupil sizes (at 3 mm, 4.5 mm and 6 mm diameter). The y-axis of the graphs shows the power breakdown for each lens model, addition and pupil size.

Figure 4.2 corresponds to the Acuvue Oasys for Presbyopia lenses. For the low- (4.2, a) and mid-power (4.2, b) addition lenses, the main power contributors were between -2.5 D and -3.5 D for the low addition lens and from -2.5 D to -3.75 D for the mid addition lens, at all pupil sizes. For both lenses, minor power contributors (around 10%) of more negative power were found at 6 mm. At the high-addition lens (4.2, c), the

main power contributors were between -1.25 D and -2.5 D. Within this interval there were two main power contributors: from -1.25 D to -1.75 D (30% at 3.00 mm) and from 2.5 D to 2.75 D (60% at 3 mm). As the pupil size increased the distribution between these areas changed: at 6 mm a low contribution of around 10% with more negative values emerged.
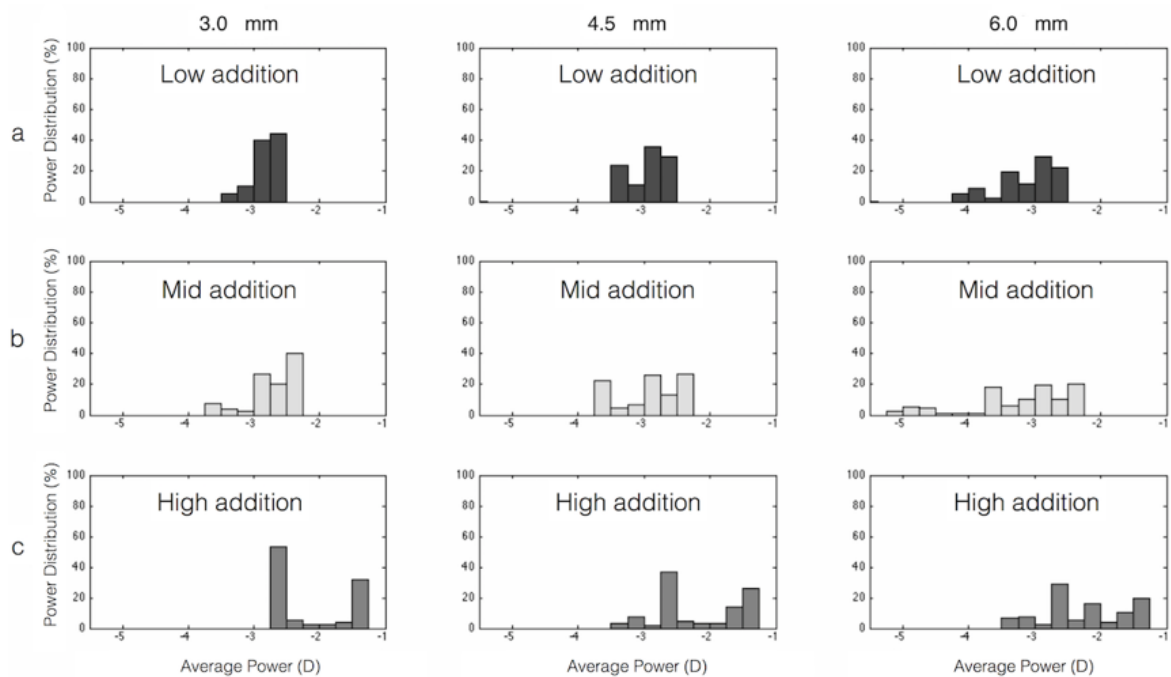

Figure 4.2. Power distribution (%) as function of pupil size (3 mm, 4.5 mm and 6 mm) for each available addition power of the Acuvue Oasys for Presbyopia lens. (a) Low-Addition lens, (b) Mid-Addition lens, (c) High-addition lens.

Similarly, Figure 3.3 corresponds to the Fusion 1 day Presbyo contact lens. At 3 mm, 60% of the power was distributed between 2 D and -2.5 D. However, as the pupil size increased, the power distribution shifted towards more negative power values.
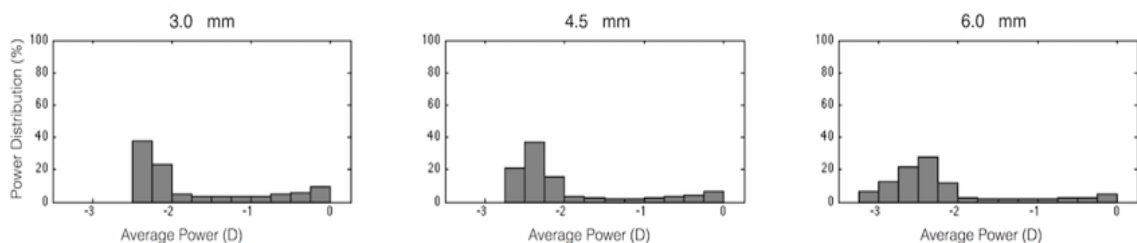

Figure 4.3 Power distribution (%) as function of pupil size (3 mm, 4.5 mm and 6 mm) for the Fusion 1 day Presbyo lens.

Finally, Figure 4.4 shows the power distribution graphs of the Biofinity CN lenses. The +1.5 D addition lens (4.4, a) had a main power contributor between -1.5 D and -1.75 D (80% of the total power) at 3 mm, a main power contributor between -2.75 D and -3.25 D (20%) at 4.5 mm, and two power contributors (40% each) at 6 mm. The +2 D addition lens (4.4, b) had similar distributions: a power contributor of more than 80% at -1 D at 3 mm whereas the distribution spread out towards more negative values as the pupil size increased. At a 6mm 40% of the power was located at -1 D and 60% between -1.25 D and -3.25 D. The +2.5 addition lens (4.4, c) showed a similar behavior. At 3 mm more than 80% of the power was concentrated between 0 D and -0.5 D, whereas at 4.5 mm and 6 mm the distribution shifted towards more negative values.
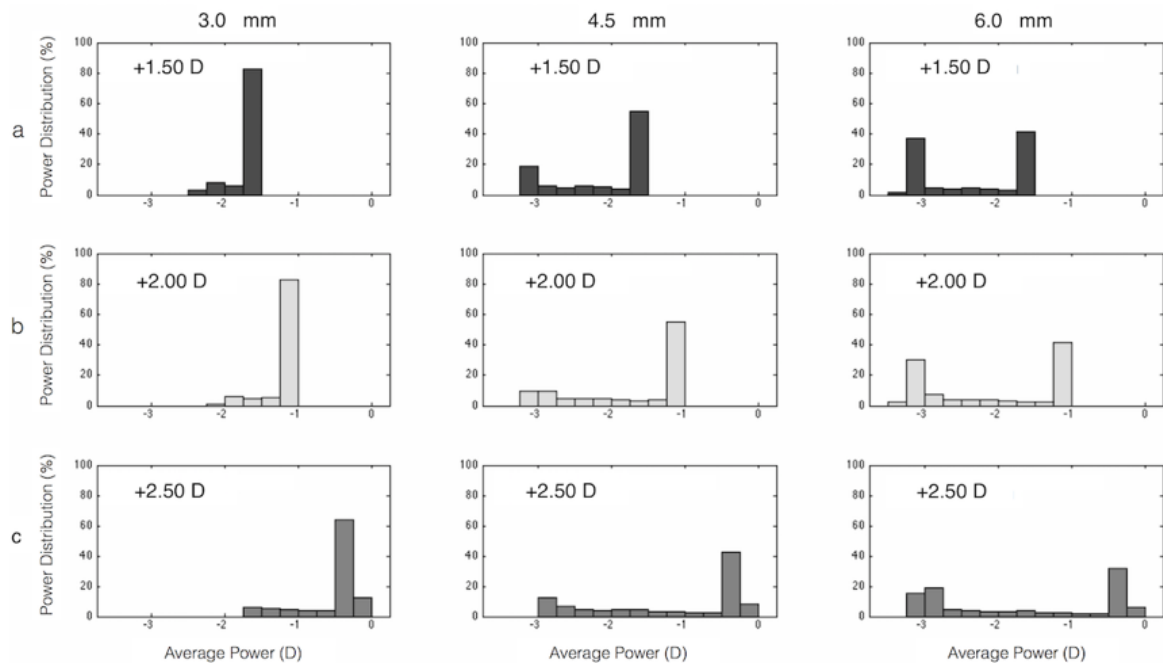
Figure 4.4: Power distribution (%) as function of pupil size (3 mm, 4.5 mm and 6 mm) for three addition powers of the Biofinity CN lenses. (a) +1.5 D, (b) +2 D, (c) +2.5 D.

4.3.3 Proportion of the lens dedicated to different vergences as a function of pupil size and cumulative power distribution

Figure 4.5 shows how the proportions of the lenses surface, dedicated to different distances, will vary with pupil size. From the graph it can be observed that the high addition Acuvue Oasys lens (4.5, a) enhanced far vision at smaller pupil sizes whereas

the Fusion 1 day Presbyo (4.5, b) and the +2.50 D Biofinity (4.5, c) lenses enhanced near vision for smaller pupil diameters. All the three lenses enhanced intermediate vision for medium pupil sizes. The lack of near vision curve for the Acuvue Oasys lens is due to the fact that this lens does not reach the refractive power proposed as threshold for near vision (the +2.50 D from the nominal power of the lens).
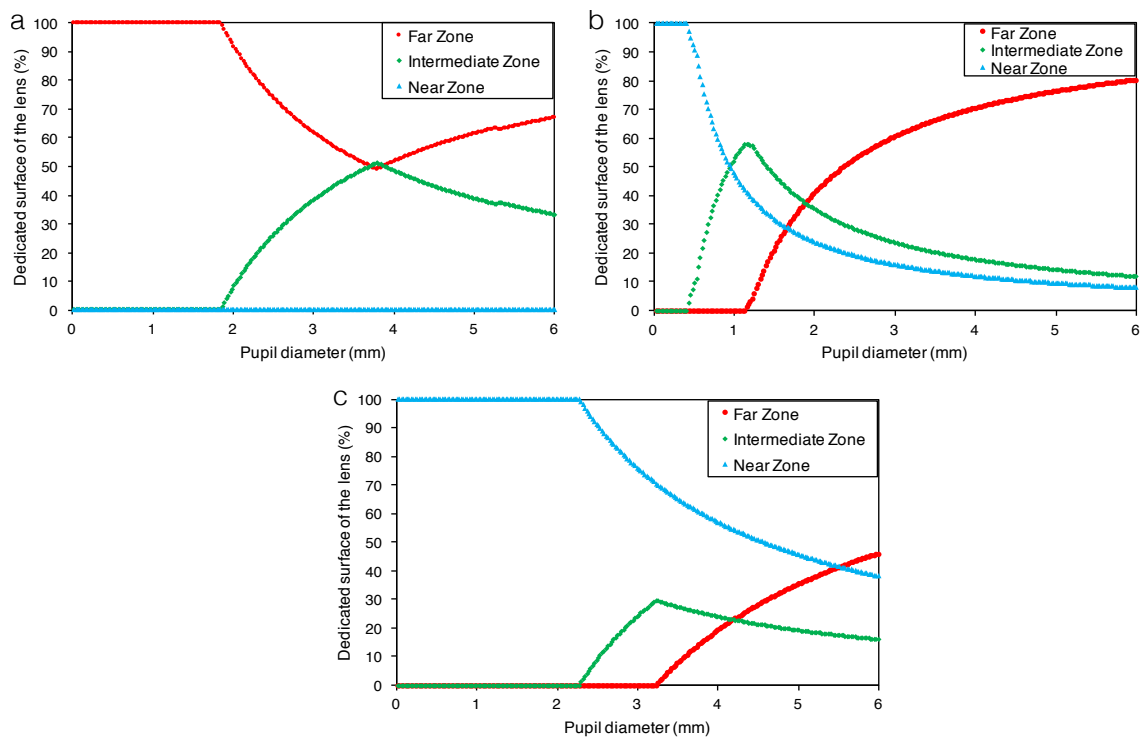
Figure 4.5: Proportion of the lens surface dedicated to different distances (far, intermediate and near vision) as a function of pupil size. (a) Acuvue Oasys for Presbyopia (High Addition), (b) Fusion 1 day Presbyo, (c) Biofinity CN Multifocal (+2.5 D addition power)

Figure 4.6 shows the cumulative power distribution of the Biofinity +2.5 D (4.6, a) and of the Fusion 1 day Presbyo lens (4.6, b) for the three different pupil diameters. The vertical dashed lines represent three different distance zones: far zone (up to -2 D), intermediate zone (-2 D to -0.5 D) and near zone (-0.5 D to 0.5 D).
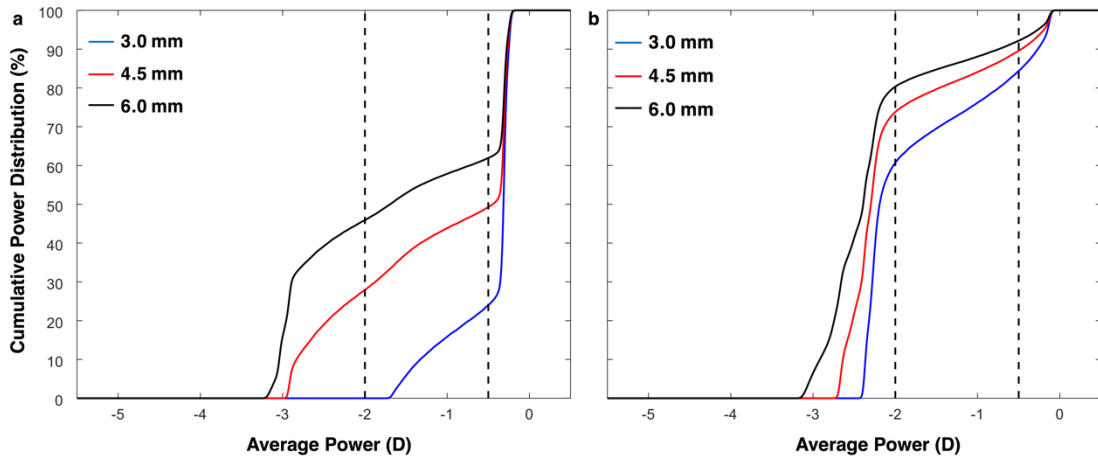
Figure 4.6. Cumulative power distribution (%) at three different pupil sizes (3 mm, 4.5 mm and 6 mm). The vertical dashed lines indicate three different vision zones: far zone (up to -2 D), intermediate zone (-2 D to -0.5 D) and near zone (-0.5 D to 0.5 D). (a) Biofinity CN lens (+2.5 D addition power), (b) Fusion 1 day presbyo lens.

As the pupil size increased the amount of the refractive power in the near vision decreased whereas the refractive power in far zone increased. For example, at 3 mm the Biofinity lens did not show power distribution in the far zone but it had around 25% of the refractive power in the intermediate zone and 75% in the near zone. At 3 mm the respective power percentages for the Fusion 1 day Presbyo lens were 60%, 20% and 20%. At 4.5 mm these percentages were 25%, 25% and 50% for the Biofinity lens and 60%, 20%, 20% for the Fusion 1 day Presbyo lens. Finally, at 6 mm the percentages were 45%, 15% and 35% for the Biofinity and 80%, 10%, 10% for the Fusion 1 day Presbyo lens.

4.4 Discussion

The aim of this work was to assess objectively the power distribution of different designs of multifocal CLs, as a function of pupil size, based on power profiles measurements. Due to the complexity of multifocal CLs designs, it is important to obtain information about the potential correction they can provide at given pupil sizes and vergences.

Figures 4.1 to 4.4 represent the power profiles and the power distribution of the multifocal CLs at different pupil sizes. The figures show the differences in power distribution with pupil size among the different lens types and also among the different addition powers.

All the lenses in this study had a nominal power of -3 D. The pupil size where each lens type reached the nominal power was different due to the addition power. For instance, the low and mid-addition CD Acuvue lenses required a pupil size of at least 3 mm to reach the nominal power, whereas the high addition lens needed a greater pupil size. The CN Fusion lens required a pupil above 5 mm and as for the CN Biofinity lenses, the differences among the three addition powers were marginal. Note that this lens comes to CN and CD design for monovision correction, hence, this combination is expected to compensate for pupil size changes.

Evaluation of multifocal CLs based on power profile analysis has been presented before. In these previous studies (Plainis, Atchison, and Charman 2013; Cardona and López 2016; Madrid-Costa et al. 2015; Vasudevan, Flores, and Gaib 2014; Belda-Salmerón et al. 2013; Wagner et al. 2015), the role of pupil size has been discussed and has been concluded that the pupil dynamics have a significant role in multifocal CLs performance. Although power profile data show the power distribution as a function of radial distance (Figure 4.1), it is however difficult to predict the impact of given pupil sizes on power distribution and how this may affect the optical performance of the lens and therefore, the subject's visual performance. The motivation of the analysis in our study was precisely this; to provide an analytical and easy-to-understand approach about the interaction between pupil size and power distribution of multifocal CLs and give some evidence about potential visual performance with these lenses.

In a study of Koch et al. (Koch et al. 1991), pupil size data corresponding to different visual tasks and illumination levels were presented for different age groups (Figure 4.7). That data showed the dependence of pupil size regarding different visual tasks and

illumination levels, and also, the variance of pupil size among individuals. The results of that study and of a previous one by Montés-Micó et al. (Montés-Micó et al. 2014), showed that the refractive power provided by a multifocal contact lensnot only varies with pupil size, but also across individuals. This observation is crucial because it means that subjects with the exact same visual demands can have different visual performance when they are fitted with the same multifocal contact lens type as a consequence of pupil size variation. Taking the latter into account, choosing between center-distance and center-near designs can be difficult if there is no sufficient information about the pupil dynamics. For instance, if the pupil size is small under bright illumination, the amount of light which enters through the periphery of the lens will decrease; hence the contribution of the refractive power corresponding to the lens' periphery will diminish too.
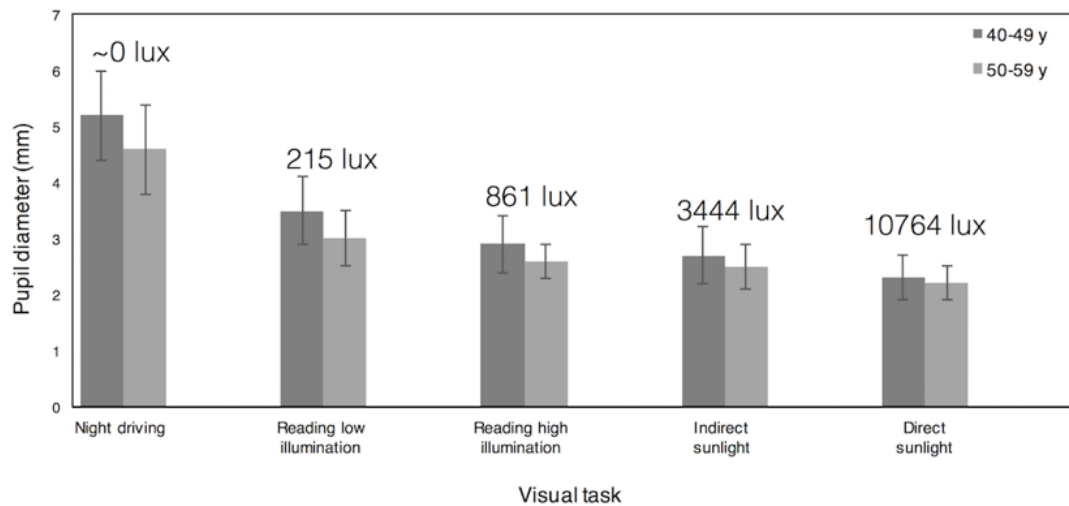

Figure 4.7. Mean pupil sizes of two presbyopic age groups, for five different tasks corresponding to different illumination levels (data obtained from the study of Koch et al. (Koch et al. 1991)).

In Figures 4.5 and 4.6 we showed the proportions of the lens surface dedicated to different distances (far, intermediate and near vision) and the cumulative power distribution respectively, to show how the proportions and the distributions change with pupil size. Since all the lenses were characterized by rotational symmetry, the proportions of profile calculated can be directly related to proportions of the lens surface. The reason of presenting only the higher addition lenses was because these lenses are conceived for people whose amplitude of accommodation is practically zero. The lower addition lenses are conceived for younger presbyopes where some amplitude of accommodation still exists in the fitted eye and it helps the subject to achieve satisfactory near vision.

Regarding pupil size, the findings of our study can provide useful information to the practitioner in selecting the appropriate lens design depending on the task that is more important to the subject. For example, according to Koch et al. (Koch et al. 1991),the typical pupil diameter for reading under low illumination (215 lux) in subjects between 50 and 59 years old is around 3 mm. Subjects with more than 55 years of age are considered to have almost zero amplitude of accommodation, hence they require lenses with high addition value (Antona et al. 2008). In Figure 4.5 we can easily see that for this pupil size, Acuvue Oasys has around 60% of its surface dedicated to far vision and 40% to intermediate vision. Subsequently, at 3 mm the Fusion offers approximately 60% of its surface for far vision, 25% for intermediate vision and 15% for near vision, whereas the Biofinity has approximately 25% of its surface for intermediate vision and 75% for near vision.

All the in-vitro measurements in this study were performed assuming the lenses were perfectly centered. Nevertheless, when a contact lens is fitted on the eye factors such as eye movements or irregularities of corneal surface can displace the lens. For soft contact lenses the estimated movement ranges between 0.5 mm and 1.0 mm (Hong, Himebaugh, and Thibos 2001). As we showed in our findings the pupil size changes the resulting provided refractive power with a multifocal contact lens. Subsequently, for a given pupil size a displacement of a multifocal contact lens could result refractive power that does not cover sufficiently the visual demands of the subject (i.e. the subject can be over- or under-corrected). Further investigation for the effect of decentration (Bakaraju et al. 2012) upon the power profiles of different designs of multifocal CLs will increase the insight about their optical behavior and to estimate the impact on visual performance.

In conclusion, although previous works (Plainis, Atchison, and Charman 2013; Madrid-Costa et al. 2015) have already shown the power profiles for some of the lenses presented here, in this work we aimed to objectively assess the impact of pupil size upon the power profiles of multifocal CLs. To achieve this, we calculated the proportion of power distribution at different pupil sizes (see Figures 4.2 to 4.4) and we also divided the power profile of the high addition lenses into different vision zones (see Figures 4.5 and 4.6) to show how the power distribution at each zone changed with pupil size. Our results, combined with the ones of previous studies (Plainis, Atchison, and Charman 2013; Madrid-Costa et al. 2015; Montés-Micó et al. 2014; Wagner et al. 2015), can enhance the present understanding of the optical behavior of multifocal CLs. Finally, the analytical approach presented here can be helpful in facilitating the proper fitting of multifocal CLs, depending on the pupil dynamics of the subjects.

Chapter 5
Temporal multiplexing with adaptive optics for simultaneous vision

5. Temporal multiplexing with adaptive optics for simultaneous vision

5.1 Introduction

Accommodation is an important mechanism of the young eye to bring nearby objects into focus and creating sharp and clear images at the retina. As the eye ages, however, its accommodation ability declines (Charman 2014a; Duane 1908; Kragha 1986) until it is lost almost completely at the early fifties, when the eye is already presbyopic. The most obvious consequence of presbyopia is blurred near vision, making hard to accomplish near tasks (e.g. reading the newspaper). Nowadays, there is a wide range of available tools for counteracting presbyopia symptoms (Charman 2014a; Charman 2014b; Bennett 2008), based on different strategies, such as ophthalmic lenses, contacts lenses (CLs), intraocular lenses (IOLs), and surgical techniques. We can distinguish two basic strategies for presbyopia treatment: simultaneous vision and alternating vision.

Simultaneous vision is based on simultaneous projection of images on the retina at the same time (Charman 2014a; Charman 2014b; Bennett 2008). Each projected image corresponds to a sharp image at a different vergence. Typically, this solution is achieved by multifocal CLs (Charman 2014a; Bennett 2008) or IOLs with refractive (Charman 2014b) or diffractive (Charman 2014b; Davison and Simpson 2006) profiles. Success of simultaneous vision relies on the ability of the human brain to select among the superimposed images a primary in-focus image (Charman 2014a), suppressing the blurred out-of-focus image. The drawback of this strategy is that suppression ability varies among individuals (Alais and Blake 2005); the out-of focus images, if not suppressed, can generate a great amount of blur and reduce the contrast sensitivity (Dick et al. 1999; Charman 2014a; Charman 2014b). Monovision (Charman 2014a; Charman 2014b; Bennett 2008), where one eye receives the correction for far vision and the other for near, can be considered as simultaneous vision if the binocular rivalry between the retinal images generates binocular suppression. Large depth-of-focus (DoF) achieved by using a pinhole in a contact lens (Miller and Meshel 1993), in a corneal inlay (Waring 2011) or near the pupil plane (David A. Atchison et al. 2016), also allows for simultaneous vision.

Alternating vision refers to images of objects at different vergences generated at the retina at different times. This is a strategy followed by bifocal, trifocal or progressive ophthalmic lenses (Charman 2014a). CLs for alternating vision (with two distinct power segments alternating with upward and downward gaze shifts) also exist(Charman 2014a; Bennett 2008). Accommodative IOLs (Ong, Evans, and Allan 2014) have been introduced that theoretically can change their power when the ciliary muscle is activated by the accommodation reflex, but their effectiveness is yet to be proven.

Although both types of multifocality are different in essence, their visual effects are identical if alternating vision is produced at a high temporal frequency. For a stimulus to be perceived as stable or smooth and without flickering, it should be presented to the eye at a rate above a threshold known as the critical flicker frequency(Kalloniatis and Luu 1995; Scharnowski, Hermens, and Herzog 2007), at around 9 Hz at scotopic light levels and 50 Hz at high photopic light levels (Roufs 1972). According to Bloch's Law (Kalloniatis and Luu 1995; Scharnowski, Hermens, and Herzog 2007), within sufficiently short time intervals (<100 ms) the visual system makes a temporal summation of brightness so that stimulus intensity and duration are reciprocally proportional to each other. Temporal multiplexing can be used to generate simultaneous vision. It allows for adjusting the proportion of time in far and near vision by direct modulation of light energy distribution between the two foci. Simultaneous vision with temporal multiplexing can be achieved artificially with high-speed optoelectronic devices, such as a tunable focal lens (Blum et al. 2012). The practical use of those devices is limited since they are relatively heavy, big, and need a power supply. However, they can be a good way to test visual performance under simulated multifocality in a presbyopic eye prior to IOLs' implantation (Dorronsoro Díaz, Alonso Sanz, and Marcos Celestino 2015).

Some simultaneous vision designs include manipulation of higher-order aberrations (HOAs), since they have been found to influence the visual performance of subjects with presbyopic solutions (Applegate, Sarver, and Khemsara 2002; Roorda 2011; Alió et al. 2008). For instance, IOLs with negative spherical aberration (SA) aim to compensate the positive SA aberration of a pseudophakic eye (Glasser and Campbell 1998). However, the presence of negative SA in IOLs can generate difficulties in vision clarity if they get displaced (D. A. Atchison 1991; Eppig et al. 2009). On the other hand, the presence of a certain amount of SA in the eye may also be useful to increase DoF

(Rocha et al. 2007; Marcos, Barbero, and Jiménez-Alfaro 2005). Within this frame, it would be desirable to explore the possibility of testing multifocality in the presence of certain values of HOAs (e.g. SA), and for instance, explore the possibility of inducing different amounts of SA for the far and near vision, mimicking the young eye where usually SA is positive for the relaxed state and negative for accommodation states larger than 2-3 D (Lopez-Gil and Fernandez-Sanchez 2010).

In this study, we used temporal multiplexing with a deformable mirror (DM) to generate simultaneous vision and to assess the through-focus optical performance (in terms of contrast) of different designs with equal and unequal distribution of energy in each focus. We also generated a toric equal energy design by inducing astigmatism and explored the effect of SA in far and near foci. Finally, we explored the effect of SA on a pseudophakic 60-year-old eye. Although our findings are based on simulated conditions, the methodology can be applied to assess visual performance with simultaneous vision designs in real subjects.

5.2 Methods

5.2.1 Experimental set-up

A diagram of the AO visual simulator (MurciAO) used in this study is shown in Figure 5.1. The system has four principal components: a 50×32 lenslets Shack-Hartmann aberrometer (HASO4 First, Imagine Eyes, Orsay, France), an electromagnetic DM (Mirao 52e, Imagine Eyes, Orsay, France) with a membrane of 52 piezoelectric actuators, a Badal system built on two flat mirrors mounted on a monitorized stage (PLS-85, PI miCos), and an 800×600 black-and-white microdisplay (eMAGIN, USA). For the experiments conducted in this study, a digital camera (E-M5, Olympus, Tokyo, Japan) was placed in the entrance pupil (5-mm) of the AO system, acting as an artificial eye. A He-Ne laser of 633 nm was used to measure and correct the aberrations of the system.
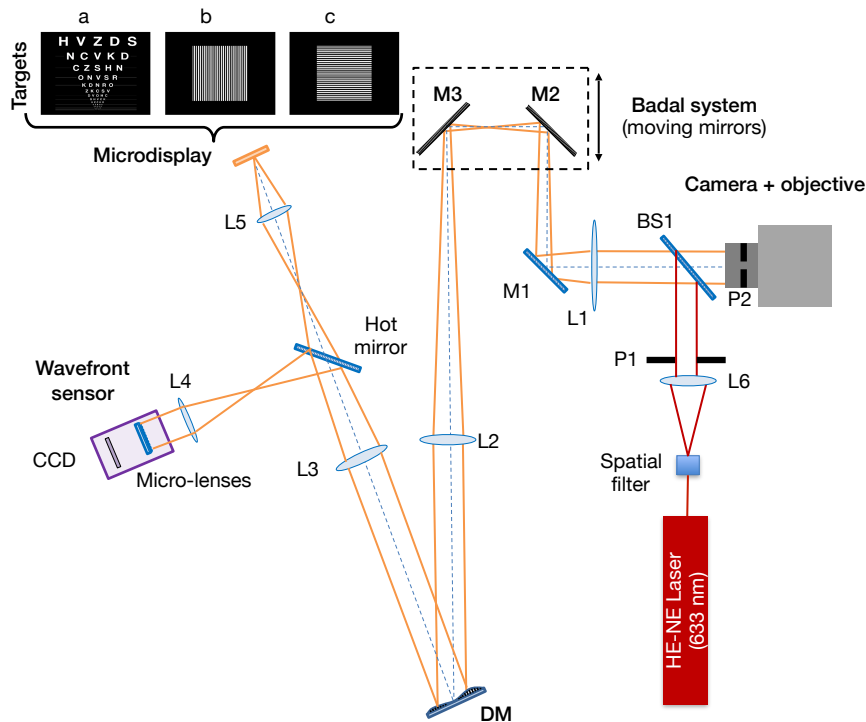
Figure 5.1. Schematic diagram of the AO system (MurciAO). Lenses L1, L2, L3, and L5 are achromatic doublets; lenses L4 and L6 are singlets; M1, M2, and M3 are flat mirrors; P1 is an artificial pupil; P2 is the camera stop; and BS1 is a pellicle beam splitter. Targets on the left side are (a) an acuity chart, (b) a vertical square grating, and (c) a horizontal square grating described in Section 2.2.

5.2.2 Measurements

Simultaneous vision patterns were generated by continuously changing the shape of the DM between two vergences: one for far focus at 0 D and one for near focus at −2.5 D, a simultaneous vision design for subjects of more than 55 years of age with near zero amplitude of accommodation (Antona et al. 2008). The residual root mean square was always below 0.1 μm for an 8.2-mm pupil diameter. To avoid flickering effects, the frequency at which the mirror changed position was 50 Hz (i.e. 20 ms) (Kalloniatis and Luu 1995; Scharnowski, Hermens, and Herzog 2007). We created two rotationally symmetrical designs for bifocal simultaneous vision: one in which the DM stayed 50% of the time in each foci and other in which the mirror stayed 60% of the time in the far focus and 40% in the near focus. These designs correspond, respectively, to the equal energy design (50/50) and the unequal energy design (60/40). Because the DM needs 5 ms to change its shape, the effective time the mirror was still in each vergence was 5 ms for the equal energy (50/50) design and 7 ms and 3 ms for the unequal (60/40) energy design. Figure 5.2 shows digital photographs of the visual acuity charts at

different vergences for three different simultaneous vision designs generated with the AO system.

For the equal-energy design, we explored toricity and SA effects on lens design. Astigmatism and SA were added using the DM (Fig. 1). First, we explored a toric bifocal design (a non rotationally symmetrical design) with −1.0 D of astigmatism at 0°. We also tested different combinations of SA (a rotationally symmetrical design) for the far and near foci to evaluate their effect on the DoF (see Table 1). The value was chosen following the amounts of negative SA that monofocal IOLs have; around −0.2 µm for a 6-mm pupil size (Wang and Koch 2007) rescaled to a 5-mm pupil.
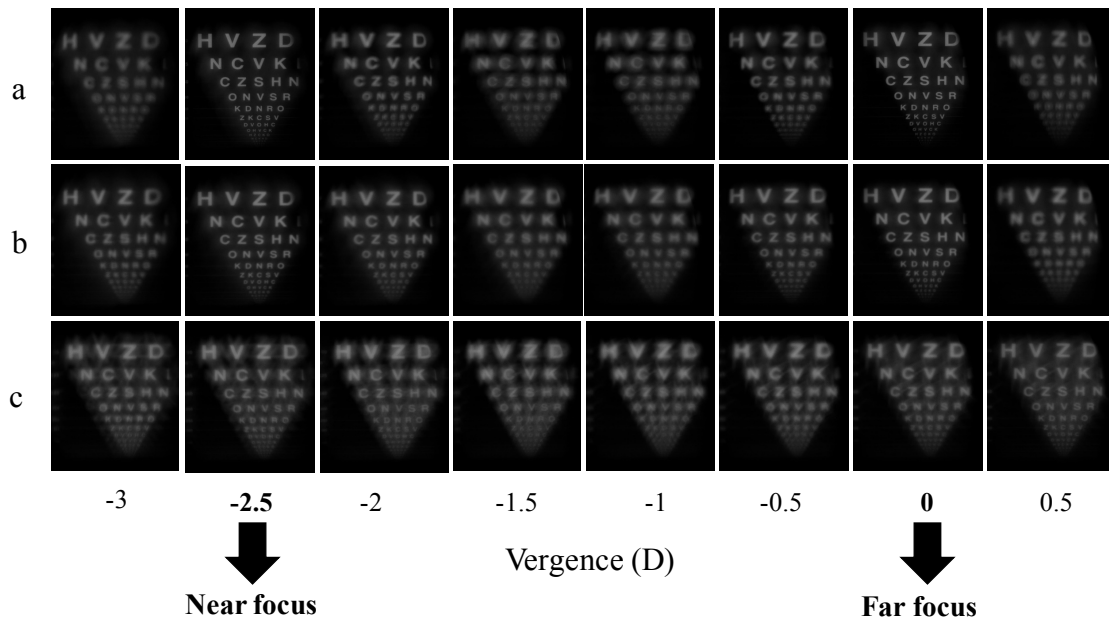

Figure 2. Through-focus photographic images of a visual acuity chart for three bifocal designs: (a) equal energy design; (b) equal energy design with negative SA at the far focus and positive SA at the near focus; (c) equal-energy design with corneal HOAs (up to 7th order). Arrows indicate the far and near foci.

Table 1 below summarizes all the designs generated in this study.

Design	Energy Distribution (%)[1]	Comments[1,2]
Equal-energy bifocal	50 (F) / 50 (N)	
Unequal-energy Bifocal	60 (F) / 40 (N)	
Bifocal Toric	50 (F) / 50 (N)	1 D of astigmatism at 0^0
Bifocal with SA	50 (F) / 50 (N)	+0.1 μm (F) / +0.1 μm (N) −0.1 μm (F) / −0.1 μm (N) −0.1 μm (F) / +0.1 μm (N) +0.1 μm (F) / −0.1 μm (N)
Bifocal + Corneal HOAs	50 (F) / 50 (N)	HOAs from a model cornea of 60 years of age
Bifocal with SA + Corneal HOAs	50 (F) / 50 (N)	−0.1 μm (F) / −0.1 μm (N) and HOAs from a model cornea of 60 years of age

[1] *N means near focus and F means far focus*
[2] *SA values are for 5-mm pupil*

Table 1. Summary of the simultaneous vision designs generated with AO. F reads for far focus and N for near focus. Note that the SA values herein are given for a 5-mm pupil diameter.

Finally, we assessed the effect of corneal HOAs of a 60-year-old eye to the bifocal 50/50 energy IOL design. The goal of this simulation was to know if the aberrations generated by the patient's cornea had an impact on the in vitro through-focus curve of a multifocal IOLs. For that purpose, up to 7th order corneal HOAs (SA +0.19 μm for a pupil size of 5 mm) were obtained from an aging model cornea (Navarro, Rozema, and Tassignon 2013). These corneal HOAs were added to the bifocal design with the DM to simulate:

a) a pseudophakic eye with a bifocal IOL of zero SA,

b) a pseudophakic eye with a bifocal IOL and −0.1 μm of SA (induced in each foci) to compensate part of the positive corneal SA of the aphakic eye (Wang and Koch 2007).

5.2.3 Measurements

Through-focus curves were recorded for each of the simulated simultaneous vision designs. A step-by-step electric motor was used to change the optical path length between L1 and L2 (Badal system) in steps of 0.125 D. The range of the through-focus curves was from +0.5 D to −3 D, except for the toric design, for which the range was

from +0.5 D to −4 D due to the astigmatic power. At each step, three different targets were successively projected on the microdisplay (luminance level at 260 cd/m^2) and an image of each target was captured with the camera while the mirror was changing its shape between the two vergences. The targets are shown in Fig. 1. They were an acuity chart, a vertical square grating, and a horizontal square grating. The gratings had a spatial frequency of 15 cpd, which is the spatial frequency typically used to evaluate in vitro optical quality of IOLs (Papadatou et al. 2016; Madrid-Costa et al. 2013). The size of each image registered with the camera was 4608x3456 pixels with a pixel size of 3.74 μm. The focal length of the camera objective used was 50 μm, therefore every pixel subtended 15.4 arcsec. The exposure time of the camera was set at 0.16 s to match the temporal summation properties of the human eye (Kalloniatis and Luu 1995).

In all measurements, we proceeded as follows. First, reference images were taken for each of the three targets in Fig. 1 with the mirror still and all the aberrations of the system corrected. Then, three through-focus curves were obtained for each target. After each through-focus curve was obtained, the aberrations of the system were corrected again and new reference images were taken prior measuring the next through-focus curve for the next simulated simultaneous vision design.

5.2.5 Data analysis

Normalized cross-correlation coefficients (Kim et al. 2011) were calculated for the acuity chart and Michelson contrast was calculated for the gratings, at each vergece of the through-focus curve. For the calculations, customized software developed in Matlab (Mathworks, Inc., Natic, MA) was used. Due to a small vignetting effect from the system's optics, a central area (150 × 200 pixels) of the images was chosen for the calculations. The normalized cross-correlation indicates the similarity between the reference image and the rest of the images in the through-focus. Contrast was normalized by dividing the contrast value of each image with the contrast value of the reference image, which was always greater than 0.9. For the rotationally symmetrical designs, where only defocus and SA were modified, the through-focus curve of the horizontal and the vertical grating were averaged.

Experimental contrast results were compared against computer simulations generated with the Fourier Optics Calculator (Thibos et al. 2004) for MatLab (Mathworks, Inc.,

Natic, MA). The selected pupil used was 5 mm, as the experimental one, and the wavelength was 550 nm.

5.3 Results

Figure 5.4 shows the experimental through-focus curves (in black) of the normalized Michelson contrast (upper panel) and of the normalized cross-correlation (lower panel) for the equal-energy, unequal-energy, and toric designs. For normalized Michelson contrast, theoretical through-focus curves are also shown in gray. Theoretical curves were not included for the cross-correlation values, since they are less sensitive to a contrast reduction caused by a secondary, out-of-focus image. For the toric design, the experimental cross-correlation peaks (marked with arrows in the lower-right panel) are located at 0 D and at −1.0 D for far vision and at −2.5 D and −3.5 D for near vision. The theoretical through-focus curves showed greater peaks than the experimental ones although, for the intermediate distance, they showed deeper valleys than the experimental curves.
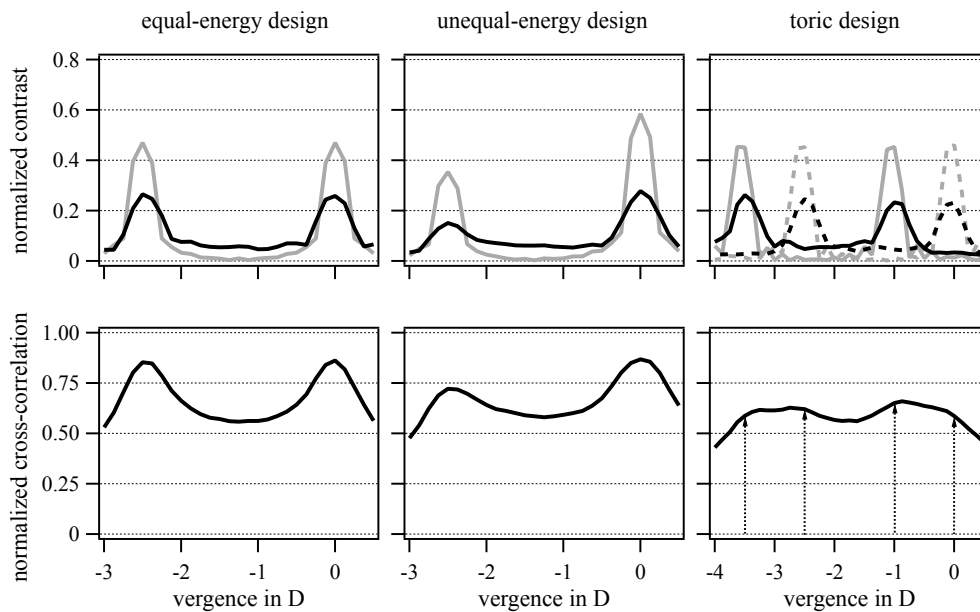
Figure 5.4. Experimental (black) and simulated (grey) through-focus curves for simultaneous vision designs: equal-energy (50/50) design (left), unequal-energy (60/40) design (center), and equal energy (50/50) toric design with 1.0 D of astigmatism at 0° (right). The dashed lines in the upper-right panel are the experimental and theoretical curves for the meridian with no astigmatic power whereas the continuous lines correspond to the meridian that has the astigmatism. The black arrows in the lower-right panel indicate the peaks for far and near vision of the toric design. Notice that the through-focus curves for the toric design are 1.0 D wider than for the rest.

76

Figure 5.5 shows experimental and simulated through-focus curves for normalized Michelson contrast for the four combinations of SA.
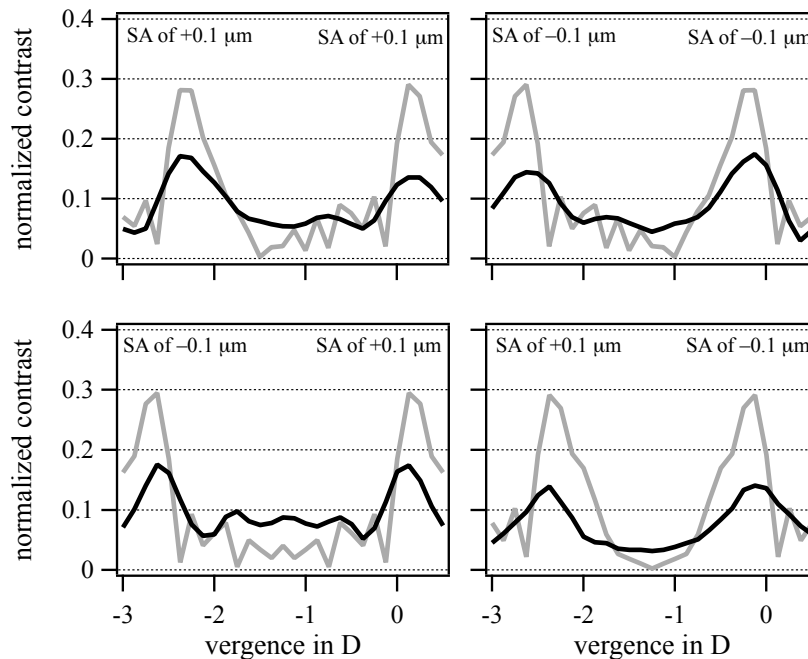
Figure 5.5. Experimental (black) and simulated (grey) through-focus curves of the normalized contrast for different combinations of SA in near and far foci. The upper panel shows through-focus curves when (left) positive SA was added to both foci and (right) negative SA was added to both foci. Lower panel shows through-focus when (left) positive SA was added to far focus and negative SA to near focus and (right) negative SA was added to far focus and positive SA to near focus. Notice that the y-axis has been rescaled for visualization purposes.

The addition of SA to the bifocal equal-energy design decreased the optical quality of the peaks but increased their width. Bumps were evident at intermediate vergences but the optical quality did not increase. Adding positive SA to both near and far foci shifted the two peaks of the curve to the right by 0.125 D. Adding negative SA had the opposite effect, shifting the curve to the left by the same amount. The addition of positive SA to the far focus and negative SA to the near focus separated the peaks from each other by 0.25 D, whereas addition of negative SA to the far focus and positive SA to the near focus brought the peaks closer together by the same amount. Figure 5.6 shows the same data as in Figure 5.5 but for the normalized cross-correlation.
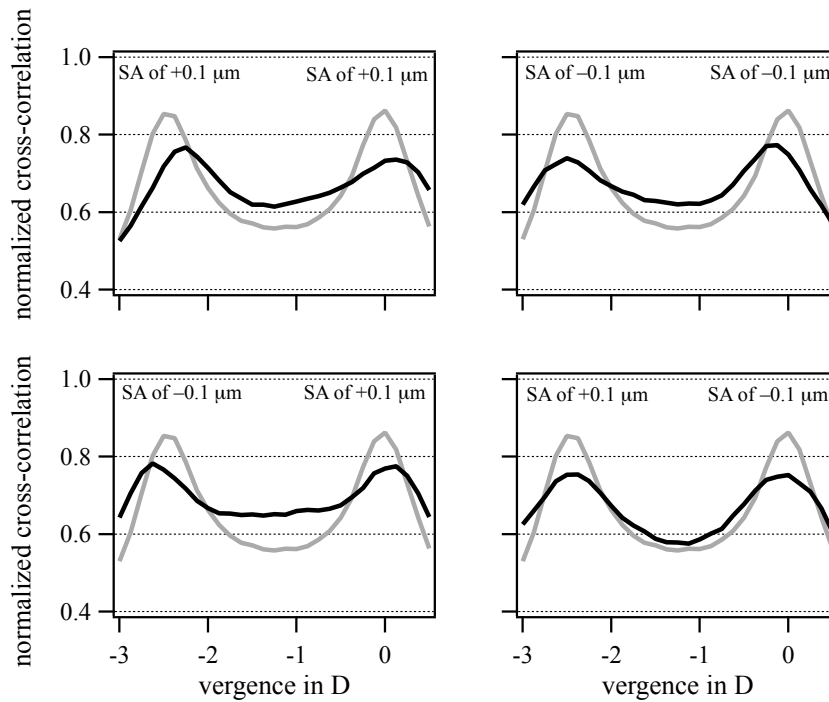
Figure 5.6. Simulated (grey) through-focus curves of the normalized cross-correlation for different combinations of SA in near and far foci. For comparison purposes, the cross-correlation curve of the equal-energy bifocal (black curve) is included in each panel. The upper panel shows through-focus curves when (left) positive SA was added to both foci and (right) negative SA was added to both foci. Lower panel shows through-focus when (left) positive SA was added to far focus and negative SA to near focus and (right) negative SA was added to far focus and positive SA to near focus.

As expected, for each combination of SA, the through-focus curves for normalized cross-correlation showed the same behavior as the through-focus curves for normalized Michelson contrast: a decrement in optical quality in peaks, an increase at intermediate vergences, and same shifts in peaks (to the right for positive SA and to the left for negative SA).

Figure 5.7 shows the experimental through-focus curves for comparing the effects of partially compensating (gray curves) or not (black curves) the SA of a normal 60-year-old pseudophakic eye with an ideal equal-energy bifocal lens.

Figure 5.7. Through-focus curves for normalized Michelson contrast (left) and normalized cross-correlation (right) for a 60-year-old pseudophakic eye wearing an ideal equal-energy bifocal lens without SA (black) and with negative SA (gray) in both foci (−0.1 μm) for partially compensating the positive SA of the model cornea (+0.19 μm). Notice that the y-axis has been rescaled for visualization purposes.
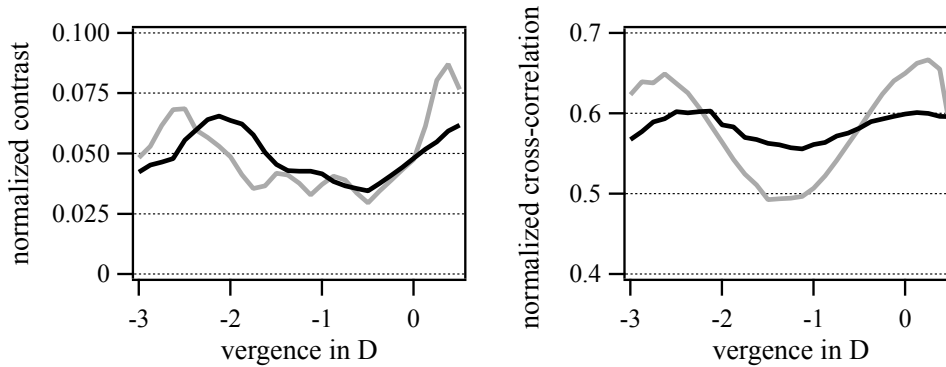
Note the changes between black and gray lines in Figure 5.7. The optical quality of the peaks dropped significantly when the corneal HOAs were added to the equal-energy bifocal lens. Additionally, they were also displaced to the right by 0.325 D for the near focus and by 0.5 D for the far focus. The addition of negative SA slightly improved the quality at the peaks and restored their placement (near peak placed at −2.5 D and far peak placed at 0.125 D).

5.4 Discussion

We propose a method based on temporal multiplexing simultaneous vision to simulate the visual optical effects of multifocal designs using AO technology. This methodology allows us to test the effects of not only defocus but also other aberrations such as astigmatism in toric designs or spherical aberration in most actual multifocal CLs and IOLs designs. It can be used to obtain a more realistic through-focus curve of multifocal solutions (CLs, IOLs) in a particular eye and also for evaluating the interactions between multifocal IOLs designs and corneal aberrations prior surgery.

This methodology can be applied for performing measurements in real subjects as long as the frequency at which the DM changes shape is equal or greater than 50 Hz, to prevent flickering (Kalloniatis and Luu 1995; Scharnowski, Hermens, and Herzog 2007). Although we did not assess subjective through-focus curves with real eyes, we observed the stimulus with our own eye (looking through the system), to ensure that there was no flickering, before conducting the experiments described here. We noted that, when the eye was not perfectly aligned with the system, the out-of-focus (ghost)

image appeared a little bit shifted with respect to the in-focus image (vergence of 0 D). Indeed, this shift is also experienced by pseudophakic eyes when having an IOL that is not well centered (Mello Jr. et al. 2000; Galor et al. 2009).

The peaks and valleys in the experimental through-focus curves for Michelson contrast were consistent with those for cross-correlation (see Figures 5.4 to 5.7). In addition, theoretical through-focus curves for Michelson contrast were consistent with our experimental measurements (see Figures 5.4 and 5.5). Yet, the peaks for the theoretical curves were systematically greater than the ones for the experimental curves. The bumps were more evident at the middle points for the theoretical curves than for the experimental ones. These differences between experimental and theoretical curves may be due to a smoothing effect generated as a consequence of the amount of time the mirror takes to change shape, as illustrated through the simulations shown in Figure 5.8. In the calculation of the theoretical curves, we implicitly assume that the mirror can move instantly from near to far focus (dotted gray curves in Figure 5.8), but in practice the mirror needed 4 ms to 5 ms (solid gray curve in Figure 5.8). This technical limitation becomes increasingly more acute as we increase the number of foci in simulate simultaneous vision (i.e. a trifocal IOL).
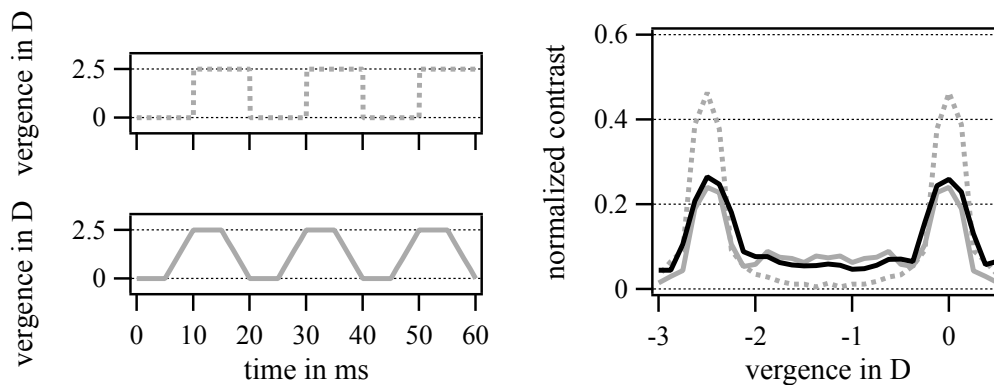
Figure 5.8. Upper left panel shows the behavior of the mirror if it changed shape instantly. Bottom left panel shows a more realistic (continuous) change of the defocus. Right panel shows simulated through-focus curves for both situations on the left (dotted gray line corresponds to the top profile change; gray solid line corresponds to the bottom profile change), and also the real through-focus curve (solid black line) for comparison purposes.

Another limitation of the methodology proposed is to reproduce the scatter effects of diffractive optics. Moreover, our methodology cannot assess the effects of diffraction caused by real IOLs with different power zones (Davison and Simpson 2006; Artigas et al. 2007). For instance, a bifocal IOL with radial center-near design has two power

zones which correspond to far and near vision, respectively. Thus, the near-focus image is formed by light passing through the central circular area, whereas the far-focus image is formed by light passing through the peripheral annulus. In our experiment, however, both images were formed from light passing through the whole circular pupil at different times. Figure 5.9 illustrates, after computational simulations, the differences respect to our approach of having two different zones, both with the same area, one for the far and one for the near focus, on normalized contrast. The differences are rather small, although the peak of the far focus decreases in the two-zone IOL simulations. For a center-distance design, the curve simply flips horizontally, that is, the lower peak would be at -2.5 D of vergence.
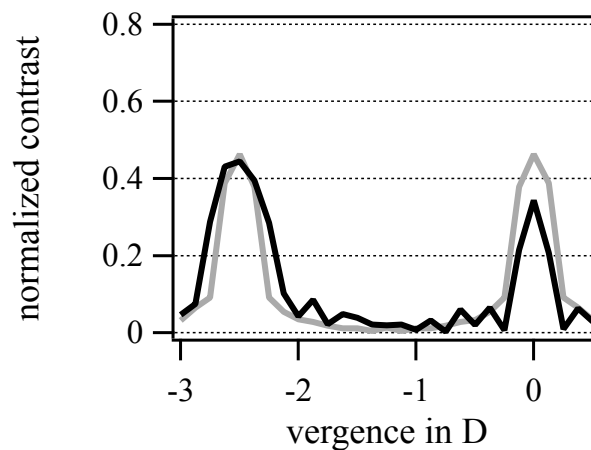
Figure 5.9. Computed simulations of the through-focus of a center-near bifocal IOL (black) and an equal-energy bifocal design, where both images share the whole pupil (grey).

Simulated simultaneous vision can also be achieved with a simpler, portable optical system with a tunable lens (Dorronsoro et al. 2015) or with two optical paths (de Gracia et al. 2013). Although a tunable lens is a good option for experiments that involve temporal multiplexing, care should be taken when using it in a vertical position since its membrane can be deformed by the action of gravity, inducing aberrations such as coma (Blum et al. 2012; Esteve-Taboada et al. 2015). A system, as the one shown in Figure 5.1, allows us also to simulate the visual effects of bifocal toric designs (see in Figure 5.4), as well as designs with different combinations of SA (see Figure 5.5 and 5.6). We tested whether the inclusion of negative SA in for far focus and positive for near focus reduced the visibility of the defocused images (hence improving the image quality) (Bradley, Kollbaum, and Thibos 2014). We tested that combination in an equal-energy design with four combinations of SA (see Fig 5.5 and 5.6). As it can be

noticed in the lower-right panel of Fig 5.5, the DoF of the peaks increased with respect to the equal-energy pattern with no SA. The opposite condition (in Fig 5.5, lower-left panel) enhanced the intermediate image quality.

Ocular SA varies significantly among older population (Rocha et al. 2007; Porter et al. 2001), therefore, the through-focus curve depends on the subject and the selected IOL's SA. As an example, the simulations with a pseudophakic 60-year-old eye implanted with an IOL with and without negative SA (Figure 5.7), showed how much the corneal aberrations may affect the quality of a bifocal design and the benefit of adding negative SA. However, the quality of the through-focus curves decreased dramatically in both cases. Nevertheless, we should keep in mind that our contrast results are based in gratings with only one spatial frequency while in typical clinical practice, several spatial frequencies are normally used (Ginsburg 2006).

In conclusion, a fast AO system can be a powerful tool for exploring different aspects of simultaneous vision. Besides the tests performed in the present work, multiple designs and combinations can be tested including trifocal lenses (Carballo-Alvarez et al. 2015; Papadatou et al. 2016; Charman 2014b; Madrid-Costa et al. 2013) and apodized lenses (Davison and Simpson 2006). Although the results of this study are based on objective measurements and computer simulations, they can be the basis for a series of experiments in subjects to test their visual performance with different multifocal designs.

Chapter 6
Visual simulation of different optical designs for presbyopia: a pilot study

6. Visual simulation of different optical designs for presbyopia: a pilot study

6.1 Introduction

Presbyopia and cataract are both related to the aging process of the crystalline lens of the human eye. Presbyopia is related to the gradual accommodative loss (Werner et al. 2000), which is perceived as impairment in near vision clarity (Charman 2008), whereas cataract is the progressive clouding of the crystalline lens (Kessel et al. 2016). Although the onset of presbyopia normally occurs earlier than the onset of cataract, at a certain point both situations might co-exist and can cause severe problems in visual performance.

When the clouding of the crystalline lens affects vision significantly (e.g. blurred vision, halos around light sources), then cataract surgery is performed for replacing the crystalline lens with an IOL (Kessel et al. 2016; Charman 2014b). In many cases, the patient receives a monofocal IOL that restores vision at one distance (usually distance). The drawback of this solution is the need of spectacles to achieve near vision (Charman 2014b). Nevertheless, some patients, especially the ones that used to be emmetropes prior to the onset of presbyopia, may consider a multifocal IOL as an option, which aims to correct vision at multiple distances, thus reducing spectacle dependence (Alió et al. 2011; Charman 2014b).

Since the implantation of the first IOL (Sarwar and Modi 2014), a wide variety of IOLs, based on simultaneous vision strategy (Charman 2014a; Charman 2014b), either refractive or diffractive, are available following different designs for achieving multifocality (Charman 2014b; Bradley, Kollbaum, and Thibos 2014). The most typical example is a diffractive IOL which distributes the light between two principal foci, offering acceptable far and near vision (Davison and Simpson 2006). The superposition of two diffractive profiles led to the creation of trifocal designs, adjusted for offering far, near and intermediate vision (Gatinel et al. 2011). More recently, extended range IOLs appeared in the market. These IOLs, as their name indicates, aim to provide good vision within an extended range of distances by increasing the DoF of the patient (Béatrice Cochener 2016).

Although all the IOLs pass some quality tests before they are approved for use in cataract surgery, the visual performance can differ from laboratory measurements

(Domínguez-Vicent et al. 2015; Montés-Micó et al. 2012; Montés-Micó et al. 2013; David Madrid-Costa et al. 2013; D. Madrid-Costa et al. 2014; Gatinel and Houbrechts 2013). A plethora of factors, described in earlier chapters of the present thesis, can be the reasons for patient's dissatisfaction with a multifocal IOL. These factors range from issues related to the lens design (Charman 2014b), dispositions of the IOL after the implantation (Petternel et al. 2004), the effect of ocular aberrations (Ortiz et al. 2008) or the suppression ability of the patient (Alais and Blake 2005).

Defocus curves are a useful tool in clinical practice for addressing the visual performance with presbyopic corrections, overcoming issues that arise with distance visual acuity measurements (Buckhurst et al. 2012; Alio et al. 2012). Defocus curves provide detailed information of VA at different levels of defocus induced with trial lenses, or at different distances, allowing for the clinician to evaluate the visual performance of the patient (Buckhurst et al. 2012; Wolffsohn et al. 2013).

In the present study, different presbyopic corrections were simulated and then defocus curves were obtained for evaluating the high and low contrast VA at different levels of defocus. The corrections included a monofocal design, an angular bifocal design, a radial bifocal design, a radial trifocal design and an extended range design. For studying the effect of HOAs in VA, corneal HOAs from a model cornea corresponding to a 60 years old eye, were also added to each design.

6.2 Methods

6.2.1 Subjects

Three subjects without any ocular pathology were enrolled to participate in this study. The mean age (mean ± SD) was 27.33 ± 1.53 years old. Two of the participants were emmetropes and the third one was myopic. All three exhibited Snellen visual acuity (VA) of 20/20 or better. The study adhered to the tenets of the Declaration of Helsinki and the participants gave written informed consent.

6.2.2 Presbyopic solutions designs

Four different multifocal and one monofocal corrections were generated (see in Figure 6.1) using custom software based on Fourier optics in Matlab (Mathworks, Inc., Natic, MA). All the designs had a diameter of 6 mm. The monofocal was generated with a wavefront containing solely –0.27 μm of SA for a 6–mm pupil. This value of SA was also used in the rest of the designs, since it is a SA value commonly used in

commercially available IOLs for compensating the positive corneal SA (Wang and Koch 2007).

The multifocal designs were created by dividing the wavefront into different zones; each of these zones had a different amount of defocus intended for different working distances (e.g. far, intermediate and near). The two bifocal designs had one zone with zero defocus (intended for far vision) and another zone with a defocus of 2.5 D, which was the addition power, intended for near vision. The difference between the two bifocals was the distribution of the zones along the wavefront, as it can be seen in Figure 6.1. One had an angular design, with the same area for both zones, whereas the other one had a radial concentric center–distance design. The central circular zone had a diameter of 3 mm, the same as the peripheral annular zone. The radial trifocal design consisted of three different concentric zones, each one with a different amount of defocus: 0 D, 1.25 D and 2.5 D, starting from the center. The central zone presented a radius of 1.10 mm, whereas the mid annular and the peripheral annular zones accounted for 0.55 mm and 1.35 mm, respectively. The last design had four concentric zones, each one of them with a refractive power of 2.5 D, 2 D, 1.75 D and 0 D starting from the center, and accounting for 0.99 mm, 0.36 mm, 0.12 mm and 1.53 mm, respectively. This design was meant to provide an extended range correction.

6.2.3 Generation of optotypes

An ETDRS optotype was used for obtaining the defocus curves for each design and subject. For this purpose, the optotype was convolved with the PSF generated by each design at different vergences (Figure 6.2). A through focus was simulated for each design by adding the proper amount of Zernike defocus (C_2^0), achieving an interval of vergences ranging from 1 D to –3.5 D, in steps of 0.25 D. Therefore, there were 19 images for each design. Also, for evaluating how corneal aberrations could affect the visual performance, 60–years old typical corneal HOAs (up to 7th order), taken by a model cornea (Navarro, Rozema, and Tassignon 2013), were added to each design's wavefront. The SA of the model cornea was +0.19 μm for a pupil size of 5 mm. All the simulations were performed for a wavelength of 550 nm and for a 4.5–mm pupil, since it has been reported as a typical pupil size for presbyopic subjects under photopic conditions (Chateau et al. 1996). Styles–Crawford apodization effect was taken into account in the simulations by applying an amplitude Gaussian function to the wavefront (David A. Atchison, Marcos, and Scott 2003).

6.2.4 Defocus curves measurements

High contrast visual acuity (HCVA) and low contrast (10%) visual acuity (LCVA) were measured monocularly for each subject and design under two conditions: without and with taking into account the corneal aberrations of the model cornea. Subjects' were instructed to read the letters of the optotypes in a screen with a luminance of approximately 100 cd/m^2 located at 1.5 meters from the participant. Participants looked at the optotypes through a 3–mm pupil, thus reducing drastically the effect of their own ocular aberrations (Liang and Williams 1997). Since all the participants were young and did not present any accommodative problem, accommodation to 1.5 m (0.67 D) was not an issue. Subjects' wore their correction, if needed, when doing the procedure. The different designs were presented randomly to each subject.

In total, 20 defocus curves were recorded per subject: five for each of the designs with the high contrast optotype, five with the low contrast optotype; the same procedure was repeated for adding to each design the corneal HOAs.

6.2.5 Calculation of the interval above VA threshold

In order to further analyze the defocus curves, the part of each defocus curve were the VA was equal or better than 0.2 logMAR was calculated. For this purpose, and to be more precise than 0.25 D, the curves were interpolated using a vergence step of 0.01 D. The 0.2 logMAR threshold can be considered as the limit where 50% of the people start to experience difficulties in reading tasks (Chateau et al. 1996).

6.3 Results

Figure 6.3 shows the mean defocus curves obtained for the monofocal design with the high and low contrast ETDRS chart. The x–axis of the charts represents the vergence (in D) whereas the y–axis expresses the VA (in logMAR). The dashed lines represent the 0.0 logMAR VA. Black curves correspond to the HCVA and grey curves account for the LCVA. The left chart of the figure shows the results without the corneal HOAs of the model cornea whereas the right chart presents the results when corneal HOAs were include. The error bars represent one SD. The peak of VA is located both for HCVA and LCVA at 0 D. HCVA was always higher compared to the LCVA, with

the effect being more pronounced in the presence of corneal HOAs. For the LCVA, after the –2.5 D of vergence, the subjects could not discriminate any letter of the chart.
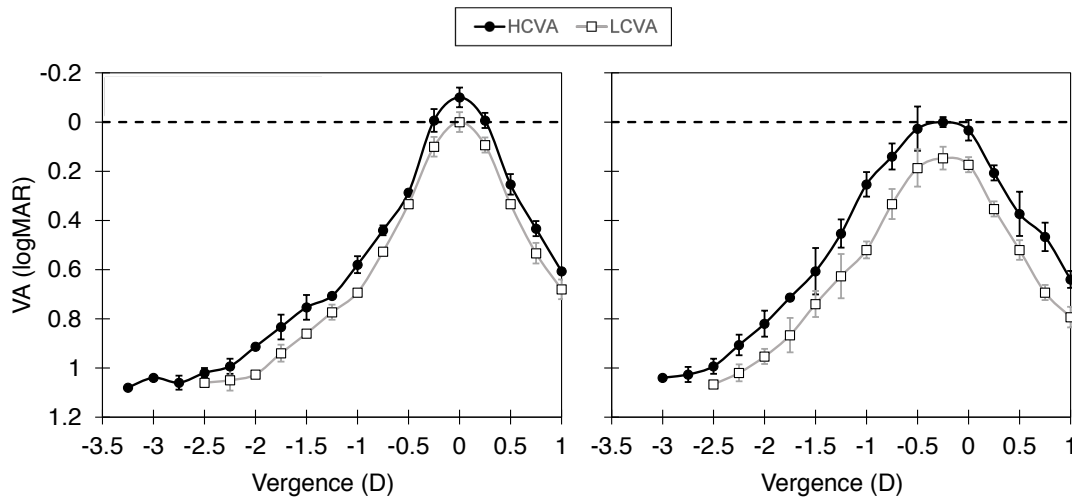

Figure 6.3: Mean defocus curves (in logMAR) obtained for the monofocal design without (left chart) and with (right chart) the addition of corneal HOAs. Black curves correspond to the HCVA, whereas grey curves present the LCVA. Error bars represent one standard deviation (SD). Note that the scale in the y-axis is backwards, for a more intuitive interpretation.

In Figure 6.4, the mean defocus curves of HCVA and LCVA are represented for the multifocal designs without the addition of corneal HOAs. In each case, the HCVA defocus curve exhibited greater VA values than the LCVA defocus curve.

The left upper chart of the figure shows the mean defocus curves for the angular bifocal design. Both HCVA and LCVA defocus curves revealed symmetry for this design, with the peaks located at 0 and -2.5 D, respectively. The right upper chart presents the defocus curves for the radial concentric center–distance bifocal design. The range of the focus for distance (peak at 0 D) was wider than the range of the focus for near (peak at –2.5 D) in both HCVA and LCVA defocus curves. The left bottom panel of the figure shows the mean defocus curves of the radial trifocal design. Although the HCVA defocus curve showed good VA outcomes at the peaks of the trifocal, the LCVA defocus curve exhibited poor VA outcomes, particularly in the distance focus. Last, the right bottom panel illustrates the mean defocus curves obtained for the extended range design. The HCVA defocus curve showed good VA for distance vision and at a range between –1.5 D and –3.5 D. The LCVA defocus curve showed poorer visual outcomes within the same range.

Figure 6.5 illustrates the mean defocus curves of the multifocal designs when the corneal HOAs were added to each design. In general, both HCVA and LCVA defocus

curves showed similar behaviour with the ones presented in Figure 6.4. Comparing to Figure 6.4, the addition of corneal HOAs to the designs led to poorer visual outcomes, most notably in the HCVA defocus curves of the trifocal and the extended range designs. The LCVA defocus curves were less affected by the corneal HOAs for the trifocal and the extended range designs. In the case of the extended range design, the LCVA defocus curve was slightly improved for near vision.

Figure 6.6 illustrates the interval of VA greater than 0.2 logMAR in the defocus curves of HCVA and LCVA, for each design. The left panel of the figure is the condition without corneal HOAs, whereas the right panel shows the results when corneal HOAs were added. The intervals decreased dramatically, especially in the cases of the radial trifocal and the extended range designs.

6.4 Discussion

The aim of this study was to evaluate the VA with different optical designs and moreover, to assess the effect of corneal HOAs from a 60 years old eye on VA outcomes with each design. For this purpose, we chose to obtain the defocus curves for HCVA and LCVA in a range of vergences from 1 D up to – 3.5 D. Although a defocus curve is a good way to test the efficacy of presbyopic solutions, previous studies have indicated issues regarding the ways of measuring it (Wolffsohn et al. 2013; Buckhurst et al. 2012). Typically, the defocus curves are measured through a range of different levels of spectacle defocus (Alfonso et al. 2009). This can lead to underestimation of the measured VA due to magnification effects induced by the lenses (although this can be resolved with a mathematical approach (Gupta, Wolffsohn, and Naroo 2008)). The latter were not the case in our study, since we presented to the subjects ETDRS optotypes that already had the proper level of defocus (see Figure 6.2), thus, the use of spectacle lenses was not necessary. Another way to obtain the defocus curve is by varying the distance from which the subject views the optotype (Hayashi, Manabe, and Hayashi 2009). However, this approach can be unattainable due to the need for controlling the angular image size and the luminance level but, in our study, the distance from the optotype and the luminance of the screen were fixed.

In the present study, we chose to measure the VA by means of obtaining defocus curves with a monofocal, an angular bifocal, a radial bifocal, a radial trifocal and an extended range design (see Figure 6.1), in an effort to cover the range of the available IOLs for

presbyopia and cataract surgery (Charman 2014a; Beatrice Cochener 2015). We evaluated the VA with a high contrast (100%) ETDRS chart and a low contrast (10%) ETDRS chart as has been described elsewhere (Regan and Neima 1983), with and without the addition of corneal HOAs. Corneal HOAs, in particular the SA that changes with aging, (D.A. Atchison 1991; Eppig et al. 2009; Rocha et al. 2007; Marcos, Barbero, and Jiménez-Alfaro 2005; Navarro, Rozema, and Tassignon 2013), have been found to affect the vision with presbyopic solutions (Applegate, Sarver, and Khemsara 2002; Roorda 2011). For simulating the effect of aging corneal HOAs on vision, we chose to add in our designs corneal HOAs of a 60 years old eye (Navarro, Rozema, and Tassignon 2013), which is more likely to undergo cataract surgery. In general, the defocus curves of every design were affected by the addition of corneal HOAs, especially the LCVA curves which is an expected outcome since HOAs affect particularly low contrast vision (Oshika et al. 2006). The least differences between HCVA and LCVA defocus curves were spotted in the case of the monofocal design when corneal HOAs were absent (see in Figure 6.3). The HCVA defocus curves in Figure 6.4 showed that the participants achieved good visual outcomes with every design without the effect of corneal HOAs. Regarding the LCVA defocus curves, both bifocal designs yielded better visual outcomes whereas the radial trifocal and the extended range design resulted in poor visual outcomes: in far vision for the trifocal and in near and intermediate vision for the extended range design. Regarding the effect of corneal HOAs on VA, in Figure 6.5, it can be observed from both HCVA and LCVA defocus curves that the VA decreased although the DoF was increased. This is the trade-off that exists between the optical quality and the DoF; aberrations make the quality worse, but they can improve DoF (Rocha et al. 2007; Marcos, Barbero, and Jiménez-Alfaro 2005). The least affected of the addition of the corneal HOAs was found to be both the HCVA and LCVA with the angular bifocal design, whereas the LCVA of the extended range design was slightly improved for near vision (after -2.5 D of vergence). Although we did not use spectacle defocus for obtaining the defocus curves, our defocus curves for HCVA are in agreement with the ones in previous studies where defocus curves were recorded for evaluating VA in eyes implanted with monofocal and bifocal IOLs (Buckhurst et al. 2012; Pieh et al. 2002; Cillino et al. 2008; Alfonso et al. 2009).

Figure 6.6 shows the total range for HCVA and LCVA equal or better than 0.2 logMAR, for each design. For the condition without the corneal HOAs, the larger range

in HCVA was achieved with the radial trifocal design and the larger range in LCVA was achieved with the extended range design. On the other hand, for the condition where the corneal HOAs were added to the designs, larger HCVA and LCVA ranges were achieved with the monofocal IOL. These results suggest that although multifocal designs can offer vision in more than one range, VA with multifocal designs is more affected by HOAs than VA with monofocal designs.

Although this study can offer a useful insight of how HCVA and LCVA behave with different optical designs for presbyopia and cataract treatment, it has several limitations. One of these limitations is the small sample of participants, which does not allow for generalizing our outcomes to the larger population. Nonetheless, it should be noticed that the outcomes did not vary greatly among the three participants. Another limitation is the fact that the designs presented here were simulated computationally. Although they can replicate the theoretical optical performance of some commercially available IOLs, they cannot substitute the optical properties of real IOLs such as visual artefacts of diffractive or refractive designs that can impact visual performance (Davison and Simpson 2006; Artigas et al. 2007; Żelichowska et al. 2008). Also, the corneal HOAs set that we used was from a model cornea and represents mean values for a healthy 60 years old cornea; however, ocular aberrations, in particular SA, can significantly vary among the population, leading to different visual outcomes among individuals, even if they are corrected with the same design (Rocha et al. 2007; Porter et al. 2001). Last, another limitation is that the designs for this study were all created assuming monochromatic light (550 nm), hence not taking into account possible effects of chromatic aberration (Thibos, Bradley, and Still 1991).

In conclusion, this study offers an evaluation of both HCVA and LCVA with simulated designs that share similarities with some available IOLs designs and evaluates also the effect of corneal HOAs on VA. The methodology followed here is easy and low-cost and can be applied for guiding the presbyopic subjects in the selection of the design that fits better their visual needs.

Chapter 7
General conclusions and future work

7. General conclusions and future work

The present PhD Thesis aimed to provide an evaluation of both optical and visual performance of different optical designs for presbyopia and cataract treatment, as well as introducing and testing new methodologies to generate presbyopic solutions. The VUaMTF metric and the straylight measurements gave the opportunity to objectively characterize the optical quality of commercially available IOLs. The power profiles of the multifocal CLs granted useful information about the power distribution of these lenses and how it varies as a function of pupil size. Moreover, the temporal multiplexing with AO methodology can be useful for evaluating the visual performance of patients who wish to try different simultaneous vision multifocal designs before surgery. Finally, the simulations of different optical designs with Fourier optics allowed for comparisons of high and low contrast VA achieved with each design, with and without corneal HOAs. This can be a helpful tool for clinicians, as it allows them to evaluate approximately how different presbyopic designs (bifocal, trifocal, extended range) behave for each patient beforehand.

The main conclusions of the studies presented in this PhD Thesis are:

- The implementation of the VUaMTF metric describes in a concise way the optical quality of IOLs (or other optical solutions) by means of defocus and spatial frequency, hence allowing for fast comparisons between different IOLs.

- The in vitro evaluation of IOLs in Chapter 3, showed that monofocal IOLs provide better optical quality for far vision comparing to diffractive IOLs. However, the latter have the potential to provide vision in other distances and their optical quality was found to be less affected by the pupil size. Hence, the selection between monofocal or multifocal IOL will depend on the patient, in the sense of his/her willing to trade-off excellent far vision for spectacle independence.

- In Chapter 3, the straylight levels of the IOLs were found to be lower than the straylight exhibited by the young healthy 20-years old crystalline lens. Diffractive IOLs found to have similar straylight values with monofocal IOLs. Subsequently, diffractive effects *per se* of these IOLs are not expected to elevate the postoperative straylight of the pseudophakic eye.

- The analysis of the power profiles of multifocal CLs provided an analytical approach for better understanding the interaction between pupil size and power distribution. Since the majority of multifocal CLs in the market are refractive and of concentric designs, the interaction between pupil size and the power distribution is paramount. Evidence about potential visual performance can be provided if the results are combined to pupil size data as shown in Chapter 4 and increase the successful fitting rate of these lenses.

- The use of temporal multiplexing and AO technology for generating presbyopic designs based on simultaneous vision has a large potential since it offers the opportunity to create different bifocal by varying the energy distributions and by manipulating aberrations like the astigmatism and the SA. Moreover, it is a non-invasive method for checking the visual performance of presbyopic patients with different designs and it can be the basis for offering customized solutions before the actual implantation of an IOL.

- Acceptable VA with multifocal designs can be achieved in multiple distances. However, it is affected by the particular design and characteristics of the presbyopic correction and the effect of aberrations, as shown in Chapter 6, especially in the cases where a trifocal or an extended range design was used. VA with a monofocal design found to be less affected both by contrast and aberrations, followed by the VA that was achieved with bifocal designs. This methodology could help also for selecting the appropriate type of presbyopic solution for each subject.

The studies of the present PhD Thesis can be the basis for future research line regarding the treatment of presbyopia:

- Combining in vitro measurements of commercially available IOLs with in vivo measurements of the same lenses in a large population, to see how well they correlate. It would be interesting to study how well the VUaMTF metric correlates with actual VA measurements in patients with IOLs implanted.

- Performing spectral analysis in explanted IOLs with elevated straylight levels for understanding the reasons behind the increased straylight in some pseudophakic eyes.

- Evaluating the effect of chromatic aberration on the optical quality of IOLs by performing in vitro measurements (as described in Chapters 2 and 3) at different wavelenghts.

- Following an analysis as the one presented in Chapter 4, to evaluate the effect of decentration on power profiles of multifocal CLs.

- Enrolling presbyopic patients for exploring the role of HOAs in visual performance with different optical designs, following non-invasive techniques such as the ones described in Chapters 5 and 6.

- Working on the creation of a device based on AO technology will allow to generate bifocal and trifocal simultaneous vision designs for evaluating the visual performance in daily clinical practice. With a faster deformable mirror, other types of correction could be achieved (e.g. trifocal, quadrafocal).

Bibliography

Bibliography

A., Fuensanta, and Nathan Doble. 2012. "The Human Eye and Adaptive Optics." In Topics in Adaptive Optics, edited by Robert Tyson. InTech. http://www.intechopen.com/books/topics-in-adaptive-optics/the-need-for-adaptive-optics-in-the-human-eye.

Agarwal, Sunita, Athiya Agarwal, and David J. Apple. 2002. Textbook of Ophthalmology. Jaypee Brothers Publishers.

Alais, David, and Randolph Blake, eds. 2005. Binocular Rivalry. Cambridge, Mass: MIT Press.

Alfonso, José F., Luis Fernández-Vega, Hussein Amhaz, Robert Montés-Micó, Beatriz Valcárcel, and Teresa Ferrer-Blasco. 2009. "Visual Function after Implantation of an Aspheric Bifocal Intraocular Lens." Journal of Cataract and Refractive Surgery 35 (5): 885–92.

Alfonso, José F., Luis Fernández-Vega, M. Begoña Baamonde, and Robert Montés-Micó. 2007. "Prospective Visual Evaluation of Apodized Diffractive Intraocular Lenses." Journal of Cataract and Refractive Surgery 33 (7): 1235–43.

Alió, Jorge L., Francisco Amparo, Dolores Ortiz, and Luis Moreno. 2009. "Corneal Multifocality with Excimer Laser for Presbyopia Correction." Current Opinion in Ophthalmology 20 (4): 264–71.

Alió, Jorge L., Bassam Elkady, Dolores Ortiz, and Gonzalo Bernabeu. 2008. "Clinical Outcomes and Intraocular Optical Quality of a Diffractive Multifocal Intraocular Lens with Asymmetrical Light Distribution." Journal of Cataract & Refractive Surgery 34 (6): 942–48.

Alió, Jorge L., David P. Piñero, Ana B. Plaza-Puche, and Maria Joanna Rodriguez Chan. 2011. "Visual Outcomes and Optical Performance of a Monofocal Intraocular Lens and a New-Generation Multifocal Intraocular Lens." Journal of Cataract and Refractive Surgery 37 (2): 241–50.

Alio, Jorge L., Ana B. Plaza-Puche, Jaime Javaloy, María José Ayala, Luis J. Moreno, and David P. Piñero. 2012. "Comparison of a New Refractive Multifocal Intraocular Lens with an Inferior Segmental near Add and a Diffractive Multifocal Intraocular Lens." Ophthalmology 119 (3): 555–63.

Alió, Jorge L., Ana B. Plaza-Puche, Raúl Montalban, and Paula Ortega. 2012. "Near Visual Outcomes with Single-Optic and Dual-Optic Accommodating Intraocular Lenses." Journal of Cataract and Refractive Surgery 38 (9): 1568–75.

Alió, Jorge L., Ana B. Plaza-Puche, David P. Piñero, Francisco Amparo, Ramón Jiménez, Jose L. Rodríguez-Prats, Jaime Javaloy, and Vanessa Pongo. 2011. "Optical Analysis, Reading Performance, and Quality-of-Life Evaluation after Implantation of a Diffractive Multifocal Intraocular Lens." Journal of Cataract and Refractive Surgery 37 (1): 27–37.

Amano, Shiro, Yuki Amano, Satoru Yamagami, Takashi Miyai, Kazunori Miyata, Tomokazu Samejima, and Tetsuro Oshika. 2004. "Age-Related Changes in Corneal and Ocular Higher-Order Wavefront Aberrations." American Journal of Ophthalmology 137 (6): 988–92.

Antona, Beatriz, Francisco Barra, Ana Barrio, Angel Gutierrez, Elena Piedrahita, and Yolanda Martin. 2008. "Comparing Methods of Determining Addition in Presbyopes." Clinical & Experimental Optometry 91 (3): 313–18.

Applegate, Raymond A., Edwin J. Sarver, and Vic Khemsara. 2002. "Are All Aberrations Equal?" Journal of Refractive Surgery (Thorofare, N.J.: 1995) 18 (5): S556–62.

Aramberri, Jaime. 2003. "Intraocular Lens Power Calculation after Corneal Refractive Surgery: Double-K Method." Journal of Cataract & Refractive Surgery 29 (11): 2063–68.

Artal, Pablo, Esther Berrio, Antonio Guirao, and Patricia Piers. 2002. "Contribution of the Cornea and Internal Surfaces to the Change of Ocular Aberrations with Age." Journal of the Optical Society of America A 19 (1): 137.

Artal, Pablo, Silvestre Manzanera, Patricia Piers, and Henk Weeber. 2010. "Visual Effect of the Combined Correction of Spherical and Longitudinal Chromatic Aberrations." Optics Express 18 (2): 1637–48.

Artigas, José M., José L. Menezo, Cristina Peris, Adelina Felipe, and Manuel Díaz-Llopis. 2007. "Image Quality with Multifocal Intraocular Lenses and the Effect of Pupil Size: Comparison of Refractive and Hybrid Refractive–diffractive Designs." Journal of Cataract & Refractive Surgery 33 (12): 2111–17.

Artigas, José M., Cristina Peris, Adelina Felipe, José L. Menezo, Isaias Sánchez-Cortina, and Norberto López-Gil. 2009. "Modulation Transfer Function: Rigid versus Foldable Phakic Intraocular Lenses." Journal of Cataract & Refractive Surgery 35 (4): 747–52.

Atchison, D. A. 1991. "Design of Aspheric Intraocular Lenses." Ophthalmic & Physiological Optics: The Journal of the British College of Ophthalmic Opticians (Optometrists) 11 (2): 137–46.

Atchison, D. A., M. J. Collins, C. F. Wildsoet, J. Christensen, and M. D. Waterworth. 1995. "Measurement of Monochromatic Ocular Aberrations of Human Eyes as a Function of Accommodation by the Howland Aberroscope Technique." Vision Research 35 (3): 313–23.

Atchison, David A., Stella Blazaki, Marwan Suheimat, Sotiris Plainis, and W. Neil Charman. 2016. "Do Small-Aperture Presbyopic Corrections Influence the Visual Field?" Ophthalmic & Physiological Optics: The Journal of the British College of Ophthalmic Opticians (Optometrists) 36 (1): 51–59.

Atchison, David A., Huanqing Guo, W. N. Charman, and S. W. Fisher. 2009. "Blur Limits for Defocus, Astigmatism and Trefoil." Vision Research 49 (19): 2393–2403.

Atchison, David A., Susana Marcos, and Dion H. Scott. 2003. "The Influence of the Stiles–Crawford Peak Location on Visual Performance." Vision Research 43 (6): 659–68.

Auffarth, Gerd. 2015. "Clinical Experience With Extended Range of Vision 1-Piece IOL." In . Ascrs. https://ascrs.confex.com/ascrs/15am/webprogram/Paper15907.html.

Babcock, H. W. 1953. "The Possibility of Compensating Astronomical Seeing." Publications of the Astronomical Society of the Pacific 65 (October): 229.

Bakaraju, Ravi C., Klaus Ehrmann, Darrin Falk, Arthur Ho, and Eric Papas. 2012. "Optical Performance of Multifocal Soft Contact Lenses via a Single-Pass Method." Optometry and Vision Science: Official Publication of the American Academy of Optometry 89 (8): 1107–18.

Barbero, Sergio, Susana Marcos, and Ignacio Jiménez-Alfaro. 2003. "Optical Aberrations of Intraocular Lenses Measured in Vivo and in Vitro." Journal of the Optical Society of America. A, Optics, Image Science, and Vision 20 (10): 1841–51.

Barbosa-Sabanero, Karla, Andrea Hoffmann, Chelsey Judge, Nicole Lightcap, Panagiotis A. Tsonis, and Katia Del Rio-Tsonis. 2012. "Lens and Retina Regeneration: New Perspectives from Model Organisms." The Biochemical Journal 447 (3): 321–34.

Barisić, Ante, Iva Dekaris, Nikica Gabrić, Maja Bohac, Ivana Romac, Ivana Mravicić, and Ratimir Lazić. 2008. "Comparison of Diffractive and Refractive Multifocal Intraocular Lenses in Presbyopia Treatment." Collegium Antropologicum 32 Suppl 2 (October): 27–31.

Baumeister, Martin, Jens Bühren, and Thomas Kohnen. 2009. "Tilt and Decentration of Spherical and Aspheric Intraocular Lenses: Effect on Higher-Order Aberrations." Journal of Cataract & Refractive Surgery 35 (6): 1006–12.

Beiko, George H. H. 2013. "Comparison of Visual Results with Accommodating Intraocular Lenses versus Mini-Monovision with a Monofocal Intraocular Lens." Journal of Cataract & Refractive Surgery 39 (1): 48–55.

Belda-Salmerón, Lurdes, David Madrid-Costa, Teresa Ferrer-Blasco, Santiago García-Lázaro, and Robert Montés-Micó. 2013. "In Vitro Power Profiles of Daily Disposable Contact Lenses." Contact Lens & Anterior Eye: The Journal of the British Contact Lens Association 36 (5): 247–52.

Bellucci, Roberto. 2013. "An Introduction to Intraocular Lenses: Material, Optics, Haptics, Design and Aberration." In ESASO Course Series, edited by J.L. Güell,

3:38–55. Basel: S. KARGER AG.
http://www.karger.com?doi=10.1159/000350902.

Bennett, Edward S. 2008. "Contact Lens Correction of Presbyopia." Clinical &
Experimental Optometry 91 (3): 265–78.

Berg, Thomas J. T. P. van den, L. J. (René) van Rijn, R. Kaper-Bongers, D. J.
Vonhoff, H. J. Völker-Dieben, G. Grabner, C. Nischler, et al. 2009. "Disability
Glare in the Aging Eye. Assessment and Impact on Driving." Journal of
Optometry 2 (3): 112–18.

Berg, T. J. van den. 1995. "Analysis of Intraocular Straylight, Especially in
Relation to Age." Optometry and Vision Science: Official Publication of the
American Academy of Optometry 72 (2): 52–59.

Bitsios, P., R. Prettyman, and E. Szabadi. 1996. "Changes in Autonomic Function
with Age: A Study of Pupillary Kinetics in Healthy Young and Old People." Age
and Ageing 25 (6): 432–38.

Blum, M., M. Büeler, C. Grätzel, J. Giger, and M. Aschwanden. 2012. "Optotune
Focus Tunable Lenses and Laser Speckle Reduction Based on Electroactive
Polymers." In , edited by Harald Schenk, Wibool Piyawattanametha, and Wilfried
Noell, 825207. doi:10.1117/12.902631.

Bonnel, Sébastien, Saddek Mohand-Said, and José-Alain Sahel. 2003. "The Aging
of the Retina." Experimental Gerontology 38 (8): 825–31.

Boreman, G. D. 2001. Modulation Transfer Function in Optical & Electro-Optical
Systems. Tutorial Texts in Optical Engineering, v. TT 52. Bellingham, Wash.,
USA: SPIE Press.

Bradley, Arthur, Peter S. Kollbaum, and Larry N. Thibos. 2014. Multifocal
correction providing improved quality of vision. US8894203 B2, filed February
27, 2012, and issued November 25, 2014.
http://www.google.ch/patents/US8894203.

Brierley, Lawrence. 2013. "Refractive Results after Implantation of a Light-
Adjustable Intraocular Lens in Postrefractive Surgery Cataract Patients."
Ophthalmology 120 (10): 1968–72.

Brigantic, Robert T., Michael C. Roggemann, Kenneth W. Bauer, and Byron M.
Welsh. 1997. "Image-Quality Metrics for Characterizing Adaptive Optics System
Performance." Applied Optics 36 (26): 6583.

Buckhurst, Phillip J., James S. Wolffsohn, Shehzad A. Naroo, Leon N. Davies,
Gurpreet K. Bhogal, Athina Kipioti, and Sunil Shah. 2012. "Multifocal Intraocular
Lens Differentiation Using Defocus Curves." Investigative Opthalmology &
Visual Science 53 (7): 3920.

Callina, Tina, and Tony P. Reynolds. 2006. "Traditional Methods for the Treatment of Presbyopia: Spectacles, Contact Lenses, Bifocal Contact Lenses." Ophthalmology Clinics of North America 19 (1): 25–33, v.

Carballo-Alvarez, Jesús, Jose M. Vazquez-Molini, Juan C. Sanz-Fernandez, Javier Garcia-Bella, Vicente Polo, Julián García-Feijoo, and Jose M. Martinez-de-la-Casa. 2015. "Visual Outcomes after Bilateral Trifocal Diffractive Intraocular Lens Implantation." BMC Ophthalmology 15: 26. doi:10.1186/s12886-015-0012-4.

Cardona, Genís, and Sílvia López. 2016. "Pupil Diameter, Working Distance and Illumination during Habitual Tasks. Implications for Simultaneous Vision Contact Lenses for Presbyopia." Journal of Optometry 9 (2): 78–84.

Carson, Daniel, Warren E. Hill, Xin Hong, and Mutlu Karakelle. 2014. "Optical Bench Performance of AcrySof(®) IQ ReSTOR(®), AT LISA(®) Tri, and FineVision(®) Intraocular Lenses." Clinical Ophthalmology (Auckland, N.Z.) 8: 2105–13.

Cerviño, Alejandro, Sarah L. Hosking, Robert Montés-Micó, and Jorge L. Alió. 2008. "Retinal Straylight in Patients with Monofocal and Multifocal Intraocular Lenses." Journal of Cataract and Refractive Surgery 34 (3): 441–46.

Chang, Daniel H., and Elizabeth A. Davis. 2006. "Phakic Intraocular Lenses." Current Opinion in Ophthalmology 17 (1): 99–104.

Chang, David F. 2008. Mastering Refractive IOLs: The Art and Science. SLACK Incorporated.

Charman, W. Neil. 2008. "The Eye in Focus: Accommodation and Presbyopia." Clinical & Experimental Optometry 91 (3): 207–25.

Charman, W. 2014a. "Developments in the Correction of Presbyopia I: Spectacle and Contact Lenses." Ophthalmic & Physiological Optics: The Journal of the British College of Ophthalmic Opticians (Optometrists) 34 (1): 8–29.

Charman, W. 2014b. "Developments in the Correction of Presbyopia II: Surgical Approaches." Ophthalmic and Physiological Optics 34 (4): 397–426.

Chateau, N., J. De Brabander, F. Bouchard, and H. Molenaar. 1996. "Infrared Pupillometry in Presbyopes Fitted with Soft Contact Lenses." Optometry and Vision Science: Official Publication of the American Academy of Optometry 73 (12): 733–41.

Cheng, Han, Justin K. Barnett, Abhiram S. Vilupuru, Jason D. Marsack, Sanjeev Kasthurirangan, Raymond A. Applegate, and Austin Roorda. 2004. "A Population Study on Changes in Wave Aberrations with Accommodation." Journal of Vision 4 (4): 272–80.

Chen, Li, Ben Singer, Antonio Guirao, Jason Porter, and David R. Williams. 2005. "Image Metrics for Predicting Subjective Image Quality." Optometry and

Vision Science: Official Publication of the American Academy of Optometry 82 (5): 358–69.

Chin, Sem Sem, Karen M. Hampson, and Edward A. H. Mallen. 2009. "Role of Ocular Aberrations in Dynamic Accommodation Control." Clinical & Experimental Optometry 92 (3): 227–37.

Cillino, Salvatore, Alessandra Casuccio, Francesco Di Pace, Raffaella Morreale, Francesco Pillitteri, Giovanni Cillino, and Gaetano Lodato. 2008. "One-Year Outcomes with New-Generation Multifocal Intraocular Lenses." Ophthalmology 115 (9): 1508–16.

Claoué, Charles. 2004. "Functional Vision after Cataract Removal with Multifocal and Accommodating Intraocular Lens Implantation: Prospective Comparative Evaluation of Array Multifocal and 1CU Accommodating Lenses." Journal of Cataract & Refractive Surgery 30 (10): 2088–91.

Cochener, Beatrice. 2015. "Patient Satisfaction With New Extended Range of Vision 1-Piece IOL." In . Ascrs. https://ascrs.confex.com/ascrs/15am/webprogram/Paper17532.html.

Cochener, Béatrice. 2016. "Clinical Outcomes of a New Extended Range of Vision Intraocular Lens: International Multicenter Concerto Study." Journal of Cataract & Refractive Surgery 42 (9): 1268–75.

Coppens, Joris E., Luuk Franssen, and Thomas J. T. P. van den Berg. 2006. "Reliability of the Compensation Comparison Method for Measuring Retinal Stray Light Studied Using Monte-Carlo Simulations." Journal of Biomedical Optics 11 (5): 054010..

Cox, Michael J. 2001. "Optics of the Human Eye D.A. Atchison, G. Smith; Butterworth-Heinemann, Oxford, 2000, 269 Pages, ISBN 0-7506-3775-7, £27.50." Ophthalmic and Physiological Optics 21 (5): 426–426.

Dai, Guangming. 2008. Correction of presbyopia using adaptive optics and associated methods. US7387387 B2, filed June 17, 2004, and issued June 17, 2008. http://www.google.ch/patents/US7387387.
Dalimier, Eugenie, and Chris Dainty. 2005. "Comparative Analysis of Deformable Mirrors for Ocular Adaptive Optics." Optics Express 13 (11): 4275.

Das, Kamal K., John C. Stover, Jim Schwiegerling, and Mutlu Karakelle. 2013. "Technique for Measuring Forward Light Scatter in Intraocular Lenses." Journal of Cataract and Refractive Surgery 39 (5): 770–78.

Datiles, M. B., and T. Gancayco. 1990. "Low Myopia with Low Astigmatic Correction Gives Cataract Surgery Patients Good Depth of Focus." Ophthalmology 97 (7): 922–26.

Davison, James A., and Michael J. Simpson. 2006. "History and Development of the Apodized Diffractive Intraocular Lens." Journal of Cataract & Refractive Surgery 32 (5): 849–58.

Dick, H. Burkhard, Frank Krummenauer, Oliver Schwenn, Romano Krist, and Norbert Pfeiffer. 1999. "Objective and Subjective Evaluation of Photic Phenomena after Monofocal and Multifocal Intraocular Lens implantation1." Ophthalmology 106 (10): 1878–86.

Dogru, Murat, Rie Honda, Masahiro Omoto, Ikuko Toda, Hiroshi Fujishima, Hiroyuki Arai, Mie Matsuyama, et al. 2005. "Early Visual Results with the 1CU Accommodating Intraocular Lens." Journal of Cataract and Refractive Surgery 31 (5): 895–902.

Domínguez-Vicent, Alberto, Jose Juan Esteve-Taboada, Antonio J. Del Águila-Carrasco, Teresa Ferrer-Blasco, and Robert Montés-Micó. 2015. "In Vitro Optical Quality Comparison between the Mini WELL Ready Progressive Multifocal and the TECNIS Symfony." Graefe's Archive for Clinical and Experimental Ophthalmology 254 (7): 1387–97.

Domínguez-Vicent, Alberto, Iván Marín-Franch, Jose Juan Esteve-Taboada, David Madrid-Costa, and Robert Montés-Micó. 2015. "Repeatability of in Vitro Power Profile Measurements for Multifocal Contact Lenses." Contact Lens & Anterior Eye: The Journal of the British Contact Lens Association 38 (3): 168–72.

Dorronsoro, Carlos, Jose Ramon Alonso-Sanz, Daniel Pascual, Aiswaryah Radhakrishnan, Miriam Velasco-OCana, Pablo Perez-Merino, and Susana Marcos. 2015. "Visual Performance and Perception with Bifocal and Trifocal Presbyopia Corrections Simulated Using a Hand-Held Simultaneous Vision Device." Investigative Ophthalmology & Visual Science 56 (7): 4306–4306.

Dorronsoro Díaz, Carlos, José Ramón Alonso Sanz, and Susana Marcos Celestino. 2015. Miniature Simultaneous Vision Simulator Instrument. WO/2015/049402, issued April 10, 2015. https://patentscope.wipo.int/search/en/detail.jsf?docId=WO2015049402.

Duane, Alex. 1908. "An Attempt to Determine the Normal Range of Accommodation at Various Ages, Being a Revision of Donder's Experiments." Transactions of the American Ophthalmological Society 11 (Pt 3): 634–41.

Elliott, D. B., and M. A. Bullimore. 1993. "Assessing the Reliability, Discriminative Ability, and Validity of Disability Glare Tests." Investigative Ophthalmology & Visual Science 34 (1): 108–19.

Eppig, Timo, Katja Scholz, André Löffler, Arthur Messner, and Achim Langenbucher. 2009. "Effect of Decentration and Tilt on the Image Quality of Aspheric Intraocular Lens Designs in a Model Eye." Journal of Cataract and Refractive Surgery 35 (6): 1091–1100.

Espandar, Ladan, Jay J. Meyer, and Majid Moshirfar. 2008. "Phakic Intraocular Lenses." Current Opinion in Ophthalmology 19 (4): 349–56.

Esteve-Taboada, José J., Antonio J. Del Águila-Carrasco, Iván Marín-Franch, Paula Bernal-Molina, Robert Montés-Micó, and Norberto López-Gil. 2015. "Opto-Mechanical Artificial Eye with Accommodative Ability." Optics Express 23 (15): 19396–404.

FAAO, Andrew Gasson FcOptom DCLP, and Judith A. Morris Msc FcOptom FAAO FIACLE. 2010. The Contact Lens Manual: A Practical Guide to Fitting, 4e. 4 edition. Edinburgh: Butterworth-Heinemann.

Felipe, A., J.M. Artigas, A. Díez-Ajenjo, C. García-Domene, and C. Peris. 2012. "Modulation Transfer Function of a Toric Intraocular Lens: Evaluation of the Changes Produced by Rotation and Tilt." Journal of Refractive Surgery 28 (5): 335–40.

Felipe, Adelina, Francisco Pastor, José M. Artigas, Amparo Diez-Ajenjo, Andrés Gené, and José L. Menezo. 2010. "Correlation between Optics Quality of Multifocal Intraocular Lenses and Visual Acuity: Tolerance to Modulation Transfer Function Decay." Journal of Cataract & Refractive Surgery 36 (4): 557–62.

Fernández, E. J., I. Iglesias, and P. Artal. 2001. "Closed-Loop Adaptive Optics in the Human Eye." Optics Letters 26 (10): 746–48.

Fernández, Enrique J., and Pablo Artal. 2003. "Membrane Deformable Mirror for Adaptive Optics: Performance Limits in Visual Optics." Optics Express 11 (9): 1056.

Fernández, Enrique J., and Pablo Artal. 2003. 2005. "Study on the Effects of Monochromatic Aberrations in the Accommodation Response by Using Adaptive Optics." Journal of the Optical Society of America. A, Optics, Image Science, and Vision 22 (9): 1732–38.

Fernández, Enrique J., Pedro M. Prieto, and Pablo Artal. 2009. "Binocular Adaptive Optics Visual Simulator." Optics Letters 34 (17): 2628.

FitzGerrell, Alan R., Edward R. Dowski, and W. Thomas Cathey. 1997. "Defocus Transfer Function for Circularly Symmetric Pupils." Applied Optics 36 (23):

Ford, Joshua, Liliana Werner, and Nick Mamalis. 2014. "Adjustable Intraocular Lens Power Technology." Journal of Cataract & Refractive Surgery 40 (7): 1205–23.

Franssen, Luuk, Joris E. Coppens, and Thomas J. T. P. van den Berg. 2006. "Compensation Comparison Method for Assessment of Retinal Straylight." Investigative Ophthalmology & Visual Science 47 (2): 768–76.

Friese, Christoph, Armin Werber, Florian Krogmann, Wolfgang Mönch, and Hans Zappe. 2007. "Materials, Effects and Components for Tunable Micro-Optics." IEEJ Transactions on Electrical and Electronic Engineering 2 (3): 232–48.

Gale, R. P., M. Saldana, R. L. Johnston, B. Zuberbuhler, and M. McKibbin. 2009. "Benchmark Standards for Refractive Outcomes after NHS Cataract Surgery." Eye (London, England) 23 (1): 149–52.

Galor, Anat, Maricely Gonzalez, David Goldman, and Terrence P. O'Brien. 2009. "Intraocular Lens Exchange Surgery in Dissatisfied Patients with Refractive Intraocular Lenses." Journal of Cataract & Refractive Surgery 35 (10): 1706–10.

Gambra, Enrique, Lucie Sawides, Carlos Dorronsoro, and Susana Marcos. 2009. "Accommodative Lag and Fluctuations When Optical Aberrations Are Manipulated." Journal of Vision 9 (6): 4.1–15.

García-Lázaro, Santiago, Teresa Ferrer-Blasco, David Madrid-Costa, César Albarrán-Diego, and Robert Montés-Micó. 2015. "Visual Performance of Four Simultaneous-Image Multifocal Contact Lenses under Dim and Glare Conditions." Eye & Contact Lens 41 (1): 19–24.

Garzón, Nuria, Francisco Poyales, Begoña Ortíz de Zárate, Jose Luis Ruiz-García, and Juan Antonio Quiroga. 2015. "Evaluation of Rotation and Visual Outcomes after Implantation of Monofocal and Multifocal Toric Intraocular Lenses." Journal of Refractive Surgery (Thorofare, N.J.: 1995) 31 (2): 90–97.

Gatinel, Damien, and Yvette Houbrechts. 2013. "Comparison of Bifocal and Trifocal Diffractive and Refractive Intraocular Lenses Using an Optical Bench." Journal of Cataract and Refractive Surgery 39 (7): 1093–99.

Gatinel, Damien, Christophe Pagnoulle, Yvette Houbrechts, and Laure Gobin. 2011. "Design and Qualification of a Diffractive Trifocal Optical Profile for Intraocular Lenses." Journal of Cataract & Refractive Surgery 37 (11): 2060–67.

Ginis, Harilaos, Onurcan Sahin, Alexandros Pennos, and Pablo Artal. 2014. "Compact Optical Integration Instrument to Measure Intraocular Straylight." Biomedical Optics Express 5 (9): 3036.

Ginsburg, Arthur P. 2006. "Contrast Sensitivity: Determining the Visual Quality and Function of Cataract, Intraocular Lenses and Refractive Surgery." Current Opinion in Ophthalmology 17 (1): 19–26.

Glasser, Adrian. 2008. "Restoration of Accommodation: Surgical Options for Correction of Presbyopia." Clinical & Experimental Optometry 91 (3): 279–95.

Glasser, Adrian, and Melanie C. W. Campbell. 1998. "Presbyopia and the Optical Changes in the Human Crystalline Lens with Age." Vision Research 38 (2): 209–29. doi:10.1016/S0042-6989(97)00102-8.

Gracia, Pablo de, Carlos Dorronsoro, and Susana Marcos. 2013. "Multiple Zone Multifocal Phase Designs." Optics Letters 38 (18): 3526–29.

Gracia, Pablo de, Carlos Dorronsoro, Álvaro Sánchez-González, Lucie Sawides, and Susana Marcos. 2013. "Experimental Simulation of Simultaneous Vision." Investigative Ophthalmology & Visual Science 54 (1): 415–22.

Grosvenor, T. 1987. "Reduction in Axial Length with Age: An Emmetropizing Mechanism for the Adult Eye?" American Journal of Optometry and Physiological Optics 64 (9): 657–63.

Gupta, Navneet, James S. W. Wolffsohn, and Shehzad A. Naroo. 2008. "Optimizing Measurement of Subjective Amplitude of Accommodation with Defocus Curves." Journal of Cataract and Refractive Surgery 34 (8): 1329–38.

Hartridge, H. 1925. "HELMHOLTZ'S THEORY OF ACCOMMODATION." The British Journal of Ophthalmology 9 (10): 521–23.

Hayashi, Ken, Shin-Ichi Manabe, and Hideyuki Hayashi. 2009. "Visual Acuity from Far to near and Contrast Sensitivity in Eyes with a Diffractive Multifocal Intraocular Lens with a Low Addition Power." Journal of Cataract and Refractive Surgery 35 (12): 2070–76.

Hayashi, K., H. Hayashi, F. Nakao, and F. Hayashi. 1999. "Intraocular Lens Tilt and Decentration after Implantation in Eyes with Glaucoma." Journal of Cataract and Refractive Surgery 25 (11): 1515–20.

Hofmann, Thomas, Bruno Zuberbuhler, Alejandro Cervino, Robert Montés-Micó, and Eduard Haefliger. 2009. "Retinal Straylight and Complaint Scores 18 Months after Implantation of the AcrySof Monofocal and ReSTOR Diffractive Intraocular Lenses." Journal of Refractive Surgery (Thorofare, N.J.: 1995) 25 (6): 485–92.

Holden, Brien A., Timothy R. Fricke, S. May Ho, Reg Wong, Gerhard Schlenther, Sonja Cronjé, Anthea Burnett, Eric Papas, Kovin S. Naidoo, and Kevin D. Frick. 2008. "Global Vision Impairment due to Uncorrected Presbyopia." Archives of Ophthalmology (Chicago, Ill.: 1960) 126 (12): 1731–39.

Holladay, J.T., P.A. Piers, G. Koranyi, der Mooren Van, and N.E.S. Norrby. 2002. "A New Intraocular Lens Design to Reduce Spherical Aberration of Pseudophakic Eyes." Journal of Refractive Surgery 18 (6): 683–91.
Hong, X., N. Himebaugh, and L. N. Thibos. 2001. "On-Eye Evaluation of Optical Performance of Rigid and Soft Contact Lenses." Optometry and Vision Science: Official Publication of the American Academy of Optometry 78 (12): 872–80.
Hong, Xin, and Myoung Choi. 2010. "Influence of Ocular Longitudinal Chromatic Aberration on the Selection of Aspheric Intraocular Lenses." Optics Express 18 (25): 26175.

"IEEE Xplore Abstract - Large-Stroke MEMS Deformable Mirrors for Adaptive Optics." 2016. Accessed July 10. http://ieeexplore.ieee.org/xpl/login.jsp?tp=&arnumber=1638484&url=http%3A%2F%2Fieeexplore.ieee.org%2Fxpls%2Fabs_all.jsp%3Farnumber%3D1638484.

"ISO 11979-2:2014 - Ophthalmic Implants -- Intraocular Lenses -- Part 2: Optical Properties and Test Methods." 2016. ISO. Accessed September 1. http://www.iso.org/iso/catalogue_detail.htm?csnumber=55682.

"ISO 11979-9:2006 - Ophthalmic Implants -- Intraocular Lenses -- Part 9: Multifocal Intraocular Lenses." 2016. ISO. Accessed September 1. http://www.iso.org/iso/catalogue_detail.htm?csnumber=40919.

Ito, Mitsutoshi, Naoko Asano-Kato, Kazumi Fukagawa, Hiroyuki Arai, Ikuko Toda, and Kazuo Tsubota. 2005. "Ocular Integrity after Anterior Ciliary Sclerotomy and Scleral Ablation by the Er:YAG Laser." Journal of Refractive Surgery (Thorofare, N.J.: 1995) 21 (1): 77–81.

Jiang, Wenhan, and Huagui Li. 1990. "Hartmann-Shack Wavefront Sensing and Wavefront Control Algorithm." In , 1271:82–93. doi:10.1117/12.20396. Joannes, Luc, Tony Hough, Xavier Hutsebaut, Xavier Dubois, Renaud Ligot, Bruno Saoul, Philip Van Donink, and Kris De Coninck. 2010. "The Reproducibility of a New Power Mapping Instrument Based on the Phase Shifting Schlieren Method for the Measurement of Spherical and Toric Contact Lenses." Contact Lens & Anterior Eye: The Journal of the British Contact Lens Association 33 (1): 3–8.

Kalloniatis, Michael, and Charles Luu. 1995. "Temporal Resolution." In Webvision: The Organization of the Retina and Visual System, edited by Helga Kolb, Eduardo Fernandez, and Ralph Nelson. Salt Lake City (UT): University of Utah Health Sciences Center. http://www.ncbi.nlm.nih.gov/books/NBK11559/.

Kaymak, H., F. Höhn, D. R. H. Breyer, P. Hagen, K. Klabe, R. H. Gerl, M. Mueller, G. U. Auffarth, M. Gerl, and F. T. A. Kretz. 2016. "[Functional Results 3 Months after Implantation of an 'Extended Range of Vision' Intraocular Lens]." Klinische Monatsblatter Fur Augenheilkunde, July.

Kessel, Line, Jens Andresen, Ditte Erngaard, Per Flesner, Britta Tendal, and Jesper Hjortdal. 2016. "Indication for Cataract Surgery. Do We Have Evidence of Who Will Benefit from Surgery? A Systematic Review and Meta-analysis." Acta Ophthalmologica 94 (1): 10–20.

Kim, Myoung Joon, Len Zheleznyak, Scott MacRae, Hungwon Tchah, and Geunyoung Yoon. 2011. "Objective Evaluation of through-Focus Optical Performance of Presbyopia-Correcting Intraocular Lenses Using an Optical Bench System." Journal of Cataract & Refractive Surgery 37 (7): 1305–12.

Koch, Douglas D., Steven W. Samuelson, Elizabeth A. Haft, and Lawrence M. Merin. 1991. "Pupillary and Responsiveness." Ophthalmology 98 (7): 1030–35.

Kohnen, Thomas, David Allen, Catherine Boureau, Philippe Dublineau, Christian Hartmann, Ekkehard Mehdorn, Pascal Rozot, and Giorgio Tassinari. 2006. "European Multicenter Study of the AcrySof ReSTOR Apodized Diffractive Intraocular Lens." Ophthalmology 113 (4): 584.e1.

Kohnen, Thomas, Rudy Nuijts, Pierre Levy, Eduard Haefliger, and José F. Alfonso. 2009. "Visual Function after Bilateral Implantation of Apodized Diffractive Aspheric Multifocal Intraocular Lenses with a +3.0 D Addition." Journal of Cataract and Refractive Surgery 35 (12): 2062–69.

Koretz, Jane F., Paul L. Kaufman, Michael W. Neider, and Patrick A. Goeckner. 1989. "Accommodation and Presbyopia in the Human Eye—aging of the Anterior Segment." Vision Research 29 (12): 1685–92.

Kozak, Igor. 2014. "Retinal Imaging Using Adaptive Optics Technology." Saudi Journal of Ophthalmology 28 (2): 117–22.

Kragha, I. K. O. K. 1986. "Amplitude of Accommodation: Population and Methodological Differences." Ophthalmic and Physiological Optics 6 (1): 75–80.

Kusel, R., and B. Rassow. 1991. "Optical Properties of the Diffractive Intraocular Lens." European Journal of Implant and Refractive Surgery 3 (2): 117–22.

Labuz, Grzegorz, Eleni Papadatou, Thomas J. T. P. Van Den Berg, Fernando Vargas-Martin, Norberto Lopez-Gil, and Nicolaas J. Reus. 2016. "Straylight from Explanted Intraocular Lenses." Investigative Ophthalmology & Visual Science 57 (12). http://iovs.arvojournals.org/article.aspx?articleid=2560380&resultClick=1.

Łabuz, Grzegorz, Nicolaas J. Reus, and Thomas J. T. P. van den Berg. 2015. "Ocular Straylight in the Normal Pseudophakic Eye." Journal of Cataract and Refractive Surgery 41 (7): 1406–15.

Łabuz, Grzegorz, Fernando Vargas-Martín, Thomas J. T. P. van den Berg, and Norberto López-Gil. 2015. "Method for in Vitro Assessment of Straylight from Intraocular Lenses." Biomedical Optics Express 6 (11): 4457–64.

Lane, Stephen S., Mike Morris, Lee Nordan, Mark Packer, Nicholas Tarantino, and R. Bruce Wallace. 2006. "Multifocal Intraocular Lenses." Ophthalmology Clinics of North America 19 (1): 89–105, vi.

Langeslag, Michelle J. M., Marrie van der Mooren, George H. H. Beiko, and Patricia A. Piers. 2014. "Impact of Intraocular Lens Material and Design on Light Scatter: In Vitro Study." Journal of Cataract and Refractive Surgery 40 (12): 2120–27.

Lapid-Gortzak, Ruth, Ivanka J. E. van der Meulen, Jan Willem van der Linden, Maarten P. Mourits, and Thomas J. T. P. van den Berg. 2014. "Straylight before and after Phacoemulsification in Eyes with Preoperative Corrected Distance

Visual Acuity Better than 0.1 logMAR." Journal of Cataract and Refractive Surgery 40 (5): 748–55.

Lens, Al, Sheila Coyne Nemeth, and Janice K. Ledford. 2008. Ocular Anatomy and Physiology. SLACK Incorporated.

Liang, Junzhong, Bernhard Grimm, Stefan Goelz, and Josef F. Bille. 1994. "Objective Measurement of Wave Aberrations of the Human Eye with the Use of a Hartmann–Shack Wave-Front Sensor." Journal of the Optical Society of America A 11 (7): 1949.

Liang, Junzhong, and David R. Williams. 1997. "Aberrations and Retinal Image Quality of the Normal Human Eye." Journal of the Optical Society of America A 14 (11): 2873.

Liang, J., D. R. Williams, and D. T. Miller. 1997. "Supernormal Vision and High-Resolution Retinal Imaging through Adaptive Optics." Journal of the Optical Society of America. A, Optics, Image Science, and Vision 14 (11): 2884–92. "Looking Deep at Extended Depth-of-Focus IOLs." 2016. Accessed July 9. http://ois.net/looking-deep-at-extended-depth-of-focus-iols/.

Lopez-Gil, N., and V. Fernandez-Sanchez. 2010. "The Change of Spherical Aberration during Accommodation and Its Effect on the Accommodation Response." Journal of Vision 10 (13): 12–12.

Lovisolo, Carlo F., and Dan Z. Reinstein. 2005. "Phakic Intraocular Lenses." Survey of Ophthalmology 50 (6): 549–87.

Lyle, W. M. 1971. "Changes in Corneal Astigmatism with Age." American Journal of Optometry and Archives of American Academy of Optometry 48 (6): 467–78.

Madrid-Costa, David, Javier Ruiz-Alcocer, Teresa Ferrer-Blasco, Santiago García-Lázaro, and Robert Montés-Micó. 2013. "Optical Quality Differences Between Three Multifocal Intraocular Lenses: Bifocal Low Add, Bifocal Moderate Add, and Trifocal." Journal of Refractive Surgery 29 (11): 749–54.

Madrid-Costa, D., J. Ruiz-Alcocer, T. Ferrer-Blasco, S. García-Lázaro, and R. Montés-Micó. 2014. "In Vitro Optical Performance of a New Aberration-Free Intraocular Lens." Eye (London, England) 28 (5): 614–20.

Madrid-Costa, D., J. Ruiz-Alcocer, S. García-Lázaro, T. Ferrer-Blasco, and R. Montés-Micó. 2015. "Optical Power Distribution of Refractive and Aspheric Multifocal Contact Lenses: Effect of Pupil Size." Contact Lens & Anterior Eye: The Journal of the British Contact Lens Association 38 (5): 317–21.

Malyugin, Boris, Suzy Antonian, and Brandon D. Lohman. 2008. "Anterior Ciliary Sclerotomy Using Collagen T-Shaped Implants for Treatment of Presbyopia." Annals of Ophthalmology (Skokie, Ill.) 40 (3-4): 130–36.

Manzanera, Silvestre, Pedro M. Prieto, Diego B. Ayala, Joseph M. Lindacher, and Pablo Artal. 2007. "Liquid Crystal Adaptive Optics Visual Simulator: Application to Testing and Design of Ophthalmic Optical Elements." Optics Express 15 (24): 16177–88.

Marcos, Susana, Sergio Barbero, and Ignacio Jiménez-Alfaro. 2005. "Optical Quality and Depth-of-Field of Eyes Implanted with Spherical and Aspheric Intraocular Lenses." Journal of Refractive Surgery (Thorofare, N.J.: 1995) 21 (3): 223–35.

Marques, Eduardo. 2015. "Visual Outcomes of New Presbyopia-Correcting Extended Range of Vision IOL." In . Ascrs. https://ascrs.confex.com/ascrs/15am/webprogram/Paper16964.html.

Marsack, Jason D., Larry N. Thibos, and Raymond A. Applegate. 2004. "Metrics of Optical Quality Derived from Wave Aberrations Predict Visual Performance." Journal of Vision 4 (4): 8.

Mello Jr., Mozart O, Ingrid U Scott, William E Smiddy, Harry W Flynn Jr., and William Feuer. 2000. "Surgical Management and Outcomes of Dislocated Intraocular Lenses." Ophthalmology 107 (1): 62–67.

Mesa, Ramon. 2015. "Reading Ability With New Extended Range of Vision 1-Piece IOL." In . Ascrs. https://ascrs.confex.com/ascrs/15am/webprogram/Paper17640.html.

Miller, David, and Leroy Meshel. 1993. Annular mask contact lenses. US5245367 A, filed November 12, 1991, and issued September 14, 1993. http://www.google.com/patents/US5245367.

Mohrenfels, Christoph Winkler von, Josefina Salgado, Ramin Khoramnia, Mathias Maier, and Chris P. Lohmann. 2010. "Clinical Results with the Light Adjustable Intraocular Lens after Cataract Surgery." Journal of Refractive Surgery (Thorofare, N.J.: 1995) 26 (5): 314–20.
.
Montés-Micó, Robert, and Jorge L. Alió. 2003. "Distance and near Contrast Sensitivity Function after Multifocal Intraocular Lens Implantation." Journal of Cataract and Refractive Surgery 29 (4): 703–11.

Montés-Micó, Robert, Enrique España, Inmaculada Bueno, W. Neil Charman, and José L. Menezo. 2004. "Visual Performance with Multifocal Intraocular Lenses: Mesopic Contrast Sensitivity under Distance and near Conditions." Ophthalmology 111 (1): 85–96.

Montés-Micó, Robert, Norberto López-Gil, Cari Pérez-Vives, Sergio Bonaque, and Teresa Ferrer-Blasco. 2012. "In Vitro Optical Performance of Nonrotational Symmetric and Refractive–diffractive Aspheric Multifocal Intraocular Lenses: Impact of Tilt and Decentration." Journal of Cataract & Refractive Surgery 38 (9): 1657–63.

Montés-Micó, Robert, David Madrid-Costa, Alberto Domínguez-Vicent, Lurdes Belda-Salmerón, and Teresa Ferrer-Blasco. 2014. "In Vitro Power Profiles of Multifocal Simultaneous Vision Contact Lenses." Contact Lens & Anterior Eye: The Journal of the British Contact Lens Association 37 (3): 162–67.

Montés-Micó, Robert, David Madrid-Costa, Hema Radhakrishnan, W. Neil Charman, and Teresa Ferrer-Blasco. 2011. "Accommodative Functions with Multifocal Contact Lenses: A Pilot Study." Optometry and Vision Science: Official Publication of the American Academy of Optometry 88 (8): 998–1004.

Montés-Micó, Robert, David Madrid-Costa, Javier Ruiz-Alcocer, Teresa Ferrer-Blasco, and Alvaro M. Pons. 2013. "In Vitro Optical Quality Differences between Multifocal Apodized Diffractive Intraocular Lenses." Journal of Cataract and Refractive Surgery 39 (6): 928–36.

Mooren, Marrie van der, Tom van den Berg, Joris Coppens, and Patricia Piers. 2011. "Combining in Vitro Test Methods for Measuring Light Scatter in Intraocular Lenses." Biomedical Optics Express 2 (3): 505–10.

Mooren, Marrie van der, Luuk Franssen, and Patricia Piers. 2013. "Effects of Glistenings in Intraocular Lenses." Biomedical Optics Express 4 (8): 1294–1304.

Mooren, Marrie van der, Roger Steinert, Farrell Tyson, Michelle J. M. Langeslag, and Patricia A. Piers. 2015. "Explanted Multifocal Intraocular Lenses." Journal of Cataract & Refractive Surgery 41 (4): 873–77.

Morgan, Philip B, Nathan Efron, Craig A Woods, and The International Contact Lens Prescribing Survey Consortium. 2011. "An International Survey of Contact Lens Prescribing for Presbyopia." Clinical and Experimental Optometry 94 (1): 87–92.

Navarro, Rafael, Jos J. Rozema, and Marie-José Tassignon. 2013. "Optical Changes of the Human Cornea as a Function of Age." Optometry and Vision Science: Official Publication of the American Academy of Optometry 90 (6): 587–98.

Nema, HV Nema, Nitin. n.d. Recent Advances in Ophthalmology - 10. Jaypee Brothers Publishers.

Ninomiya, Sayuri, Takashi Fujikado, Teruhito Kuroda, Naoyuki Maeda, Yasuo Tano, Tetsuro Oshika, Yoko Hirohara, and Toshifumi Mihashi. 2002. "Changes of Ocular Aberration with Accommodation." American Journal of Ophthalmology 134 (6): 924–26.

Nio, Y. K., N. M. Jansonius, V. Fidler, E. Geraghty, S. Norrby, and A. C. Kooijman. 2002. "Spherical and Irregular Aberrations Are Important for the Optimal Performance of the Human Eye." Ophthalmic & Physiological Optics: The Journal of the British College of Ophthalmic Opticians (Optometrists) 22 (2): 103–12.

Nishi, Yutaro, Kamiar Mireskandari, Peng Khaw, and Oliver Findl. 2009. "Lens Refilling to Restore Accommodation." Journal of Cataract and Refractive Surgery 35 (2): 374–82.

Olson, Randall J., Liliana Werner, Nick Mamalis, and Robert Cionni. 2005. "New Intraocular Lens Technology." American Journal of Ophthalmology 140 (4): 709–16.

Ong, Hon Shing, Jennifer R. Evans, and Bruce D. S. Allan. 2014. "Accommodative Intraocular Lens versus Standard Monofocal Intraocular Lens Implantation in Cataract Surgery." The Cochrane Database of Systematic Reviews, no. 5: CD009667.

Ortiz, Dolores, Jorge L. Alió, Gonzalo Bernabéu, and Vanessa Pongo. 2008. "Optical Performance of Monofocal and Multifocal Intraocular Lenses in the Human Eye." Journal of Cataract and Refractive Surgery 34 (5): 755–62.

Oshika, Tetsuro, Chikako Okamoto, Tomokazu Samejima, Tadatoshi Tokunaga, and Kazunori Miyata. 2006. "Contrast Sensitivity Function and Ocular Higher-Order Wavefront Aberrations in Normal Human Eyes." Ophthalmology 113 (10): 1807–12.

Ossma, Ivan L., Andrea Galvis, Luis G. Vargas, Michelle J. Trager, M. Reza Vagefi, and Stephen D. McLeod. 2007. "Synchrony Dual-Optic Accommodating Intraocular Lens. Part 2: Pilot Clinical Evaluation." Journal of Cataract and Refractive Surgery 33 (1): 47–52.

Pallikaris, Ioannis G., and Sophia I. Panagopoulou. 2015. "PresbyLASIK Approach for the Correction of Presbyopia." Current Opinion in Ophthalmology 26 (4): 265–72.

Pallikaris, Ioannis G, Sotiris Plainis, and W. N Charman. 2012. Presbyopia: Origins, Effects, and Treatment. http://site.ebrary.com/id/10824143.

Papadatou, Eleni, Antonio J. Del Águila-Carrasco, José J. Esteve-Taboada, David Madrid-Costa, and Robert Montés-Micó. 2016. "Assessing the in Vitro Optical Quality of Presbyopic Solutions Based on the Axial Modulation Transfer Function." Journal of Cataract and Refractive Surgery 42 (5): 780–87.

Pascal JI, and Ludvigh E. 1938. "INtroduction to Physiological Optics." Archives of Ophthalmology 19 (2): 316–19. doi:10.1001/archopht.1938.00850140158020. Peng, Cheng, Jiangyue Zhao, Liwei Ma, Bo Qu, Qi Sun, and Jinsong Zhang. 2012. "Optical Performance after Bilateral Implantation of Apodized Aspheric Diffractive Multifocal Intraocular Lenses with +3.00-D Addition Power." Acta Ophthalmologica 90 (8): e586–93.

Pennos, Alexandros, Harilaos S. Ginis, Adrian Gambin, and Pablo Artal. 2016. "Straylight Measurements in Intraocular Lenses with an Optical Integration Method." Investigative Ophthalmology & Visual Science 57 (12): 3116–3116.

Pepose, J.S., D. Wang, and G.E. Altmann. 2012. "Comparison of through-Focus Image Sharpness across Five Presbyopia-Correcting Intraocular Lenses." American Journal of Ophthalmology 154 (1): 20–28.

Pérez-Vives, Cari, Teresa Ferrer-Blasco, Alberto Domínguez-Vicent, Santiago García-Lázaro, and Robert Montés-Micó. 2013. "Optical and Visual Quality of the Visian Implantable Collamer Lens Using an Adaptive-Optics Visual Simulator." American Journal of Ophthalmology 155 (3): 499–507.e1.
.
Pérez-Vives, Cari, Robert Montés-Micó, Norberto López-Gil, Teresa Ferrer-Blasco, and Santiago García-Lázaro. 2013. "Crystalens HD Intraocular Lens Analysis Using an Adaptive Optics Visual Simulator." Optometry and Vision Science: Official Publication of the American Academy of Optometry 90 (12): 1413–23.

Perreault, Julie A., Thomas G. Bifano, B. Martin Levine, and Mark N. Horenstein. 2002. "Adaptive Optic Correction Using Microelectromechanical Deformable Mirrors." Optical Engineering 41 (3): 561–66. doi:10.1117/1.1447230.
Petrash, J. Mark. 2013. "Aging and Age-Related Diseases of the Ocular Lens and Vitreous Body." Investigative Ophthalmology & Visual Science 54 (14): ORSF54–59.

Petternel, Vanessa, Rupert Menapace, Oliver Findl, Barbara Kiss, Matthias Wirtitsch, Georg Rainer, and Wolfgang Drexler. 2004. "Effect of Optic Edge Design and Haptic Angulation on Postoperative Intraocular Lens Position Change." Journal of Cataract and Refractive Surgery 30 (1): 52–57.

Pieh, Stefan, Christian Kellner, Georg Hanselmayer, Birgit Lackner, Gerald Schmidinger, Tony Walkow, Markus Sticker, Herbert Weghaupt, Adolf Friedrich Fercher, and Christian Skorpik. 2002. "Comparison of Visual Acuities at Different Distances and Defocus Curves." Journal of Cataract and Refractive Surgery 28 (11): 1964–67.

Piers, Patricia A., Enrique J. Fernandez, Silvestre Manzanera, Sverker Norrby, and Pablo Artal. 2004. "Adaptive Optics Simulation of Intraocular Lenses with Modified Spherical Aberration." Investigative Ophthalmology & Visual Science 45 (12): 4601–10.

Plainis, Sotiris, David A. Atchison, and W. Neil Charman. 2013. "Power Profiles of Multifocal Contact Lenses and Their Interpretation." Optometry and Vision Science: Official Publication of the American Academy of Optometry 90 (10): 1066–77.

Plainis, Sotiris, George Ntzilepis, David A. Atchison, and W. Neil Charman. 2013. "Through-Focus Performance with Multifocal Contact Lenses: Effect of Binocularity, Pupil Diameter and Inherent Ocular Aberrations." Ophthalmic & Physiological Optics: The Journal of the British College of Ophthalmic Opticians (Optometrists) 33 (1): 42–50.

Pons, A. M., A. Lorente, C. Albarrán, R. Montés, and J. M. Artigas. 1998. "Characterization of the Visual Performance with Soft Daily Wear Disposable Contact Lenses." Ophthalmic & Physiological Optics: The Journal of the British College of Ophthalmic Opticians (Optometrists) 18 (1): 40–48.

Porter, J., A. Guirao, I. G. Cox, and D. R. Williams. 2001. "Monochromatic Aberrations of the Human Eye in a Large Population." Journal of the Optical Society of America. A, Optics, Image Science, and Vision 18 (8): 1793–1803.

Prieto, Pedro M., Fernando Vargas-Martín, Stefan Goelz, and Pablo Artal. 2000. "Analysis of the Performance of the Hartmann–Shack Sensor in the Human Eye." Journal of the Optical Society of America A 17 (8): 1388.

Putnam, Nicole M., Heidi J. Hofer, Nathan Doble, Li Chen, Joseph Carroll, and David R. Williams. 2005. "The Locus of Fixation and the Foveal Cone Mosaic." Journal of Vision 5 (7): 632–39.

Regan, David, and David Neima. 1983. "Low-Contrast Letter Charts as a Test of Visual Function." Ophthalmology 90 (10): 1192–1200.

Reggiani Mello, Glauco H., and Ronald R. Krueger. 2011. "Femtosecond Laser Photodisruption of the Crystalline Lens for Restoring Accommodation." International Ophthalmology Clinics 51 (2): 87–95.

Remón, Laura, Augusto Arias, Arnau Calatayud, Walter D. Furlan, and Juan A. Monsoriu. 2012. "Through-Focus Response of Multifocal Intraocular Lenses Evaluated with a Spatial Light Modulator." Applied Optics 51 (36): 8594.

Rocha, Karolinne Maia, Eduardo S. Soriano, Wallace Chamon, Maria Regina Chalita, and Walton Nosé. 2007. "Spherical Aberration and Depth of Focus in Eyes Implanted with Aspheric and Spherical Intraocular Lenses: A Prospective Randomized Study." Ophthalmology 114 (11): 2050–54.

Rocha, Karolinne Maia, Laurent Vabre, Nicolas Chateau, and Ronald R. Krueger. 2009. "Expanding Depth of Focus by Modifying Higher-Order Aberrations Induced by an Adaptive Optics Visual Simulator." Journal of Cataract & Refractive Surgery 35 (11): 1885–92.

Roddier, François. 1988. "Curvature Sensing and Compensation: A New Concept in Adaptive Optics." Applied Optics 27 (7): 1223. doi:10.1364/AO.27.001223. Roorda, A. 2011. "Adaptive Optics for Studying Visual Function: A Comprehensive Review." Journal of Vision 11 (5): 6–6.

Rosen, E., and C. Gore. 1998. "Staar Collamer Posterior Chamber Phakic Intraocular Lens to Correct Myopia and Hyperopia." Journal of Cataract and Refractive Surgery 24 (5): 596–606.

Rossi, Ethan A., and Austin Roorda. 2010. "The Relationship between Visual Resolution and Cone Spacing in the Human Fovea." Nature Neuroscience 13 (2): 156–57.

Roufs, J. A. 1972. "Dynamic Properties of Vision. I. Experimental Relationships between Flicker and Flash Thresholds." Vision Research 12 (2): 261–78.

Ruiz-Alcocer, Javier, David Madrid-Costa, Santiago García-Lázaro, Teresa Ferrer-Blasco, and Robert Montés-Micó. 2014. "Optical Performance of Two New Trifocal Intraocular Lenses: Through-Focus Modulation Transfer Function and Influence of Pupil Size." Clinical & Experimental Ophthalmology 42 (3):

Sáles, Christopher S., and Edward E. Manche. 2015. "Managing Residual Refractive Error after Cataract Surgery." Journal of Cataract and Refractive Surgery 41 (6): 1289–99.

Salvi, S M, S Akhtar, and Z Currie. 2006. "Ageing Changes in the Eye." Postgraduate Medical Journal 82 (971): 581–87. doi:10.1136/pgmj.2005.040857. Sarwar, H., and N. Modi. 2014. "Sir Harold Ridley: Innovator of Cataract Surgery." Journal of Perioperative Practice 24 (9): 210–12.

Schachar, Ronald A. 2004. "Qualitative Effect of Zonular Tension on Freshly Extracted Intact Human Crystalline Lenses: Implications for the Mechanism of Accommodation." Investigative Ophthalmology & Visual Science 45 (8): 2691–

Scharnowski, Frank, Frouke Hermens, and Michael H. Herzog. 2007. "Bloch's Law and the Dynamics of Feature Fusion." Vision Research 47 (18): 2444–52.

Sebag, J. 1987. "Age-Related Changes in Human Vitreous Structure." Graefe's Archive for Clinical and Experimental Ophthalmology = Albrecht Von Graefes Archiv Für Klinische Und Experimentelle Ophthalmologie 225 (2): 89–93.

Strenk, Susan A., Lawrence M. Strenk, and Jane F. Koretz. 2005. "The Mechanism of Presbyopia." Progress in Retinal and Eye Research 24 (3): 379–93.

"SYMFONY IOL | Eurotimes.org." 2016. Accessed July 9. http://www.eurotimes.org/node/1737.
"TECNIS® - Safer, Sharper Vision after Cataract Surgery." 2016. Accessed July 9. http://www.tecnisiol.com/eu/tecnis-symfony-iol.htm.

Telandro, Alain. 2004. "Pseudo-Accommodative Cornea: A New Concept for Correction of Presbyopia." Journal of Refractive Surgery (Thorofare, N.J.: 1995) 20 (5 Suppl): S714–17.

Thibos, Larry N., Xin Hong, Arthur Bradley, and Raymond A. Applegate. 2004. "Accuracy and Precision of Objective Refraction from Wavefront Aberrations." Journal of Vision 4 (4): 329–51.

Thibos, L. N., A. Bradley, and D. L. Still. 1991. "Interferometric Measurement of Visual Acuity and the Effect of Ocular Chromatic Aberration." Applied Optics 30 (16): 2079–87.

Tomás-Juan, Javier, and Ane Murueta-Goyena Larrañaga. 2015. "Axial Movement of the Dual-Optic Accommodating Intraocular Lens for the Correction of the Presbyopia: Optical Performance and Clinical Outcomes." Journal of Optometry 8 (2): 67–76.

Torricelli, André AM, Jackson B Junior, Marcony R Santhiago, and Samir J Bechara. 2012. "Surgical Management of Presbyopia." Clinical Ophthalmology (Auckland, N.Z.) 6: 1459–66.

Toshida, Hiroshi, Kozo Takahashi, Kazushige Sado, Atsushi Kanai, and Akira Murakami. 2008. "Bifocal Contact Lenses: History, Types, Characteristics, and Actual State and Problems." Clinical Ophthalmology (Auckland, N.Z.) 2 (4): 869–77.

Tucker, J., and E. P. Rabie. 1980. "Depth-of-Focus of the Pseudophakic Eye." The British Journal of Physiological Optics 34: 12–21.

Tyson, Robert K. 2015. Principles of Adaptive Optics, Fourth Edition. CRC Press. Van Den Berg, Thomas J. T. P., L. J. René Van Rijn, Ralph Michael, Christian Heine, Tanja Coeckelbergh, Christian Nischler, Helmuth Wilhelm, et al. 2007. "Straylight Effects with Aging and Lens Extraction." American Journal of Ophthalmology 144 (3): 358–63.

Vasudevan, Balamurali, Michael Flores, and Sara Gaib. 2014. "Objective and Subjective Visual Performance of Multifocal Contact Lenses: Pilot Study." Contact Lens & Anterior Eye: The Journal of the British Contact Lens Association 37 (3): 168–74.

Veselá, M., D. Baráková, D. Bujalková, and D. Garajová. 2016. "[The Effect of Multifocal Toric Lens Rotation on Visual Quality]." Ceská a Slovenská Oftalmologie: Casopis Ceské Oftalmologické Spolecnosti a Slovenské Oftalmologické Spolecnosti 72 (2): 3–11.

Villegas, Eloy A., Encarna Alcón, Sandra Mirabet, Inés Yago, José María Marín, and Pablo Artal. 2014. "Extended Depth of Focus with Induced Spherical Aberration in Light-Adjustable Intraocular Lenses." American Journal of Ophthalmology 157 (1): 142–49.

Villegas, Eloy A., Encarna Alcon, Elena Rubio, José M. Marín, and Pablo Artal. 2014. "Refractive Accuracy with Light-Adjustable Intraocular Lenses." Journal of Cataract and Refractive Surgery 40 (7): 1075–84.e2.

Vos, J.J. 1984. "DISABILITY GLARE - A STATE OF THE ART REPORT." CIE-Journal 3 (2): 39–53.

Vries, Niels E. de, Luuk Franssen, Carroll A. B. Webers, Nayyirih G. Tahzib, Yanny Y. Y. Cheng, Fred Hendrikse, Khiun F. Tjia, Tom J. T. P. van den Berg, and Rudy M. M. A. Nuijts. 2008. "Intraocular Straylight after Implantation of the Multifocal AcrySof ReSTOR SA60D3 Diffractive Intraocular Lens." Journal of Cataract and Refractive Surgery 34 (6): 957–62.

Wagner, Sandra, Fabian Conrad, Ravi C. Bakaraju, Cathleen Fedtke, Klaus Ehrmann, and Brien A. Holden. 2015. "Power Profiles of Single Vision and Multifocal Soft Contact Lenses." Contact Lens & Anterior Eye: The Journal of the British Contact Lens Association 38 (1): 2–14.

Wang, Li, and Douglas D. Koch. 2007. "Custom Optimization of Intraocular Lens Asphericity." Journal of Cataract & Refractive Surgery 33 (10): 1713–20.

Waring, George O. 2011. "Correction of Presbyopia with a Small Aperture Corneal Inlay." Journal of Refractive Surgery (Thorofare, N.J.: 1995) 27 (11): 842–45.

Wells, Jered R., and James T. Dobbins. 2012. "Estimation of the Two-Dimensional Presampled Modulation Transfer Function of Digital Radiography Devices Using One-Dimensional Test Objects." Medical Physics 39 (10): 6148–60.

Werner, John S., Sarah L. Elliott, Stacey S. Choi, and Nathan Doble. 2009. "Spherical Aberration Yielding Optimum Visual Performance: Evaluation of Intraocular Lenses Using Adaptive Optics Simulation." Journal of Cataract & Refractive Surgery 35 (7): 1229–33.

Werner, Leonardo, Fernando Trindade, Frederico Pereira, and Liliana Werner. 2000. "Physiology of Accommodation and Presbyopia." Arquivos Brasileiros de Oftalmologia 63 (6): 487–93.
.
Wilkins, Mark R., Bruce D. Allan, Gary S. Rubin, Oliver Findl, Emma J. Hollick, Catey Bunce, and Wen Xing. 2013. "Randomized Trial of Multifocal Intraocular Lenses versus Monovision after Bilateral Cataract Surgery." Ophthalmology 120 (12): 2449–55.

Winn, B., D. Whitaker, D. B. Elliott, and N. J. Phillips. 1994. "Factors Affecting Light-Adapted Pupil Size in Normal Human Subjects." Investigative Ophthalmology & Visual Science 35 (3): 1132–37.

Wolffsohn, James S., Amit N. Jinabhai, Alec Kingsnorth, Amy L. Sheppard, Shehzad A. Naroo, Sunil Shah, Phillip Buckhurst, Lee A. Hall, and Graeme Young. 2013. "Exploring the Optimum Step Size for Defocus Curves." Journal of Cataract and Refractive Surgery 39 (6): 873–80.

Wolffsohn, James Stuart, Olivia Anne Hunt, Shehzad Naroo, Bernard Gilmartin, Sunil Shah, Ian Andrew Cunliffe, Mark Timothy Benson, and Sanjay Mantry. 2006. "Objective Accommodative Amplitude and Dynamics with the 1CU Accommodative Intraocular Lens." Investigative Ophthalmology & Visual Science 47 (3): 1230–35.

Woodward, Maria A., J. Bradley Randleman, and R. Doyle Stulting. 2009. "Dissatisfaction after Multifocal Intraocular Lens Implantation." Journal of Cataract & Refractive Surgery 35 (6): 992–97.

Yamauchi, Tomofusa, Hitoshi Tabuchi, Kosuke Takase, Hideharu Ohsugi, Zaigen Ohara, and Yoshiaki Kiuchi. 2013. "Comparison of Visual Performance of Multifocal Intraocular Lenses with Same Material Monofocal Intraocular Lenses." PloS One 8 (6): e68236.

Yang, H. C., S. K. Chung, and N. H. Baek. 2000. "Decentration, Tilt, and near Vision of the Array Multifocal Intraocular Lens." Journal of Cataract and Refractive Surgery 26 (4): 586–89.

Yi, Fan, D. Robert Iskander, and Michael Collins. 2011. "Depth of Focus and Visual Acuity with Primary and Secondary Spherical Aberration." Vision Research 51 (14): 1648–58.

Yoon, Geun-Young, and David R. Williams. 2002. "Visual Performance after Correcting the Monochromatic and Chromatic Aberrations of the Eye." Journal of the Optical Society of America. A, Optics, Image Science, and Vision 19 (2): 266–75.

Żelichowska, Beata, Marek Rękas, Andrzej Stankiewicz, Alejandro Cerviño, and Robert Montés-Micó. 2008. "Apodized Diffractive versus Refractive Multifocal Intraocular Lenses: Optical and Visual Evaluation." Journal of Cataract & Refractive Surgery 34 (12): 2036–42.

Appendix A

Appendix A – Publications from the thesis

This PhD Thesis has resulted in the following peer-reviewed publications:

1. Assessing the in vitro optical quality of presbyopic solutions based on the axial modulation transfer function. *Journal of Cataract & Refractive Surgery* 2016; *42*(5):780-787. Impact factor: 3.020.
   http://www.sciencedirect.com/science/article/pii/S0886335016300967
   DOI: 10.1016/j.jcrs.2015.11.049

2. Temporal multiplexing with adaptive optics for simultaneous vision. *Biomedical Optics Express* 2016. 7: 4102-4113. Impact factor: 3.344.
   https://www.osapublishing.org/boe/abstract.cfm?uri=boe-7-10-4102
   DOI: 10.1364/BOE.7.004102

3. Objective assessment of the effect of pupil size upon the power distribution of multifocal contact lenses. *International Journal of Ophthalmology* 2017; 10(1) Impact factor: 0.939.
   Scheduled to be published in January 2017

Parts of the present Thesis have been presented to the following scientific congresses:

1. XXXIII congress of the European Society of Cataract & Refractive Surgeons (ESCRS), 4-8 September 2015, Barcelona, Spain. *A new metric for quantifying intraocular lenses optical quality by means of axial modulation transfer function*. Proceedings of XXXIII congress of the ESCRS, abstract book, September 2015.

2. The International OSA Network of Student (IONS) congress, Iberian Chapter, 24-26 September 2015, Valencia, Spain. *A new metric to assess the quality of optical elements based on the axial modulation transfer function.* Proceedings of IONS Valencia congress, abstract book, September 2015.

3. Congreso Internacional de Optometría, Contactología y Óptica Oftálmica (OPTOM) 2016, 8-10 Abril 2016, Madrid, Spain**. *Una métrica para cuantificar la calidad óptica de las lentes intraoculares por medio de la función de transferencia de la modulación axial*. Proceedings of OPTOM congress, abstract book, April 2016.

4. The Association for Research in Vision and Ophthalmology (ARVO) Annual Meeting, 1-5 May, 2016, Seattle, Washington, USA. *Assessing the optical quality of commercially available intraocular lenses by means of modulation transfer function and straylight*. Proceedings of ARVO Annual Meeting, abstract book, May 2016.

5. 8th European Meeting on Visual and Physiological Optics (VPO), 22-24 August 2016, Antwerp, Belgium. *Simultaneous vision with adaptive optics*. Proceedings of VPO congress, abstract book, August 2016.